

Identification and Modeling of
Parameters that Influence Microdialysis
Sampling *in vitro* and *in vivo*

by Julie Ann Stenken

1995

Submitted to the Department of Chemistry
and the Faculty of the Graduate School of the
University of Kansas in partial fulfillment of the
requirements for the degree of Doctor of Philosophy

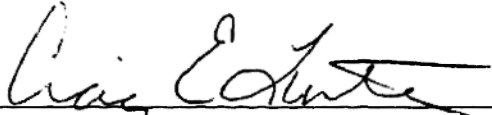
Identification and Modeling of Parameters that Influence Microdialysis Sampling *in vitro* and *in vivo*.

by

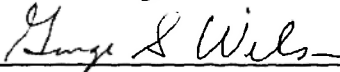
Julie Ann Stenken
B.S., University of Akron, Ohio, 1990

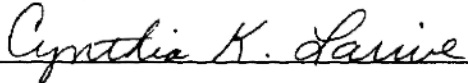
Submitted to the Department of Chemistry and the Faculty of the Graduate School of the University of Kansas in partial fulfillment of the requirements for the degree of Doctor of Philosophy

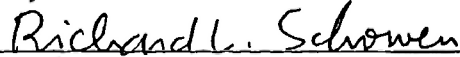
Diss
1995
S746
c.2
(Science)




(Professor in Charge)









(Committee Members)

Date Defended: October 11, 1995

Dedicated to my mother, Audrey Stenken (1936-1981), who has been unable to witness the many accomplishments of her children.

Abstract

Microdialysis sampling has matured into a standard technique for sampling the rat brain *in vivo*. Microdialysis is beginning to be used for sampling from other tissues in laboratory animals. It has also been used in humans. The amount of material that enters or leaves a microdialysis probe is dependent upon many factors, some of which are presented in this dissertation. These factors include forced convection around the dialysis membrane, hindered diffusion through the membrane, and kinetic processes that occur in the tissue space. The aims of these studies were to identify factors that affect extraction efficiency in microdialysis systems and to develop methods to quantitate these factors.

By setting up a specialized flow apparatus the effects of forced convection around a microdialysis membrane fiber were studied. From this same apparatus, values of the membrane permeability for hydroquinone, caffeine, theophylline, and theobromine were found for cuprophane, cellulose acetate and polyacrylonitrile membranes. A mathematical model was developed to determine the membrane permeability, and it fit the data well.

The effects of inhibition of phenacetin and antipyrine metabolism in the liver and acetylcholine metabolism in the brain on the amount of each substance lost from the probe was studied. It was found through the development of a mechanistic model that microvasculature exchange rates dominate metabolism rates in the liver. Inhibition of metabolism in the liver did not change the amount of material lost from the microdialysis probe during a local infusion. Acetylcholine is removed from the brain through only metabolic processes, thus inhibition affects the amount of material that is lost from the microdialysis probe after a local infusion of acetylcholine in the brain.

A human study evaluated the usefulness of microdialysis for determining low levels of caffeine taken *ad lib*. This final study shows that microdialysis sampling although originally developed for brain studies in the rat, is finding more use in human studies.

Acknowledgements

Associate Professor Craig Lunte has served as a patient and encouraging advisor over the years. Dr. Lunte has indeed encouraged me to pursue the many different aspects of microdialysis that are included in this dissertation.

Associate Professor Marylee Southard of the Department of Chemical and Petroleum Engineering has been more than generous with her time, effort and energy during the development of the mathematical parts of this dissertation.

To Docent Lars Ståhle at the Karolinska Institute in Stockholm, I say that you and your family deserve a thousand *tack for senaste's*. Lasse provided an excellent environment in which an individual could work both from an intellectual and a social standpoint.

Professors George Wilson and Richard Schowen were instrumental in encouraging and helping me obtain the J. William Fulbright Fellowship to study in Sweden. Their insights and mentoring have been most helpful.

Donna Iannotti, Dianne Runk, Carolyn Moran, and John Rasmussen have provided good friendship and support through some of my roughest days in graduate school.

Paul Hancock provided stimulating conversation about heat and fluid flow and modeling of these processes during many bike rides throughout the Lawrence area. His insights in these areas were most helpful.

Natasja Borg of the Karolinska Institute provided expert rat watching assistance when I would need to eat lunch at 3 pm during long rat experiments. I am also most appreciative of Natasja being one of the few individuals in the department who would consistently speak to me in Swedish (whether I wanted to or not) so that my language skills would improve. *En tusind tack så mycket's till dig!*

The following scientists, laboratory assistants and secretarial staff at the Department of Clinical Pharmacology in Sweden are acknowledged for allowing me to feel most welcome including Professor Folke Sjöquist, Leif Bertilsson, Gunnar Alvan, Lennart Meurling, Marja-Liisa Dahl, Elisabeth Samuelson, Monique Wakelkamp, Sanna Hulkko, Ming Chang, Margareta Lind, Lilleba Bohman, Ulla Petersson, Gunnel Tybring, Christina Alm, Eva Götharsson and Jan Nordin.

Grover and Carolyn Everett who graciously gave me a place to work and sleep after

returning from Stockholm to Lawrence.

Lunte group members: Dennis Scott, Howard Hendrickson, Rita Palsmeier, Mike Hadwiger and Malonne Davies for answering questions on instrumentation, computers or for discussions on the quantitative aspects of microdialysis.

My family, especially my brother Joe and my father for always being willing to listen to me and for their support even though at times they did not understand why I was occupied with what I was doing.

Finally I need to acknowledge the many avenues of financial support that I have obtained during my graduate career. For my first three years I obtained support through the federally funded Patricia Roberts Harris fellowship for minorities and women. For several months of my third year I was supported by funds obtained by my advisor through the National Institutes of Health. During my final year, I obtained support through the Procter & Gamble Bioanalytical Chemistry Fellowship and a J. William Fulbright Fellowship.

Table of Contents

Chapter 1. Introduction: Methods used to Characterize Processes Affecting Microdialysis.	1
1.1 Problem Statement	1
1.2. Basic Principles of Microdialysis Sampling	1
1.2.1 Modes of Microdialysis Operation	2
1.2.1.1 Recovery	4
1.2.1.2 Delivery	6
1.2.3 Mass Transfer Resistance in Microdialysis	6
1.2.3.1 Tissue Resistance	8
1.2.3.2 Membrane Resistance	9
1.2.3.3 Dialysis Resistance	10
1.3 Controllable Conditions in the Microdialysis Experiment	11
1.4 Microdialysis Applications	11
1.5 Calibration Methods and Issues	12
1.5.1 <i>In vitro</i> Calibrations	13
1.5.2 Mass Transfer Coefficient Determinations	13
1.5.3 No-net Flux Determinations	14
1.5.4 Internal Standards	15
1.6 Predictive Modeling in Microdialysis	17
1.6.1 Introduction to Mathematical Model Building	17
1.6.1 Microdialysis Diffusion-based Models	17
1.6.2 Methods Based on Diffusive and Kinetic Processes	19
1.7 Use of Microdialysis Mathematical Models for Use in Tissues Other than Brain	23
1.8 References	26
Chapter 2. Examination of Recovery Profiles for a Microdialysis System Under Hydrodynamic Conditions.	32
2.1 Introduction	32
2.1.1 Membrane Terminology	33
2.1.2 Microdialysis in a Fluid Space	35
2.2 Materials and Methods	37
2.2.1 Chemicals	37
2.2.2 Microdialysis	37
2.2.3 Liquid Chromatographic Analyses	40
2.2.4 Rotating Disk Electrochemistry	40
2.2.5 Determination of the Membrane Permeability	41
2.2.6 Determination of Membrane Partition Coefficients	43
2.3 Results and Discussion	43

2.3.1 Recovery Experiments	43
2.3.2 Mass Transfer Coefficient Determinations	47
2.3.3 Permeability Determinations	50
2.3.4 Permeation Through the Membrane	53
2.4 Conclusions	56
2.5 References	56

Chapter 3. Development and Analysis of Mechanistic Models to Describe the Extraction Efficiency in Microdialysis Experiments.	59
3.1 Development of Models to Describe Microdialysis Experiments	59
3.2 Analytical methods	60
3.2.1 Analytical assumptions	61
3.2.2 Analytical Solution	63
3.2.3 Addition of Membrane Diffusion	65
3.3 Numerical Methods	68
3.3.1 Numerical Method Assumptions	70
3.3.2 Solution of the Numerical Equations	71
3.3.2.1 Tissue Space	71
3.3.2 Membrane mass balance	74
3.3.3 Dialysate mass balance	75
3.4 Solving the system of equations for microdialysis	78
3.5 Specifics Needed for the FORTRAN code	82
3.6 Adaptations to the Original Program	85
3.6.1 Euthanasia of the Animal	85
3.6.2 Metabolite formation	88
3.6.3 Non-linear kinetics in microdialysis	88
3.7 Strengths and limitations of the model	90
3.8 References	93

Chapter 4. Liver microdialysis: Identification of processes that contribute to the flux from the probe using model compounds phenacetin, antipyrine, and acetaminophen.	96
4.1 Introduction	96
4.1.2 Inhibition Studies	97
4.1.3 Metabolite Studies	101
4.2 Materials and Methods	101
4.2.1 Materials	101
4.2.2. Ethical Statements	102
4.2.3 <i>In Vitro</i> Experiments	102
4.2.4 <i>In vivo</i> Experiments	103
4.2.5 LC Analyses	106

4.3 Results and Discussion	106
4.3.1 Inhibition Studies	107
4.3.2 Euthanasia Studies	115
4.3.3. Portal Vein Ligation	121
4.3.4 Metabolite Studies	121
4.4 Summary	124
4.5 References	126
Chapter 5. The effect of acetylcholinesterase inhibition on the flux of ¹⁴ C-acetylcholine in microdialysis delivery experiments.	131
5.1 Introduction	131
5.2 Materials and Methods	132
5.3 Results and Discussion	134
5.4 Summary	140
5.5 References	141
Chapter 6. Determination of sub-cutaneous caffeine levels in a humans after voluntary caffeine ingestion	141
6.1 Introduction	141
6.2 Materials and Methods	142
6.2.1 Microdialysis	142
6.2.2 Caffeine Consumption Procedure	143
6.2.3 LC Analyses	144
6.3 Results and discussion	144
6.4 References	149
Chapter 7. Summary	150
Appendix 1. Development of the membrane permeability equations for microdialysis	154
Appendix 2. Development of Simplified Equations to Describe Microdialysis Flux	159
A.2.1 Flux From a Cylinder	159
A.2.2 Flux from the Membrane with Membrane Diffusion Included	162
A.2.3 References	166
Appendix 3. Development of the Far-Field Boundary Condition in a Recovery Microdialysis Experiment	167
Appendix 4. FORTRAN Code.	169

Chapter 1

Introduction: Methods used to Characterize Processes Affecting Microdialysis.

1.1 Problem Statement

The aims of the microdialysis studies described in this dissertation were two-fold. The first goal was to identify the factors of the microdialysis system that affect microdialysis extraction efficiency *in vitro* and *in vivo*, primarily in rats. The microdialysis system consists of the dialysis probe and the environment in which the probe is placed. This goal was accomplished through the experimental studies described in Chapters 2, 4 and 5 of this dissertation. Briefly, Chapter 2 discusses the limiting role of the membrane in hydrodynamic situations. Chapters 4 and 5 discuss the implications of metabolic inhibition on the flux of material from the microdialysis probe in liver and brain. The second goal was to develop methods to quantitate, through empirical and theoretical approaches, the factors indentified after completion of the first goal. A model that describes the diffusivity of substances through the membrane while the membrane is placed in a flowing fluid is presented in Chapter 2 and derived in Appendix 1. Chapter 3 develops a numerical model that predicts the concentration of substances as they exit the dialysis tubing under various conditions.

1.2. Basic Principles of Microdialysis Sampling

Much research *in vivo* in animals as well as in humans has focused on the collection of biological fluids, such as blood, urine, and feces to assess disease states or to determine the concentration of drugs or endogenous compounds. Although these routes of collection may give some indication as to the pathway that a compound may traverse, they are far removed from the site of action of the compound. These methods cannot be used to determine where a compound is concentrated or its local metabolism in a specific tissue site. To identify processes that occur at the site of action, such as local metabolism or transport rates, the use of other invasive and more

destructive techniques becomes necessary. Techniques used to quantify metabolism include: liver perfusion, tissue slices, whole cell studies or the use of subcellular fractions such as liver microsomes. Although these techniques have greatly advanced the understanding of metabolic and transport processes, they do disrupt or destroy the normal physiological processes that are interconnected and interdependent upon each other such as blood flow and metabolism in the liver.

Microdialysis is a sampling technique that involves the use of a hollow fiber dialysis membrane to separate low molecular weight compounds from larger compounds such as proteins at the site being sampled. This separation from the tissue space provides protein-free samples that can be directly analyzed without further clean-up procedures. The membrane length can vary from one to five mm for rat studies and up to 30 mm for human studies. The membrane lumen is perfused with a saline solution which allows diffusion of substances across the membrane into the dialysate perfusion fluid. Microdialysis was introduced as a sampling method for *in vivo* analyses almost thirty years ago and was used to sample the extracellular fluid (ECF) of brain tissue and blood plasma in dogs [Bito et al., 1966]. However, Urban Ungerstedt's research group at the Karolinska Institute in Stockholm, Sweden, is credited for developing and popularizing microdialysis sampling through the late 1970's and early 1980's. Microdialysis has allowed researchers and clinicians to observe the chemical events that are directly related to the tissue that is sampled rather than in a biological space unrelated to, or removed from, the tissue of interest.

1.2.1 Modes of Microdialysis Operation

Microdialysis is utilized in two different operating modes as shown in Figure 1. In both modes of operation, the dialysis fiber lumen is perfused with a solution that closely matches the ionic composition of the surrounding tissue space. This causes the

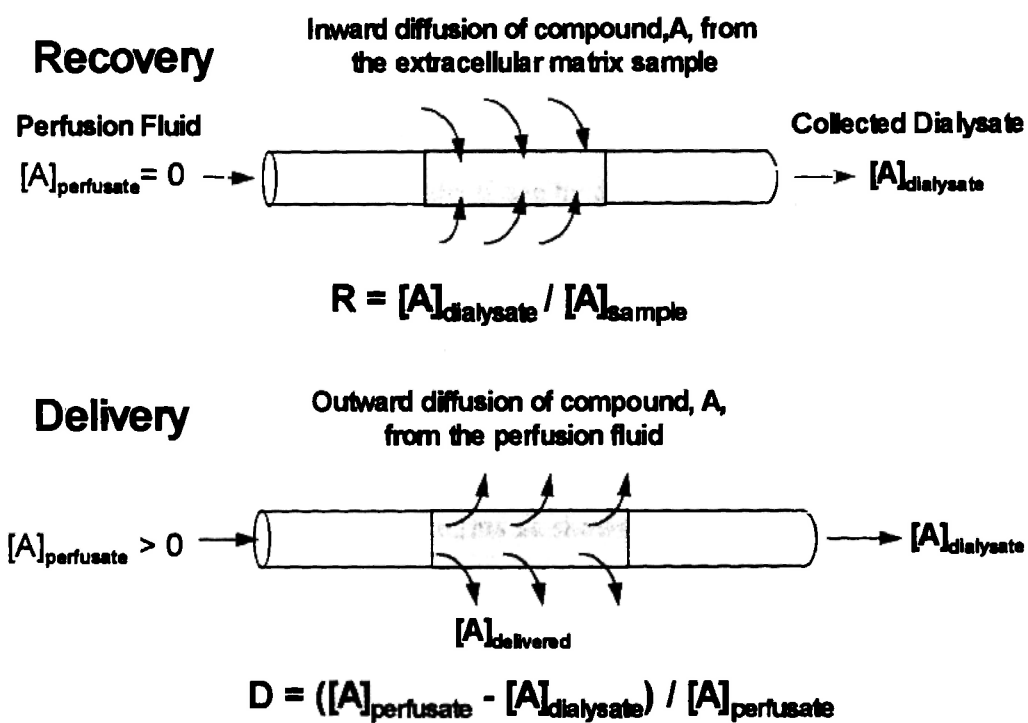


Figure 1. A linear microdialysis probe. $[A]$ denotes the concentration of the analyte.

mechanism of transport of molecules from the tissue space into the dialysis probe to be driven only by diffusion (concentration gradient) and not by osmotic pressure. Because transport into the dialysis fiber lumen is diffusive, there will be no net loss of fluid from the extracellular fluid space or the fiber lumen itself. This allows the fiber to behave as an artificial blood vessel in which low molecular weight substances (the analytes of interest) can be recovered from or delivered to the ECF space.

1.2.1.1 Recovery

The experiment that is most often performed using microdialysis sampling is called recovery. In a recovery experiment the analyte is removed from the extracellular fluid (ECF) space of the tissue by diffusion into the dialysis fiber lumen. It is important to note that microdialysis only samples analytes that are located in the ECF space and not the intracellular fluid space (ICF). The extraction fraction or recovery, R , which is the percentage of a substance that diffuses from one side of the membrane to the other, is described by the first equation shown in Figure 1. Most researchers use the term recovery to describe the relative recovery of the substance, which is defined in concentration terms as shown in Figure 1. The relative recovery value will decrease with increasing flow rates as shown in Figure 2 for hydroquinone. The term, mass recovery can also be used to describe the extraction efficiency of the microdialysis probe. Mass recovery will increase with increasing flow rates. This is because at higher flow rates the dialysis perfusion fluid in the hollow fiber becomes a sink and thus drives the movement of mass into the fiber lumen. Mass recovery is a difficult term to work with because in an *in vivo* situation the total amount of mass of a substance is unknown, thus the mass recovery would be difficult to calculate. Although the relative recovery may also be difficult to obtain *in vivo*, it can be obtained *in vitro* and is then applied *in vivo*. With mass recovery, the values will be different depending upon the volume of the standard in which the dialysis probe is placed. This is the reason for use of the relative recovery to describe the extraction

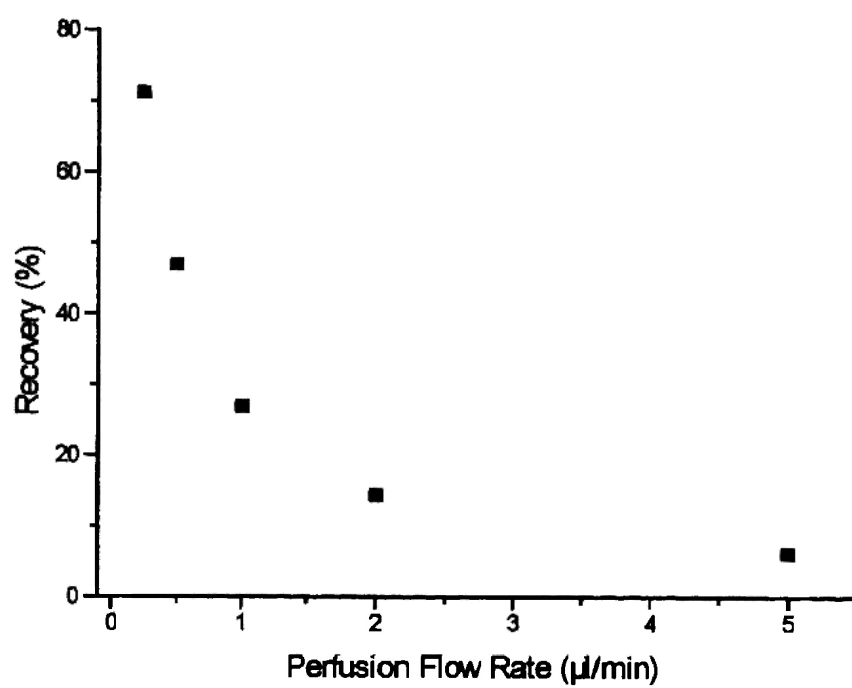


Figure 2. Hydroquinone recovery through a 3mm PAN membrane in a stirred solution.

efficiency of the microdialysis membrane fiber. Substances in the ECF space can pass through the fiber membrane by diffusion and be swept away by the perfusion fluid to be detected. In general during a recovery experiment, the concentration of the substance of interest is zero in the perfusion fluid that enters the microdialysis fiber lumen as shown in Figure 1, but in principle only needs to be less than the concentration in the sample ECF space in order for net diffusion into the probe to occur.

1.2.1.2 Delivery

When the transport of the analyte is in the opposite direction to that in the recovery experiment, the experiment is called delivery. In this mode, a known concentration of the analyte is included in the perfusion fluid. The analyte diffuses across the probe membrane into the ECF space, where it diffuses away from the probe, and is removed from the ECF by local metabolism or transport processes such as capillary permeation. An advantage of a delivery experiment is that a potentially toxic chemical can be delivered directly to the tissue space rather than through the circulatory system which may cause dysfunction of organs in the animal being studied. The delivery experiment can also be used to study local metabolism, which is discussed in Chapters four and five of this dissertation.

1.2.3 Mass Transfer Resistance in Microdialysis

The percentage of a substance that enters or leaves the microdialysis probe is a complex function of a variety of factors of which only a few can be experimentally manipulated or measured. The driving force for mass transport in the microdialysis experiment is a concentration gradient between the outside tissue space and the dialysate perfusion fluid. Figure 3 shows how a compound must pass through three distinct regions, the extracellular fluid space of the tissue, the membrane, and the dialysate perfusion fluid itself prior to be carried away by the dialysate. The mass

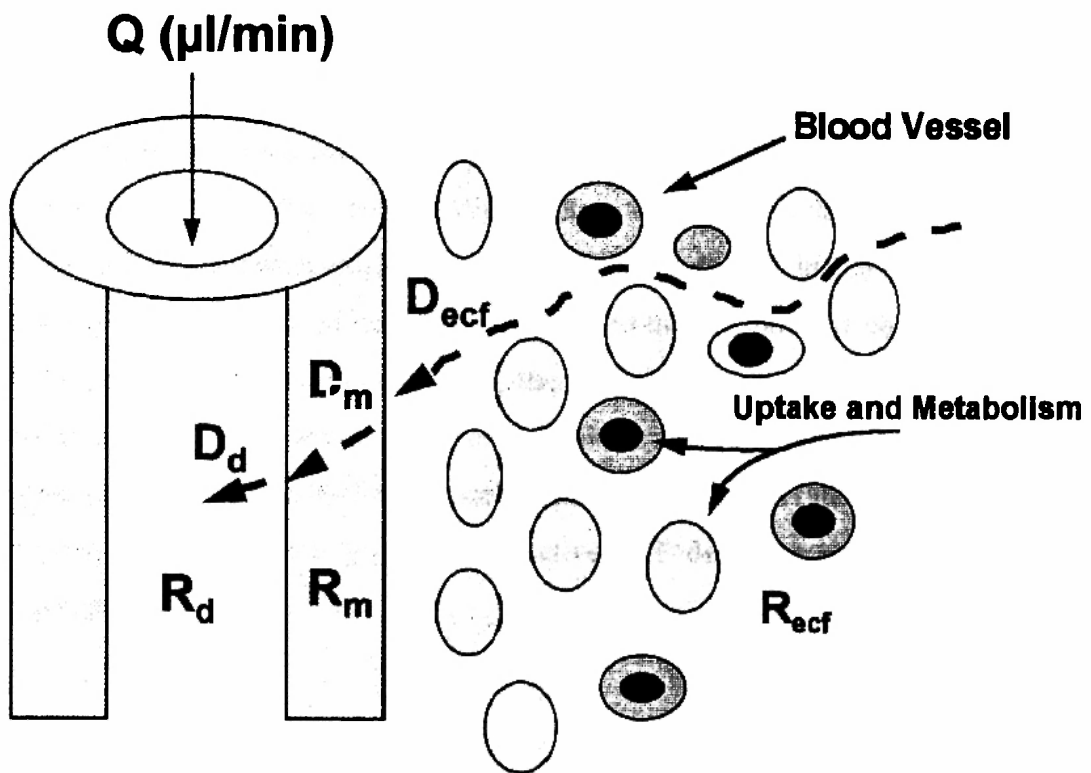


Figure 3. Conceptual view of microdialysis transport resistances based on diffusion.

transfer resistance provided by each of these spaces can be better understood by considering each space as a resistance placed in a series configuration. In this case, the resistance is in series because the effects of each of the spaces is additive and the amount of substance that passes through is a function of these additive resistances: the resistance by the tissue ECF space, R_{ecf} , the resistance given by the membrane, R_m , and the resistance given by the dialysate, R_d .

1.2.3.1 Tissue Resistance

In the tissue space, the analyte undergoes a tortuous path around cells and blood vessels to reach the dialysis fiber membrane. This tortuous path increases the distance that the molecule must diffuse and thus reduces the diffusion coefficient through the use of a tortuosity factor that accounts for the increased path length. In brain tissue, this factor is usually considered to have a value of about 1.5 to 1.6 and differs between the various regions in the brain [Nicholson and Phillips, 1981]. The diffusion coefficient that is used to describe transport through the tissue space is generally the aqueous diffusion coefficient at 37°, D_{aq} divided by the square of a tortuosity factor, λ , thus giving an effective ECF diffusion coefficient described in Equation 1:

$$D_{ECF} = \frac{D_{AQ}}{\lambda^2} \quad (1)$$

Iontophoretic injections of inert anions to produce a point source of substance away from an ion-selective electrode in order to determine the tortuosity of different brain regions has been reported [Nicholson, 1993]. This work verified Equation 1 for the use of these inert substances. For dopamine, a cation, use of Equation 1 to describe its *in vivo* diffusion coefficient was found to be incorrect. The *in vivo* diffusion coefficient for dopamine was found to be an order of magnitude lower than other

anionic or neutral compounds of similar molecular weight and structure [Rice et al., 1985]. It was suggested that the glycoaminoglycan content in tissue has a hindering effect on the *in vivo* diffusion coefficient of dopamine. This indicates that caution should be used when applying *in vitro* diffusion measurements to *in vivo* situations.

The tissue resistance is a combination of the diffusion coefficient of the analyte in the ECF space, the volume fraction through which the analyte can pass, and the uptake and metabolism constants that may affect the concentration of the analyte. These uptake processes include capillary permeation into the local vascular space or reuptake of neurotransmitters in the brain. In general, it is assumed by most researchers in the microdialysis field that the major resistance to mass transport is provided by the lower tissue diffusion coefficients of substances. However, situations in which the kinetics of transport or metabolism in the tissue space are very rapid could alter this scenario such that the membrane resistance and the ECF resistance approach each other in their effects on regulating the mass transport to the inner fiber lumen. It is known from the mass transport literature that kinetic processes coupled with diffusion can influence the rate of mass transport tremendously [Cussler, 1984]. This problem will be further discussed in Chapter 3.

1.2.3.2 Membrane Resistance

From the perspective of the recovery experiment, after the molecule of interest has passed through the tissue space, it must pass through the dialysis membrane in order to be collected by the perfusion fluid. The dialysis membrane resistance is caused by the thickness and length of the membrane as well as the diffusivity of the analyte through the membrane. The most common membranes used in microdialysis include a proprietary polycarbonate membrane used by CMA/Microdialysis in their commercially available microdialysis probes, cellulose acetate, cuprophan, and polyacrylonitrile (PAN). These membranes have different chemical structures and

variations in molecular weight cutoff. Charged small molecules seem to interact in different ways with each of these membranes despite having molecular weights far below the molecular weight cutoffs of these membranes. For instance, acetaminophen glucuronide (MW 350) is poorly extracted by PAN membranes despite the 29,000 molecular weight cutoff designated to the PAN membrane. This is because PAN carries a negative charge due to the cyano groups; thus, hindered diffusion of polar or charged species could be expected with this membrane. This change in the diffusion rate from interaction with the membrane will result in an increased resistance due to the decrease in the value of the diffusivity.

The membrane surface area and length are also known to influence the recovery [Johnson and Justice, 1983]. Since transport through the membrane is diffusion controlled, it is reasonable to expect the recovery to change as a function of the surface area of the probe as the total flux into the probe is dependent upon the surface area. Further work on the role of the membrane in microdialysis will be presented in Chapter 2 of this dissertation.

1.2.3.3 Dialysis Resistance

The mass transfer resistance in the dialysate is due to the diffusion coefficient of the analyte in the perfusion fluid in the dialysis fiber lumen and to some extent the perfusion flow rate of the perfusion fluid. This resistance will be the least contributing factor to the overall resistance to mass transfer in either a recovery experiment or a delivery experiment. This is because the diffusion coefficient of any analyte in the aqueous perfusion fluid will be greater than in the membrane or the tissue because there will be no tortuosity or volume fraction effects in the dialysate. Higher flows of the perfusion fluid will create a greater sink in the dialysis fiber lumen, due to the formation of a thinner static fluid layer, thus preventing the possibilities of back-diffusion. An exception to the role of the dialysate resistance

would be when the combination of membrane surface area and perfusion flow rate allow for 100 percent recovery or delivery of the analyte. In the recovery case, this would indicate an equilibrium has occurred, whereas in the delivery case it would indicate that the tissue has the ability to efficiently extract the analyte from the dialysis probe. In the 100 percent recovery case, it would be difficult to ascertain which particular kinetic rate in the tissue would most affect the dialysis experiment. For studies in which a perturbation is made to the tissue space, it is necessary to use flow conditions in which an observed change in the relative recovery can be assured.

1.3 Controllable Conditions in the Microdialysis Experiment

Microdialysis experiments are performed to help answer questions about specific molecules. The basic properties of the specific molecule such as its *in vitro* and *in vivo* diffusivity and its uptake cannot be altered by the researcher. The choice of the membrane that can be used for the microdialysis probe may be limited to that used by a commercial manufacturer's probe. Given this, the diffusion properties of the molecule and its interactions with the membrane are also fixed. The researcher can vary the flow rate of the perfusion fluid or the length of the dialysis membrane. It may be possible to vary the kinetic properties of the tissue through pharmacological means such as the use of uptake inhibitors for the neurotransmitter dopamine.

1.4 Microdialysis Applications

Microdialysis has become a standard technique in the field of neuroscience and has been used in blood-brain barrier studies, [de Lange et al., 1995] neurotransmitter and neuropeptide sampling [Robinson and Justice, 1991]. Microdialysis sampling strategies have also been developed for sampling from the extracellular fluid (ECF) matrix of other tissues such as the skin [Ault et al., 1992, 1994], liver [Scott et al., 1990, 1993], kidney, heart [Van Wylen et al., 1993], muscle [Deguchi et al., 1991], and solid tumors [Palsmeier and Lunte, 1994a, 1994b]. Microdialysis sampling has

been used in humans [Stähle et al., 1991c, Lonroth et al., 1987, Bolinder et al., 1989] and has been approved for use in humans for determining levels of glucose in diabetics in Sweden. Microdialysis sampling has not only been used to gain information about the concentration of a substance in the ECF space of a tissue, but it has also been used to sample and obtain pharmacokinetic information from the blood [Stähle, 1993] and tissue of an animal [Lunte et al., 1991, Wong 1993]. The technique has also found extensive promise in drug distribution studies [Stähle et al., 1991a, 1991b, Ljungdahl-Stähle et al., 1992, Van Belle et al., 1995]. It is important to reiterate that microdialysis samples substances that have passed into the ECF space and not those in the intracellular space (ICF). However, microdialysis has tremendous promise as a sampling technique because it allows sampling of organs in their native environment which preserves the organ integrity and allows the animal to serve as its own control. Even though microdialysis sampling does allow sampling from an intact organ it is also important to note that the insertion of the microdialysis probe does cause some initial damage to the tissue.

1.5 Calibration Methods and Issues

In the neurosciences, microdialysis is often used to monitor events that can be reported in terms of percent variation from a control value. In these cases, the issue of *in vivo* calibration of the microdialysis probe is often avoided. It is assumed in these cases that the recovery remains constant despite a pharmacological challenge. However, if it is desired to quantitate the local concentration of a substance in the tissue space, then it becomes necessary to calibrate the microdialysis probe. The calibration methods used only obtain a value of the concentration of substances in the tissue space and do not aid in the understanding of the processes that can affect microdialysis transport. The initial use of models was to apply a mathematical function to *in vitro* calibration data and thus arrive at a predicted value of the local tissue concentration [Benveniste and Hüttemeier, 1990]. Kehr has extensively

reviewed these calibration techniques, the various models used in microdialysis, and their utility [Kehr, 1993]. Since this thesis is not focused upon calibration, but rather parameters that affect microdialysis, only a brief review of calibration methods will be provided for readers not familiar with these techniques in microdialysis.

1.5.1 *In vitro* Calibrations

An initial method for calibration involved placement of the dialysis probe in a standard solution as a way of characterizing the membrane [Ungerstedt et al., 1982]. For brain tissue it has been shown that an *in vitro* calibration does not correlate well to the results obtained *in vivo* for various neurotransmitters and exogenous substances [Hsiao et al., 1990]. This method serves to correct for probe to probe differences in membrane length or heterogeneity in the membrane fiber [Johnson and Justice, 1983].

1.5.2 Mass Transfer Coefficient Determinations

Jacobson et al. presented an early *in vivo* calibration method based on mass transport in kidney dialysis and incorporated the use of mass transfer resistances [Jacobson et al. 1985]. The perfusion rate, Q , was varied to obtain an effective mass transfer coefficient, K , for the tissue and membrane as shown in Equation 2, where C is the concentration of the analyte in the dialysate, C_o is the concentration of the analyte in the tissue space and A is the surface area of the dialysis membrane.

$$C/C_o = 1 - e^{(-KA/Q)} \quad (2)$$

A difficulty with this approach as with most of the *in vivo* calibration methods is that the method does not include any terms to describe the underlying physiology outside the microdialysis membrane. This was observed by Jacobson et al. as the

variation of the mass transfer coefficient changes for various amino acids in the brain.

As an extension of Jacobson's work, Menacherry et al. presented the idea of using a low perfusion flow, which is limited by analytical considerations such as low sample volume, long collection times due to the 60 nl/min flow rate, and possible evaporation of the sample [Menacherry et al., 1992]. In this case the extraction efficiency or the recovery of the membrane approaches 100 percent and thus the concentration of the analyte in the dialysate is approximately that in the outside sample space.

1.5.3 No-net Flux Determinations

The no-net flux method attributed to Lönnroth [Lönnroth et al., 1987] and mathematically described by Stähle et al. [Stähle et al. 1991d] is a straight-forward method for determining an *in vivo* concentration and the *in vivo* recovery. This method requires that a steady-state of the analyte exists in the tissue space. Additionally, this method is based upon the assumption that mass transport processes in a microdialysis experiment are bi-directional. That is, that the flux of an analyte to and from the dialysis probe remains equal under the experimental conditions employed.

The no-net-flux experiment involves perfusing the site or fluid of interest with varying concentrations of the analyte of interest. These concentrations should be above and below the expected ECF concentration. The difference between the outlet and inlet concentrations of the dialysate is plotted as a function of the inlet concentration of the dialysate. The x-intercept of the regressed line is considered the true concentration of the analyte in the sample space. The slope of the line is the recovery of the analyte of interest. An example of this particular method is depicted in Figure 4. This method has now become the most frequently used and "validated"

method for determining the ECF concentration of an analyte of interest particularly in the brain [Justice, 1993]. If a steady-state is not achieved or the transport of the analyte of interest is not bi-directional, then a poorly regressed line would be expected.

1.5.4 Internal Standards

Using the same assumption that the flux of molecules is the same bi-directionally, the internal standards approach attempts to perform an *in vivo* calibration with a calibrator other than the analyte species under investigation. These methods are assumed to correct for possible tissue differences in the probe or tissue space. Various internal standards that have been presented include $^3\text{H}_2\text{O}$, [Larsson, 1991] antipyrine, [Yokel et al., 1991], AZT analogs [Wang et al., 1993], and various nucleosides [Stähle, 1994]. Although this technique may be useful for determining changes in the surrounding tissue space, it still does not address the fundamental rate processes that can affect the flux of a substance to the microdialysis probe. Additionally, questions still arise as to whether or not the calibrator interferes with any of the processes *in vivo* and thus inadvertently affects the results. For example, erroneous results may be possible with an internal standard that may bind or interact with the same transport protein that the studied analyte drug interacts with. To date, it seems as if every internal standard must be experimentally verified prior to use.

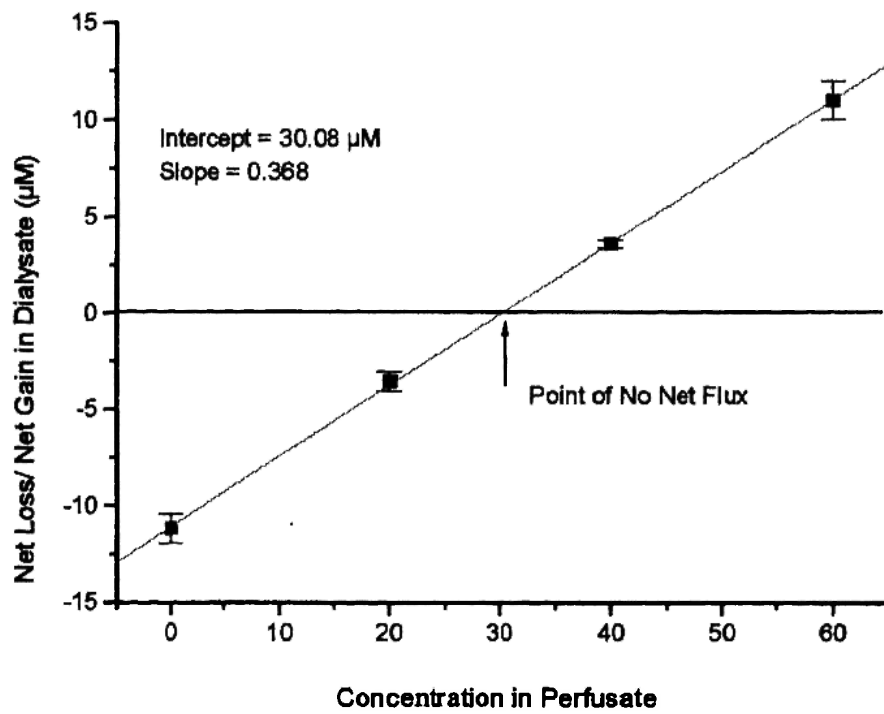


Figure 4. Lonnroth plot. Simulated data points are plotted here to illustrate this method of calibration.

1.6 Predictive Modeling in Microdialysis

1.6.1 Introduction to Mathematical Model Building

A mathematical model is a simplified construct that describes a part of reality by using mathematical symbols and is created for a specific purpose. There exist many reasons for creating mathematical models. Models can be used to predict certain outcomes of events that may be expensive or impractical to determine through experimentation. Models can also be used to aid the understanding of a particular process.

Model building is a cyclical process that first begins with the formulation of a problem, which describes the information that is sought by the model creator. The next step involves outlining the model. This involves the determination of the input or independent variables, the output or dependent variables, and the variables or events that will be considered not to affect the model or that are too difficult to model. The third step involves deciding if the model is useful. In this case, it must be decided if the needed data for the model are available to make the predictions desired. Finally the model is tested against data or by using common sense. These steps can then be repeated if the data and the model do not agree or if the model creator wishes to incorporate some of the neglected variables back into the model. Further information on the model building process can be found in various textbooks [Bender, 1978, Box et al., 1978 and Rubinstein and Firstenberg, 1995].

1.6.1 Microdialysis Diffusion-based Models

Benveniste first reported the use of a mechanistic model which incorporated the effects of volume fraction and tortuosity differences on the diffusion properties of substances in the tissue space for microdialysis experiments [Benveniste, 1989]. The goal of her mathematical model was to be able to use the model in conjunction with *in vitro* recovery experiments to determine the concentration of substances in the brain

extracellular fluid space. She also presented in her review of brain microdialysis processes that can affect microdialysis sampling such as: substance interaction with the dialysis membrane, temperature, membrane surface area, composition of perfusion fluid, and drainage [Benveniste and Hüttemeier, 1990].

In her development of a descriptive model for use in determining the recovery of a substance, Benveniste starts with the general equation to describe flux. This is important as it is the flux to the probe or away from the probe that will affect the extraction fraction of a substance from the tissue or the dialysis probe. Benveniste considered a diffusion only approach for substances to be transported between the interstitial space and the microdialysis probe. This was done only because it was claimed that a solution to the problem utilizing the uptake rate constants would be too difficult to solve, not because she did not understand the role of the microenvironment in which the dialysis probe resided. Using Fick's Law for a steady state concentration versus time profile, the flux to the microdialysis probe in tissue is described as:

$$J = -\phi_{\text{ecf}} \frac{D}{\lambda^2} \frac{dC}{dr} \quad (3)$$

where ϕ_{ecf} describes the volume fraction of fluid in the ECF through which a molecule can diffuse and λ is the tortuosity factor that describes the increased diffusion pathway *in vivo* due to the presence of cells and their impermeable membranes. It was assumed that the value of the volume fraction of the ECF space was about 0.2 and the tortuosity was 1.5 [Nicholson and Phillips, 1981]. The combination of the diffusion coefficient, the tortuosity coefficient and the volume fraction of the tissue ECF space gives an effective diffusion coefficient of a molecule through the ECF space. Equation 3 was solved and the results of the flux with those from an *in vitro* recovery experiment are used to determine the concentration of the substance in the ECF. One

limitation of this model is that the parameters such as the volume fraction, diffusion coefficient *in vivo* and the tortuosity factor need to be determined for each individual substance. However the true physiological diffusion coefficients for many substances found in the brain have not been determined and are estimated from *in vitro* values at 37° C. Benveniste's final solution which relates the dialysate outflow, C_o to the concentration in the interstitial fluid, C_i is shown in Equation 4.

$$C_i = [K\lambda^2 / \phi_{ecf}] \frac{C_o}{\text{Recovery}_{in vitro}} \quad (4)$$

K is a factor used to describe the differences between dialysis experiments performed *in vitro* and *in vivo*. K is assumed to be the same for all substances studied in the brain [Benveniste, 1989] and has a value of 0.7.

Amberg and Lindfors [Amberg and Lindfors, 1989; Lindfors, et al. 1989] presented a more complete and complicated mathematical model to describe the microdialysis process in brain. Although this model did not include transport processes that may occur in the tissue, it did provide the reader with various important points to consider. Their work allowed for readers to understand some of the finer points in microdialysis including: 1) the idea that the recovery of a substance actually reaches a pseudo-steady state with time, 2) the relative distance that is affected by the microdialysis probe as a function of time and 3) the possibility of membrane interactions with molecules being dialyzed. The severe limitation of their work is in the presentation of the complex mathematics to solve for a concentration of a substance in the ECF space. The mathematics presented become a hinderance to understanding their work for many researchers utilizing microdialysis.

1.6.2 Methods Based on Diffusive and Kinetic Processes

It is known from the chemical engineering mass transport literature that kinetic processes coupled with diffusion can greatly affect flux [Cussler, 1984]. Since the recovery of an analyte is a function of the flux of that analyte to and from the microdialysis probe, it makes sense that the role of kinetic processes should be included in a mechanistic model that would describe microdialysis. Although the modeling work presented by Benveniste, Amberg and Lindefors has advanced the understanding of the role of diffusion in microdialysis, their models did not incorporate the role of tissue reactions such as uptake and metabolism. Bungay et al. presented an improved model of the transport processes that affect the microdialysis experiment at steady state in the brain [Bungay et al., 1990]. This improved model included linear terms for transport into and out of the microvasculature, uptake into and out of cells, and metabolism. This model predicted the recovery or delivery of a substance as well as the substance's concentration profile away from the microdialysis probe. At steady-state, the extraction fraction, which is a generalized term that describes the recovery or delivery ratios, can be obtained by using Equation 5.

$$E_d = 1 - \exp\left(-\frac{1}{Q_d(R_d + R_m + R_e)}\right) \quad (5)$$

The extraction fraction, E_d is a function of the dialysis volumetric flow rate, Q_d and the independent resistances of the dialysate, membrane and extracellular fluid space denoted by R_d , R_m and R_e . The formulas for the resistances are given by Bungay.

The model of Bungay et al. has been further extended for use in transient situations in the brain by Morrison et al. [Morrison et al., 1991a, 1991b]. The same assumptions used in Bungay's model apply to Morrison's work. A complex analytical solution is obtained that must be evaluated numerically. The equations obtained are

not printed here because they will not aid in the understanding of microdialysis models. Interested readers are referred to Morrison's work for further details.

The model of Morrison et al. may not be useful for use with microdialysis sampling in other tissues as it is currently formulated for several reasons. The first is an assumption which requires all kinetic processes to be linear. This assumption is necessary in order to achieve an analytical solution to the mass-balance equations. An analytical solution was desired by Morrison et al. so that the general microdialysis community could gain an understanding of the complex role that various parameters play in determining the recovery of an analyte. Because this assumption is used, substances which undergo active transport or have metabolism which is saturable under Michaelis-Menten kinetics cannot be solved using Morrison's model. However, an approximation of the effects of saturable metabolism could be obtained through the use of limiting cases of the Michaelis-Menten kinetics in the model. The linear kinetic assumption and the numerical integration that is used to evaluate the analytical solution, limit the model's use to compounds with recoveries under 70 percent. However, this is a reasonably safe assumption because recoveries would only exceed 70 percent in the brain at very low flow rates (less than 0.5 $\mu\text{l}/\text{min}$). Another assumption incorporates the membrane and dialysis systems into the overall solution because it is assumed that the resistance to mass transport in the brain ECF is the greatest. These assumptions have not been validated for other tissue systems because the work of Morrison has only been applied to brain, where the transport of most substances to and from the microdialysis probe is believed to be relatively slow in the tissue as compared to the membrane and dialysate. In particular, the theory of Bungay predicts that as the overall sum of the transport and metabolic rate constants increases, the resistance in the ECF to mass transport decreases. The microvasculature permeability rate constant is relatively small in brain compared to other tissues because of the blood-brain barrier. In other tissues such as the liver, skin, or solid

tumors it is expected that the microvasculature permeability will be larger. As the rates of the kinetic and metabolic processes increase, the tissue resistance will decrease and it is possible that the membrane and the tissue ECF resistances will approach each other. This indicates that the assumptions of collapsing the membrane and dialysate resistance into the solution of the concentration profile in the ECF may not be valid for other tissues such as the skin or liver where there is no barrier to drug permeation or cases in which the kinetic rate processes are rapid as in dopamine re-uptake processes [Smith and Justice, 1994].

The same research group that developed Morrison's model also developed experiments to validate that model. This was performed by locally delivering sucrose [Dykstra et al., 1992] and AZT in the brain [Dykstra et al., 1993] over various time periods. The experimental results of the amount of substance lost from the local delivery and the concentration profile of these substances in the tissue space determined by quantitative autoradiography were compared to the model predictions. In both of these validation papers, the data fit the model predictions once the value of the volume fraction of the ECF space was adjusted from a value of 0.2 to 0.4. This adjustment was made because it was shown that edema had affected the microenvironment around the probe.

The work by Dykstra et al. illustrates one of the difficulties of validation of microdialysis modeling. That is, there are only two dependent variables that are used in the model, the value of the concentration of the substance in the dialysate and the concentration profile away from the dialysis probe. This makes model testing difficult as the concentration profile away from the probe can only be verified through imaging methods such as autoradiography or possibly fluorescence imaging. Additionally the input variables such as the diffusion coefficient and kinetic rate constants for a

compound that is being modeled are fixed and cannot be varied to stress the model.

Microdialysis sampling in combination with a mathematical model is just beginning to be used to determine transport parameters in the brain as illustrated in Morrison and Dykstra's work. Microdialysis modeling has not been applied to tissues such as the liver or skin. There has been a recent adaptation of Bungay's model by Wallgren et al. [Wallgren et al., 1995] to determine the local blood flow in muscle from the infusion of ethanol through the microdialysis probe. This model was tested using data obtained from isolated muscle tissue. This model is a modification of the work of Bungay et al. and has included a more comprehensive mathematical description of the flow of the dialysis perfusion fluid, which does not improve the model of Bungay. This is because the most uncertain factor in the model was the diffusivity of ethanol in the muscle.

With an extended and general model, microdialysis could be used in attempts to determine transport and rate constants in these tissues. However, metabolism and transport processes in these systems are more complex and will require a more complex model that takes into account all three systems through which mass transport occurs, i.e., the tissue ECF, the membrane, and the dialysate. While the new model will be more complicated to solve, it will be applied for more general use in organs such as the skin or liver. In these organs, metabolism and transport across the capillaries is expected to occur at a faster rate than in the brain, thus reducing the resistance to mass transport in the tissue space and making the membrane and dialysate more limiting to mass transfer.

1.7 Use of Microdialysis Mathematical Models for Use in Tissues Other than Brain

As mentioned above, microdialysis has become a standard technique for use in sampling from the extracellular fluid of the brain. Extensive fundamental work by

Professor Urban Ungerstedt's group at the Karolinska Institute in Stockholm, Drs. Paul Morrison and Peter Bungay at NIH, and Professor J. Justice's group at Emory University have provided the microdialysis community a greater understanding of the many factors that influence microdialysis sampling *in vivo* in brain tissue as well as the potential uses of microdialysis. The fundamental work that has been used for brain microdialysis can be applied to microdialysis sampling in other tissues.

An exciting use of microdialysis sampling coupled with a mathematical model would be the estimation of uptake and metabolic rates in the area of liver metabolism research. The liver is a highly complex organ and most experimental work that has focused upon liver research has been *in vitro*. *In vitro* studies of liver processes generally include: 1) microsomal studies to determine the role of the various cytochrome P450 isozyme's metabolism, 2) hepatocytes to determine the roles of other enzymes or 3) liver perfusion studies to determine the uptake of various compounds [Blom et al., 1982, Snell and Mullock, 1987].

Microsomes are prepared by isolation of the subcellular endoplasmic reticulum of the hepatocyte [Snell and Mullock, 1987]. Microsomal fractions of liver are advantageous because these subcellular fractions contain principally the cytochrome P450 mixed function oxidases and the UDP-glucuronyltransferases. The enzymes in these fractions can be induced and inhibited. Microsomal fractions have proven to be useful in testing the metabolism of *in vivo* marker compounds such as antipyrine and theophylline [Matthew, 1990a, 1990b]. Our present-day fundamental understanding of drug metabolism comes from work that has incorporated microsomes.

The next step in complexity in drug metabolism utilizes the isolated hepatocyte in drug uptake, transport and metabolism studies [Cheney, 1988]. Here the isolated cell keeps the integrity of both the membrane bound enzymes such as the Cytochrome

P450's and the cytosolic enzymes such as the sulfotransferases. Utilization of isolated rat hepatocytes has the advantage that the heterogeneity normally found in the intact liver is disrupted. This allows a comparison of metabolite kinetics to be made with the intact perfused liver [Pang et al., 1985].

Perhaps the most widely used technique to study the liver is that of liver perfusion [Bartosek et al., 1973]. This technique has been used widely to determine the rates at which substances are taken up by the liver [Goresky and Schwab, 1988], and the rates of metabolism of substances through the perfused liver. Without this technique, an understanding of basic hepatic pharmacology in the intact liver would have been difficult to obtain [Bass and Keiding, 1988].

There are few methods available to study the fate of drugs and other compounds *in vivo* in rat. Micro-light guides have been used to determine the fluorescence of NADH in the liver [Lemasters, 1986] and the metabolism of other fluorescent substances [Conway et al., 1982, 1984]. The utility of this technique is quite limited as it is only useful for drugs or compounds which fluoresce. There has been one paper that describes a method for collecting bile in an awake and freely moving rat [Kanz, 1992].

The present tools used to study drug metabolism and pharmacology in the liver will continue to be used, however, microdialysis can serve as an additional tool to study the liver *in vivo*. The rest of this dissertation focuses on some of the important processes that need to be considered when using microdialysis in tissues other than brain. The development of mathematical methods to describe and model the microdialysis experiment will provide understanding into the roles that the various mass transfer resistances provide in liver and brain. The development of the model

is discussed in chapter three and examples of the model used with experiments in liver and brain are presented in chapters four and five.

1.8 References

Amberg, G.; Lindfors, N. Intracerebral Microdialysis: II. Mathematical studies of diffusion kinetics. *J. Pharmacol. Methods*. 1989, 22, 157-183.

Ault, J.M.; Lunte, C.E.; Meltzer, N.M.; Riley, C.M. Microdialysis sampling for the investigation of dermal drug transport. *Pharm. Res.* 1992, 9, 1256-1261.

Ault, J.M.; Riley, C.M.; Meltzer, N.M.; Lunte, C.E. Dermal microdialysis sampling *in vivo*. *Pharm. Res.* 1994, 11, 1631-1639.

Bartosek, I.; Guaitani, A.; Miller, L.L. *Isolated liver perfusion and its applications*. Raven Press: New York, 1973.

Bass, L.; Keiding, S. Physiological based models and strategic experiments in hepatic pharmacology. *Biochem. Pharmacol.* 1988, 37, 1425-1431.

Bender E. A. *An introduction to mathematical modeling*. John Wiley & Sons: New York, 1978.

Benveniste, H. Brain microdialysis. *J. Neurochem.* 1989, 52, 1667-1679.

Benveniste, H.; Hüttemeier, C. Microdialysis-Theory and Application. *Prog Neurobiol.* 1990, 35, 195-215.

Bito, L.; Davson, H.; Levin, E.; Murray, M.; Snider, N. The concentrations of free amino acids and other electrolytes in cerebrospinal fluid. *In vivo* dialysate of brain and the blood plasma of the dog. *J. Neurochem.* 1966, 13, 1057-1067.

Blom, A.; Scaf, A. H. J.; Meijer, D. K. F. Hepatic drug transport in the rat: A comparison between isolated hepatocytes, the isolated perfused liver and the liver *in vivo*. *Biochem. Pharmacol.* 1982, 31, 1553-1565.

Bolinder, J.; Hagström, E.; Ungerstedt, U.; Arner, P. Microdialysis of subcutaneous adipose tissue *in vivo* for continuous glucose monitoring in man. *Scand. J. Clin. Lab. Invest.* 1989, 49, 465-474.

Box, G.E.P.; Hunter, W.G.; Hunter, J.S. *Statistics for Experimenters: An Introduction to Design, Data Analysis, and Model Building*, John Wiley & Sons: New York, 1978.

Bungay, P.M.; Morrison, P.F.; Dedrick, R.L. Steady-state theory for quantitative microdialysis of solutes and water *in vivo* and *in vitro*. *Life Sci.* **1990**, *46*, 105-119.

Cheney, R.J.; The utility of hepatocytes in drug metabolism studies. In *Progress in Drug Metabolism, Vol. 11*, G.G. Gibson, ed. 1988, 217-265.

Conway J.G.; Kauffman F.C.; Thurman, R. G. Rates of sulfation and glucuronidation of 7-hydroxycoumarin in periportal and pericentral regions of the liver lobule. *Mol. Pharmacol.* **1982**, *22*, 509-516.

Conway J.G.; Kauffman F.C.; Tsukada T.; Thurman R.G. Glucuronidation of 7-hydroxycoumarin in periportal and pericentral regions of the liver lobule. *Mol. Pharmacol.* **1984**, *25*, 487-493.

Cussler, E.L. *Diffusion: Mass Transport in Fluid Systems*. Cambridge University Press: Cambridge, 1984, pp. 346-377.

Deguchi, Y.; Terasaki, T.; Kawasaki, S.; Tsuji, A. Muscle microdialysis as a model study to relate the drug concentration in tissue interstitial fluid and dialysate. *J. Pharmacobio-Dyn*, **1991**, *14*, 483-492.

de Lange, E.C.M.; Hesselink, M.B.; Danhof, M.; de Boer, A.G.; Breimer, D.D. The use of intracerebral microdialysis to determine changes in blood-brain barrier transport characteristics. *Pharm Res.* **1995**, *12*, 129-133.

Dykstra, K.H.; Hsiao, J.K.; Morrison, P.F.; Bungay, P.M.; Mefford, I.N.; Scully, M.M.; Dedrick, R.L. Quantitative examination of tissue concentration profiles associated with microdialysis. *J. Neurochem.* **1992**, *58*, 931-940.

Dykstra, K.H.; Arya, A.; Arriola, D.M.; Bungay, P.M.; Morrison, P.F.; Dedrick, R.L. Microdialysis study of zidovudine (AZT) transport in rat brain. *J. Pharmacol. Exp. Ther.* **1993**, *267*, 1227-1236.

Goresky, C.A.; Schwab, A.J. Flow, cell entry, and metabolic disposal: Their interactions in hepatic uptake. in I.M. Arias, W.B. Jakoby, H. Popper, D. Schachter and D.A. Shafritz, eds. *The Liver: Biology and Pathobiology, Second edition*. Raven press: New York, 1988, 807-831.

Hsiao, J.K.; Ball, B.A.; Morrison, P.F.; Mefford, I.N.; Bungay, P.M. Effects of different semi-permeable membranes on in vitro and in vivo performance of microdialysis probes. *J. Neurochem.* 1990, 54, 1449-1452.

Jacobson, I.; Sandberg, M.; Hamberger, A. Mass transfer in brain dialysis devices - a new method for the estimation of extracellular amino acids concentration. *J. Neurosci. Meth.* 1985, 15, 263-268.

Johnson, R.D.; Justice, J.B. Model studies for brain dialysis. *Brain Res. Bull.* 1983, 10, 567-571.

Justice, J.B. Jr. Quantitative microdialysis of neurotransmitters. *J. Neurosci. Methods.* 1993, 48, 263-276.

Larsson, C.I. The use of an "internal standard" for control of the recovery in microdialysis. *Life Sciences* 1991, 49, P1-73-P1-75.

Lemasters, J.J.; Sungchul, J.; Thurman, R.G. New micro methods for studying sublobular structure and function in the isolated, perfused rat liver. In *Regulation of Hepatic Metabolism: Intra- and Intercellular Compartmentation*. R.G. Thurman; F.C. Kauffman; K. Jungermann, eds. Plenum Press: New York, 1986. 159-184.

Lindfors, N; Amberg, G.; Ungerstedt, U. Intracerebral microdialysis I: Experimental studies of diffusion kinetics. *J. Pharmacol. Methods* 1989, 22, 141-56.

Ljungdahl-Stähle, E.; Guzenda, E.; Bottiger, D.; Wahren, B.; Öberg, B.; Stähle, L. Penetration of zidovudine and 3'-fluro-3'-deoxythymidine into the brain, muscle tissue and veins in cynomolgus monkeys: Relation to antiviral action. *Antimicrob. Agents Chemother.* 1992, 36, 2418-2422.

Lunte, C.E.; Scott, D.O.; Kissinger, P.T. Sampling living systems using microdialysis probes. *Anal. Chem.* 1991, 63, 773A-780A.

Lönroth, P.; Jansson, P.A.; Smith, U. A microdialysis method allowing characterization of intracellular water space in humans. *Am. J. Physiol.* 1987, 256, E250-E255.

Kanz, M.F.; Whitehead, R.F.; Ferguson, A.E.; Kaphalia, L.; Moslen, M.T. Biliary function studies during multiple time periods in free moving rats: A useful system and set of marker solutes. *J. Pharmacol. Methods* 1992, 27, 7-15.

Kehr, J. A survey on quantitative microdialysis: theoretical models and practical implications. *J. Neurosci. Meth.* **1993**, *48*, 251-261.

Matthew, D.E.; Houston, J.B. Drug metabolizing capacity in vitro and in vivo - I. Correlations between hepatic microsomal monooxygenase markers in β -naphthoflavone-induced rats. *Biochem. Pharmacol.* **1990a**, *40*, 743-749

Matthew, D.E.; Houston, J.B. Drug metabolizing capacity in vitro and in vivo - II. Correlations between hepatic microsomal monooxygenase markers in phenobarbital-induced rats. *Biochem. Pharmacol.* **1990b**, *40*, 751-758.

Menacherry, S.; Hubert, W.; Justice, J.B. In vivo calibration of microdialysis probes for exogenous compounds. *Anal. Chem.* **1992**, *64*, 577-583.

Morrison, P.F.; Bungay, P.M.; Hsiao, J.K.; Ball, B.A.; Mefford, I.N.; Dedrick, R.L. Quantitative microdialysis: Analysis of transients and application to pharmacokinetics in brain. *J. Neurochem.* **1991a**, *57*, 103-119.

Morrison, P.F.; Bungay, P.M.; Hsiao, J.K.; Mefford, I.V.; Dykstra, K.H.; Dedrick, R.L. Quantitative microdialysis. In *Microdialysis in the Neurosciences*. T.E. Robinson and J.B. Justice Jr., eds. Elsevier: Amsterdam, 1991b, 47-80.

Nicholson, C; Phillips, J.M. Ion-diffusion modified by tortuosity and volume fraction in the extracellular environment of rat cerebellum. *J. Physiol. (London)* **1981**, *321*, 225-257.

Nicholson, C. Ion-selective microelectrodes and diffusion measurements as tools to explore the brain cell microenvironment. *J. Neurosci. Meth.* **1993**, *48*, 199-213.

Palsmeier, R.K.; Lunte, C.E. Microdialysis sampling of tumors for the study of the metabolism of antineoplastic agents. *Cancer Bull.* **1994a**, *46*, 58-66.

Palsmeier, R.K.; Lunte, C.E. Microdialysis sampling in tumor and muscle: Study of the disposition of 3-amino-1,2,4-benzotriazine-1,4-di-N-oxide (SR4233). *Life Sci.*, **1994b**, *55*, 815-825.

Pang, K.S.; Kong, P.; Terrell, J.A.; Billings, R.E. Metabolism of acetaminophen and phenacetin by isolated rat hepatocytes: A system in which the spatial organization inherent in the liver is disrupted. *Drug Metab. Dispos.* **1985**, *13*, 42-50.

Rice, M.E.; Gerhardt, G.A.; Hierl, P.M.; Nagy, G.; Adams, R.N. Diffusion coefficients of neurotransmitters and their metabolites in brain extracellular fluid space. *Neuroscience*, 1985, 15, 891-902.

Robinson, T.E.; Justice, J.B. Jr., eds. *Microdialysis in the Neurosciences*. Elsevier: Amsterdam, 1991.

Rubinstein, M.F.; Firstenberg, I.R. *Patterns of Problem Solving, 2nd edition*. Prentice Hall: Englewood Cliffs, New Jersey, 1995.

Scott, D.O.; Sorenson, L.R.; Lunte, C.E. In vivo microdialysis sampling coupled to liquid chromatography for the study of acetaminophen metabolism. *J. Chromatogr.* 1990, 506, 461-469.

Scott, D.O.; Lunte, C.E. In vivo microdialysis sampling in the bile, blood, and liver of rats to study the disposition of phenol. *Pharm. Res.* 1993, 10, 335-342.

Smith A.D.; Justice, J.B. The effect of inhibition of synthesis, release, metabolism and uptake on the microdialysis extraction fraction of dopamine. *J. Neurosci. Methods* 1994, 54, 75-82.

Snell, K.; Mullock, B. *Biochemical Toxicology: A practical approach*. IRL Press: Oxford, 1987.

Stähle, L. Drug distribution studies with microdialysis: I. Tissue dependent difference in recovery between caffeine and theophylline. *Life Sci.* 1991a, 49, 1835-1842.

Stähle, L.; Segersvärd, S.; Ungerstedt, U. Drug distribution studies with microdialysis. II. Caffeine and theophylline in blood, brain, and other tissues in rats. *Life Sci.* 1991b, 49, 1843-1852.

Stähle, L.; Arner, P.; Ungerstedt, U. Drug distribution studies with microdialysis. III: Extracellular concentration of caffeine in adipose tissue in man. *Life Sci.* 1991c, 49, 1853-1858.

Stähle, L., Segersvärd, S., Ungerstedt, U. A comparison between three methods for estimation of extracellular concentrations of exogenous and endogenous compounds by microdialysis. *J. Pharmacol. Methods* 1991d, 25, 41-52.

Stähle, L. Microdialysis in pharmacokinetics. *Eur.J Drug Metab. Pharmacokinet.* 1993, 18, 89-96.

Stähle L. Zidovudine and alovudine as cross-wise recovery internal standards in microdialysis experiments? *J. Pharmacol. Toxicol. Meth.* **1994**, *31*, 167-169.

Van Belle, K.; Sarre, S.; Ebinger, G.; Michotte, Y. Brain, liver, and blood distribution kinetics of carbamazepine and its metabolic interaction with clomipramine in rats: A quantitative microdialysis study. *J. Pharmacol Exp. Ther.* **1995**, *272*, 1217-1222.

Van Wylen, D.G.L.; Schmit, T.J.; Lasley, R.D.; Gingell, R.L.; Mentzer, R.M. Cardiac microdialysis in isolated rat hearts - interstitial purine metabolites during ischemia. *Am. J. Physiol.* **1992**, *262*, H1934-H1938.

Wallgren, F.; Amberg, G.; Hickner, R.C.; Ekelund, U.; Jorfeldt, L.; Henriksson, J. A mathematical model for measuring blood flow in skeletal muscle with the microdialysis ethanol technique. *J. Appl. Physiology* , **1995** in press.

Wang, Y.F.; Wong, S.L.; Sawchuck, R.J. Microdialysis calibration using retrodialysis and zero-net-flux-application to a study of the distribution of zidovudine to rabbit cerebrospinal fluid and thalamus. *Pharm. Res.* **1993**, *10*, 1411-1419.

Wong, S.L.; van Belle, K.; Sawchuk, R.J. Distributional transport kinetics of zidovudine between plasma and brain extracellular fluid/cerebrospinal fluid in the rabbit: Investigation of the inhibitory effect of probenecid utilizing microdialysis. *J. Pharmacol. Exp. Ther.* **1993**, *264*, 899-909.

Ungerstedt, U.; Herrera-Marschitz, M.; Jungnelius, U.; Stähle, L.; Tossman, U.; Zetterström, U. Dopamine synaptic mechanisms reflected in studies combining behavioural recordings and brain dialysis. In *Advances in Dopamine Research*. Kohsaka, M.; Shohmori, T.; Tsukada, Y.; Woodruff, G.N. eds. Pergamon Press: Oxford, 1982, pp. 219-231.

Yokel, R.A.; Allen, D.D.; Burgio, D.E.; McNamara, P.J. Antipyrine as a dialyzable reference to correct differences in efficiency among and within sampling devices during in vivo microdialysis. *J. Pharmacol. Toxicol. Meth.* **1992**, *27*, 135-142.

Chapter 2

Examination of Recovery Profiles for a Microdialysis System Under Hydrodynamic Conditions.

2.1 Introduction

Chapter 1 described the usefulness of microdialysis for separating larger biomolecules from the tissue extracellular fluid space. This makes the analysts' job easier as there is no sample clean-up necessary prior to analysis. This has allowed the development of on-line sample detection systems for rapid and real time sampling for microdialysis [Church and Justice, 1987, Kehr and Ungerstedt, 1988, Newton and Justice, 1994, Chen and Lunte, 1995]. In addition, to sampling from a tissue space microdialysis has also been used to sample from fluids such as the bile [Scott and Lunte, 1993], blood [Steele et al., 1991] and fermentation broths [Marko-Varga et al., 1993].

Despite the over 2200 papers cited in the literature that use microdialysis, [CMA/Microdialysis, 1994] there have been few fundamental studies describing how the membrane can affect microdialysis sampling. Johnson and Justice presented one of the first fundamental studies on the role of the membrane and studied the effects of the flow rate, length, and geometry on the relative recovery of a dialysis membrane [Johnson and Justice, 1983]. As would be expected from a technique that is based upon the flux of a substance into the membrane, the recovery increased with increased membrane length and decreased perfusion flow rates. Other methodological studies have been performed that have focused on the pressure through the dialysis membrane [Keipers and Korf, 1994] and the diffusion of substances away from the dialysis probe [Ruggeri et al., 1990]. The effects of protein binding on membranes that have been used to sample fermentation broths have been investigated [Buttler et al., 1995]. Since microdialysis sampling is used in various fluids and tissues that may have

limiting effects on the membrane, it seems important to study the behavior of the membrane under controlled fluid flow conditions.

2.1.1 Membrane Terminology

A membrane can be considered to be a selective barrier between two phases. In microdialysis separations, the membrane is a barrier between the inner dialysate perfusion fluid flowing through the inner fiber lumen and the outside sample space. The microdialysis fiber is used to separate large biomolecules from the dialysis perfusion fluid which is similar to kidney dialysis separations. This feature of microdialysis allows the analyst to directly analyze the dialysate solution without any sample clean-up procedures. Typical fibers that are used for microdialysis are Cuprophan, a regenerated cellulose membrane, Cellulose acetate, PAN a polyacrylonitrile membrane, and a proprietary polycarbonate copolymer used for commercially available probes. Many of these fibers are actually asymmetric [Sakei, 1994], which means they are a composite of two polymers consisting of a thin outer skin of approximately 0.5 μm and a thicker supporting porous underlayer of approximately 50-200 μm . This top layer or skin can often determine the transport rate through the membrane rather than the porous underlayer. These fibers also have different values for their molecular weight cutoff, which is a value used to define the retentive properties of the membrane in the kidney dialysis case. These molecular weight cutoff determinations are measured by performing solute rejection measurements [Mulder, 1991]. Cutoff is defined as the molecular weight at which 90 percent of the solute in the sample is rejected by the membrane. Additionally membranes can have what is termed sharp cut-off or diffuse cut-off. An example of these two types of cut-off's is shown in Figure 1. Unfortunately it is not possible to define the characteristics of microdialysis membranes toward a particular analyte based on the molecular weight cutoff. Other factors also control the membrane separation process including fouling, adsorption, the shape of the solute and its

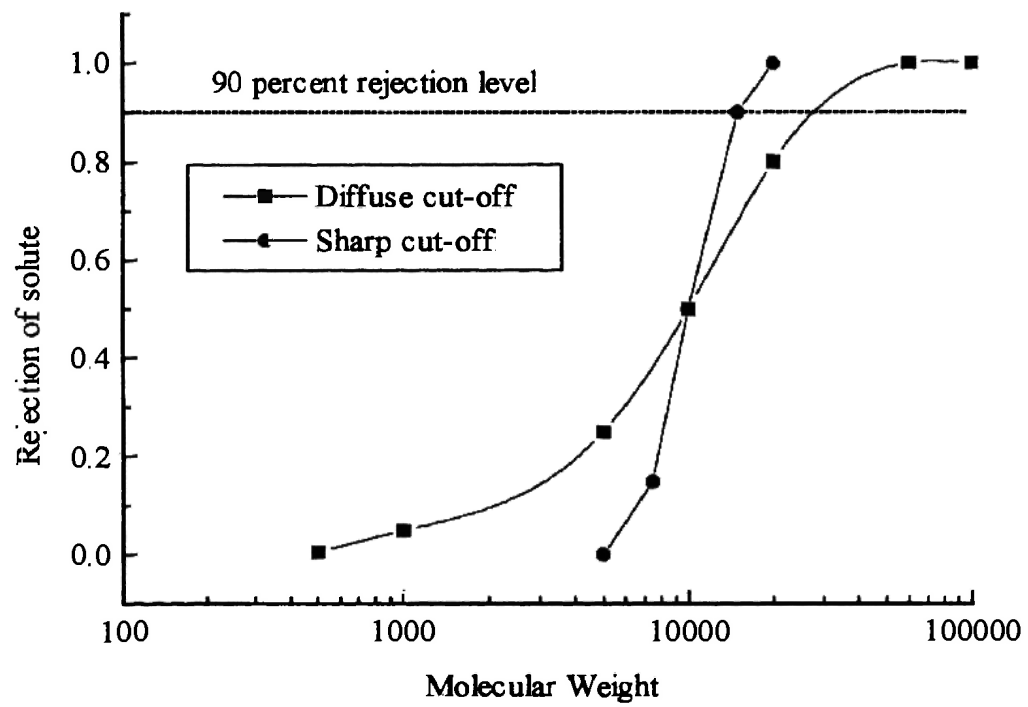


Figure 1. Comparison of membranes with diffuse and sharp cut-offs for solute rejection.

interactions with the membrane (hindered diffusion).

2.1.2 Microdialysis in a Fluid Space

Since microdialysis is used to sample matrices besides brain tissue, such as the blood, bile, and fermentation liquids, it is important to determine how the membrane affects relative recovery in these situations. The recovery and delivery of an analyte in microdialysis is a mass transport controlled process. There are three regions where mass transport occurs in the microdialysis experiment which must be considered: the sample solution, the dialysis membrane, and the dialysate inside the membrane (i.e. the solution inside the fiber lumen). In general it has been suggested that the resistance to mass transport is greatest in the tissue space, with the membrane and dialysis fluid contributing a lesser resistance to the diffusion of an analyte [Hsiao et al., 1990]. Transport in the dialysate is generally considered unimportant relative to other regions when the perfusion rate is greater than $0.25 \mu\text{l}/\text{min}$.

Because the majority of microdialysis applications have focused on the brain, theoretical considerations have focused on this tissue. Recently, microdialysis has been used to sample from hydrodynamic systems such as blood and bile and in highly perfused tissues such as the liver. The effects of external fluid flow on the recovery of analytes through the microdialysis membrane are therefore relevant. In systems which include convective diffusion to the membrane, membrane resistance and any concentration boundary layer formed by fluid flow both on the outside and inside of the membrane will contribute to the recovery as shown in Figure 2. This boundary layer forms in conjunction with the hydrodynamic or Prandtl boundary layer. The Prandtl boundary layer is developed by the frictional drag of the fluid flowing near the membrane. As the Prandtl boundary layer forms, the concentration or diffusion boundary layer, grows in proportion with it. It is the diffusion layer that defines the concentration gradient next to the membrane. In applications involving hydrodynamic

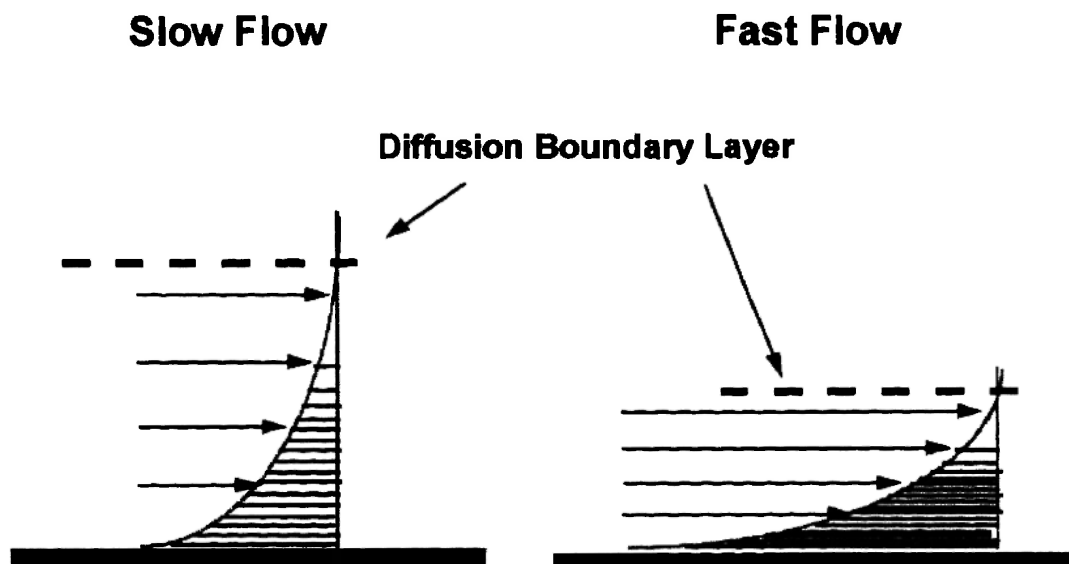


Figure 2. Diffusion boundary layer formation due to fluid flow across a flat plate.

fluids or highly perfused tissues, it would be expected that a diffusion layer forms around the membrane. This diffusion layer dictates the rate of recovery because its thickness defines the concentration gradient to the membrane. This chapter discusses the effect of controlled linear fluid velocity on the relative recovery of the analyte hydroquinone. The results obtained will be described using different theories from the mass transport literature. Hydroquinone was chosen as the initial analyte because its detection is amenable to electrochemical techniques, allowing ready determination of diffusion coefficients in various media by rotating disk voltammetry.

2.2 Materials and Methods

2.2.1 Chemicals

Hydroquinone, caffeine, theophylline, theobromine, and phenacetin were purchased from Sigma (St. Louis, MO). All other chemicals were reagent grade or better. Ringer's solution contains 155 mM NaCl, 5.6 mM KCl and 2.4 mM CaCl₂.

2.2.2 Microdialysis

A combination dialysis fiber-sample flow system was designed for these experiments as shown in Figure 3. Three different dialysis membranes were used in this experiment: PAN (a polyacrylonitrile membrane with a molecular weight cutoff (MWCO) of 29,000) o.d. 340 μm , i.d. 240 μm , Cuprophan (MWCO 12,000) o.d. 222 μm , i.d. 200 μm , and cellulose acetate (MWCO 5,000) o.d. 250 μm , i.d. 232 μm . The PAN and Cuprophan membranes were gifts from Ivan Mefford at NIH and can be currently purchased from CGH Medical Inc. (Lakewood, CO). The cellulose acetate membranes were a gift from Bob Cross at the University of Kansas Medical School and can be purchased from Baxter Health Care (Chicago, IL). Pieces of fused silica (o.d. 147 μm , i.d. 75 μm Polymicro Technologies Incorporated, Phoenix, AZ) approximately 6 cm in length were inserted into each end of the dialysis fiber and

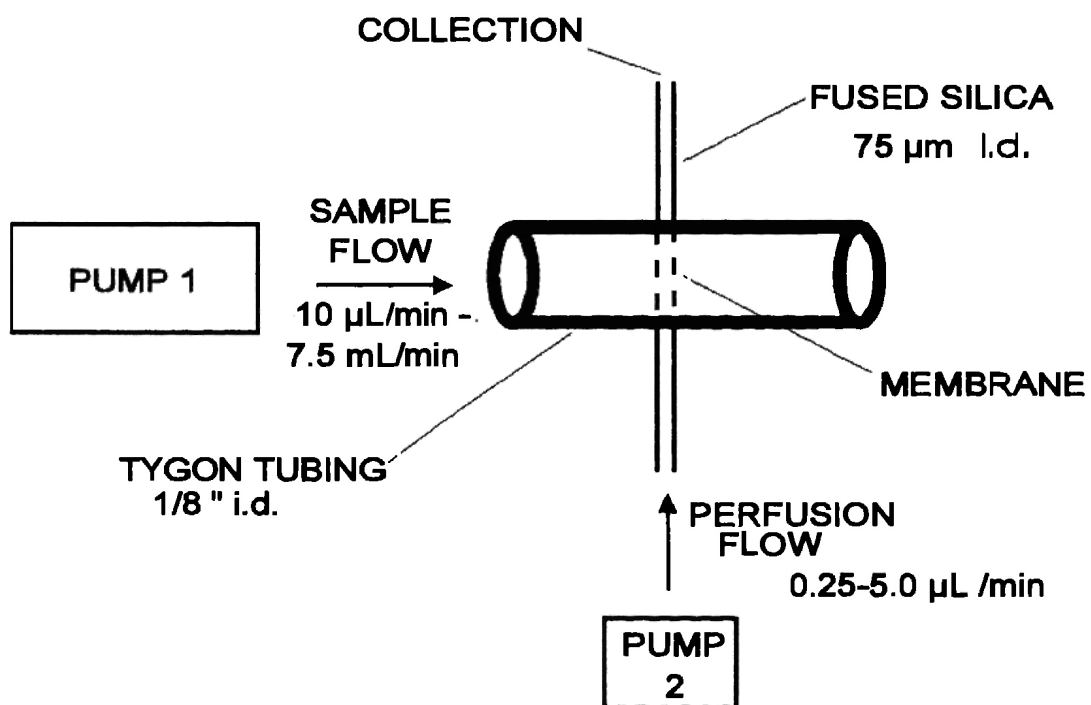


Figure 3. Set-up of microdialysis controlled velocity experiment.

were affixed using UV curable epoxy (UVEXS Inc. Sunnyvale, CA). Connection of one end of the fused silica was made to a syringe needle by slipping a piece of PE-10 tubing (o.d. 610 μm , i.d. 280 μm , Clay Adams, Parsippany, NJ) over the fused silica. A piece of PE-50 tubing (o.d. 965 μm i.d. 580 μm) was inserted over the PE-10 and was glued. With the aid of an 18 gauge needle, the other end of the probe was inserted into a 4 cm piece of Tygon tubing (o.d. 1/4", i.d. 1/8" Fisher Scientific) and positioned such that the dialysis fiber was centered in the tubing.

The flow scheme used in these experiments is shown in Figure 3. A Harvard Apparatus 22 syringe pump (South Natick, MA) was used to pump the analyte across the dialysis membrane. A CMA/100 (CMA/BAS West Lafayette, IN) syringe pump was used to perfuse Ringer's solution through the dialysis fiber. The flow rate of the Harvard pump was adjusted between 10 $\mu\text{l}/\text{min}$ and 5 ml/min to give the desired velocity of the analyte solution. For this experimental arrangement, the Reynolds number (Re) of the sample fluid ranged from 0.7-33.5. The Reynolds number being defined as the product of velocity and a characteristic length (in the case of a cylinder this is the diameter) divided by the kinematic viscosity (0.01 cm^2/s in these experiments). A Reynolds number of less than 2000 is used as indication of laminar flow. The CMA/100 syringe pump was adjusted between 0.25 $\mu\text{l}/\text{min}$ and 5 $\mu\text{l}/\text{min}$. This gives a Re number between 0.02 and 0.4 for the flow through the dialysis fiber. The system was allowed to equilibrate between each change in flow rate for 5 minutes. Samples were collected for 5 minutes at each of the perfusion rates and were diluted with 95 μl of Ringer's solution to prevent evaporation effects. The percent recovery is defined as the ratio of the dialysate concentration to the concentration outside of the dialysis membrane. The sample solution consisted of 150 $\mu\text{g}/\text{ml}$ hydroquinone in Ringer's solution. Three samples were collected at each sample flow rate and perfusion flow rate. For clarity, the flow of solution through the dialysis

fiber will be termed perfusate flow, and the flow of solution around the dialysis fiber will be termed sample flow.

2.2.3 Liquid Chromatographic Analyses

The concentration of the dialysate was determined by LC-EC. An ODS-Hypersil 4.6 mm x 15 cm column (packed in-house) was used to achieve separation. The mobile phase was 0.05 M sodium phosphate buffer, pH 2.5, with 10 % (v/v) acetonitrile. A 20 μ l Rheodyne injection loop was used. The amperometric detector was a BAS LC-4C (BioAnalytical Systems, West Lafayette, IN). A glassy carbon electrode was used at a potential of +800 mV vs. Ag/AgCl. The retention time for hydroquinone under these conditions was 3.4 minutes, and the void volume eluted at 1.7 minutes. The system was calibrated in the range of 0.5 μ g/mL to 75 μ g/mL hydroquinone and was linear within this range.

The methylxanthines were analyzed by using LC with UV detection. The ODS-Hypersil column was used with a mobile phase of 0.05 M sodium phosphate buffer, pH 2.5 with 15% (v/v) acetonitrile. The Shimadzu UV detector was set to 275 nm.

2.2.4 Rotating Disk Electrochemistry

The diffusion coefficient for hydroquinone in the Ringer's solution was determined using a rotating disk electrode (Pine Instruments Co., Grove City, PA). The rotation rate was varied between 200 and 2000 rpm. The potential was scanned between +100 and +900 mV vs. Ag/AgCl. The limiting current was plotted versus the square root of the frequency which gives the familiar Levich plot for determining diffusion coefficients [Bard and Faulkner, 1980]. The diffusion coefficient for hydroquinone was found to be $0.85 \times 10^{-5} \text{ cm}^2/\text{s}$ in Ringer's solution. This agrees with

literature values for hydroquinone in other ionic media [Kolthoff and Orlemann, 1941].

2.2.5 Determination of the Membrane Permeability

The membrane permeability can be determined by using the following equation: (See Appendix 1 for the derivation.)

$$\frac{[C_o - C_{out}]}{C_{out}} = Q \frac{\ln(R_o/R_i)}{2\pi L D_{mem} K} - \ln(R_o/R_i) \quad (1)$$

where C_o is the concentration in the bulk ($\mu\text{g/ml}$), C_{out} is the concentration in the dialysate ($\mu\text{g/ml}$), R_o is the outer radius of the fiber (cm), R_i is the inner radius of the fiber (cm), L is the length of the fiber (cm), D_{mem} is the diffusion coefficient in the membrane (cm^2/s), K is the partition coefficient between the membrane and aqueous solution and Q is the flow rate through the fiber (cm^3/s). The permeability can be defined as the product of the diffusion coefficient and partition coefficient, ($D_{mem}K$). For the permeability experiments, the flow of the sample was set at 3.0 ml/min, which is sufficient to reduce the diffusion boundary layer around the membrane. Although the chosen flow rate does not have any particular physiological significance, this flow rate lies on the plateau portion of the recovery curve for the membranes studied (Figure 4). A flow rate of 3.0 ml/min gives a linear velocity of 0.7 cm/s. A typical blood velocity through the main veins of a dog which have an inner diameter of 2.4 mm (close to our tube which is 3 mm) is 1.48 cm/s [Lightfoot, 1974]. This high flow rate allows the assumption of a steady-state process which is necessary in order to use the above equation.

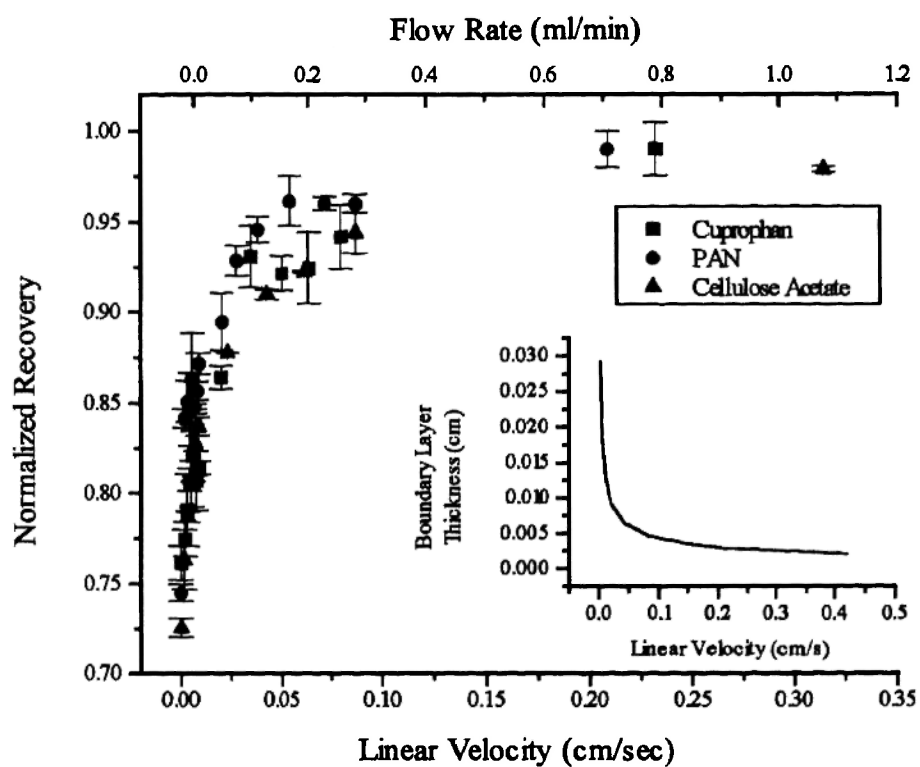


Figure 4. Normalized percent recoveries versus sample flow velocity. The inset shows the effect of velocity on boundary layer thickness.

2.2.6 Determination of Membrane Partition Coefficients

A 50 $\mu\text{g/ml}$ solution of phenacetin was prepared for use in an equilibrium study with the cellulose acetate dialysis fibers. Membrane fibers were placed into a tared 5 ml vial to approximately one half of the volumetric capacity of the vial. The weight of the fibers was recorded and 3 mls of the phenacetin solution were added to the vial. The weight was recorded again after the addition of the phenacetin. The vial was placed in a sonic bath to remove air bubbles that had formed. Additional membrane fibers were added until the vial was full. The weight was recorded a final time. Control samples of 3 mls of phenacetin were also prepared. All solutions were stored in the dark to prevent the photo-oxidation of phenacetin. After preparation of all the solutions, 15 μl were removed for LC analysis. This procedure was repeated 24 and 48 hours after the initial sample preparation.

2.3 Results and Discussion

2.3.1 Recovery Experiments

A plot of the normalized percent recoveries for each membrane versus the linear velocity of the sample solution is shown in Figure 4. The normalization is calculated by dividing each recovery obtained for a particular membrane by the highest recovery obtained for that membrane. The linear velocity of the solution is determined by dividing the flow rate of the solution by the cross-sectional area of the tube through which the solution passes. This calculation provides the average fluid flow through a tube. Since the Reynolds numbers for the flow experiments are much less than 2000, the flow is considered laminar. The recovery is affected by the change in velocity only at very low linear velocities. As shown in Figure 4 the percent recovery increases with increased velocity until a plateau value is reached. Linear velocity, rather than flow rate, is the critical factor as identical curves are obtained using Tygon tubing of different internal diameter and flow rates to achieve equivalent linear velocities as shown in Figure 5.

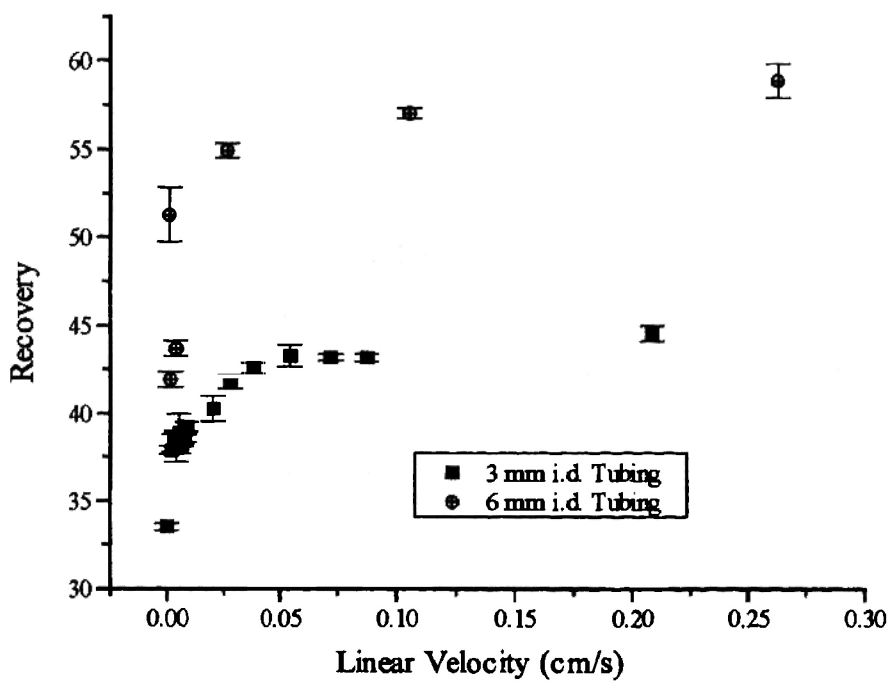


Figure 5. Hydroquinone recovery through a PAN membrane using two different probe diameters.

Although the sample solution flows around a cylindrical microdialysis tube, its flow pattern can be described more simply by approximating it as flow across a flat plate. This simplification is accurate here because of the low Reynolds numbers for flow on the sample side ($0.7 < Re < 33$). Levich has shown that the complex flow separation and reversal which are characteristic of flow over curved surfaces exist only at Reynolds numbers greater than 20 [Levich,1962]. Because all but the highest flow experiments had a sample side $Re < 20$, the flat plate approximation is used in this study.

For flow across a flat plate, the diffusion layer thickness has been shown to be proportional to the inverse of the square root of the velocity [Levich, 1962]. Here, the flat surface length has been taken to be half the circumference of the dialysis membrane. A plot of the diffusion layer thickness is shown in the inset of Figure 4. As the linear velocity increases the diffusion layer formed around the membrane decreases, making the concentration gradient in the boundary layer steeper. The rate of mass transfer is increased according to Fick's law of diffusion. At a limiting velocity, the diffusion layer around the membrane has become so thin that any further increase in linear velocity does not affect its thickness. In such a case, diffusion through the membrane becomes the limiting factor in mass transport. This limiting condition is shown in Figure 4, where the percent recovery, which is a function of the mass transfer rate, remains constant at higher sample solution velocities.

The flux of a solute can be expressed as:

$$N = k (C_{interface} - C_{bulk}) \quad (2)$$

where k is the rate constant for mass transfer from the membrane/solution interface to the bulk solution. To further characterize the recovery data in terms of a boundary layer being formed around the membrane and to determine the limiting factor in the recovery data, boundary layer theory can be used. From boundary layer theory the mass transfer rate can be determined as [Cussler, 1984]:

$$k = 0.626 \frac{D}{L} \left(\frac{L v^0}{\nu} \right)^{1/2} \left(\frac{\nu}{D} \right)^{1/3} \quad (3)$$

where, k is the mass transfer rate (cm/s), D is the diffusion coefficient (cm²/s), L is the length of the membrane (cm), ν is the kinematic viscosity (cm²/s), and v^0 is the maximum velocity of the fluid (cm/s).

From the above equation, a plot of percent recovery (or mass transfer rate) versus the square root of the velocity, v^0 , should be a straight line in cases in which a diffusion layer exists. Figure 7 shows the percent recovery for a cuprophan membrane as a function of the square root of the velocity, v^0 ^(1/2). As the fluid velocity approaches zero, Equation 3 can no longer be used as there is no convection in the system. At zero sample velocity, the mass transfer rate constant is described in the purely diffusional case by

$$k = D/h \quad (4)$$

where h is the diffusion layer thickness which would include the sample fluid and the membrane. Thus, the percent recovery approaches a nonzero value at zero sample velocity.

Figure 6 shows the percent recovery for a cellulose acetate membrane plotted versus the square root of the velocity. This plot exhibits three regions corresponding to whether mass transport through the sample solution or through the membrane is most important in determining the sample recovery. The first region occurs at low linear velocities where the diffusion layer is large. This region shows a linear dependence of recovery on the square root of sample velocity. In this region mass transport is limited by diffusion through the sample diffusion layer and not diffusion through the membrane. In the second region, the diffusion layer is rapidly decreasing and the concentration gradient to the membrane is increasing. The relation of recovery to sample velocity is nonlinear in this transitional region. As the sample diffusion layer decreases, mass transport through the membrane becomes more important relative to transport through the sample. In this transitional region, recovery is controlled by both sample transport and membrane transport. The third region is the plateau at high sample velocity, in which recovery is independent of sample velocity. In this region the sample diffusion layer has decreased to the point that mass transport is primarily controlled by diffusion through the membrane.

2.3.2 Mass Transfer Coefficient Determinations

In Figure 7, the mass transport coefficients for a PAN membrane are plotted according to the method of Jacobson as described in Chapter 1 [Jacobson et al., 1985]. Mass transfer coefficients can be obtained from these plots as the slope is equal to the product of the mass transfer coefficient and the surface area. The calculated mass transfer coefficients are presented in Table 1. As can be seen, the slopes for linear velocities greater than 0.211 cm/s are essentially overlapping, indicating that the membrane resistance controls mass transport rather than the solution resistance. As mentioned above the terminal veins of a dog have a blood velocity of 1.3 cm/s and the large veins of a dog have a blood velocity of 3.6 cm/s

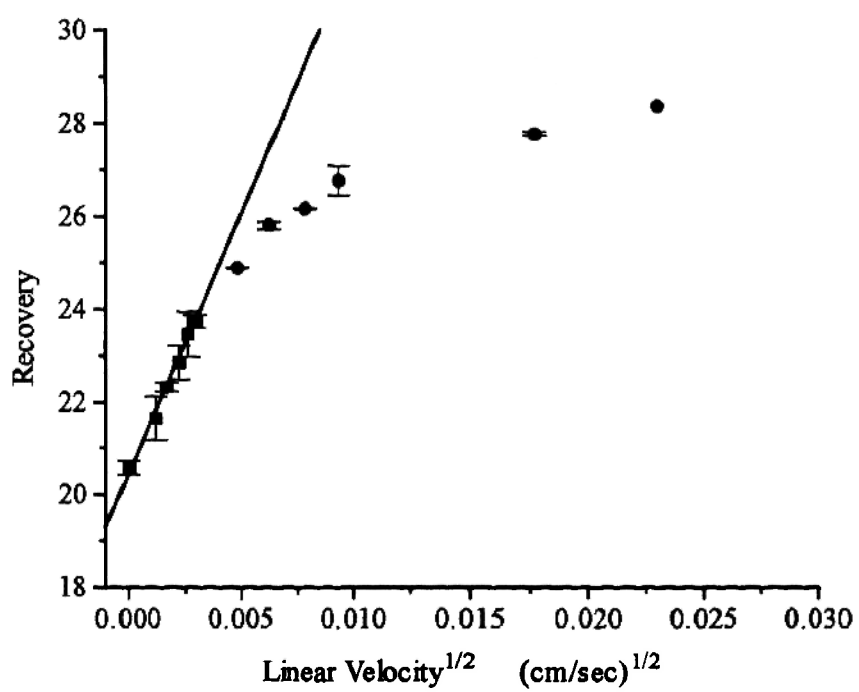


Figure 6. Plot of the percent recovery vs. $(\text{linear velocity})^{1/2}$ for a cellulose acetate membrane.

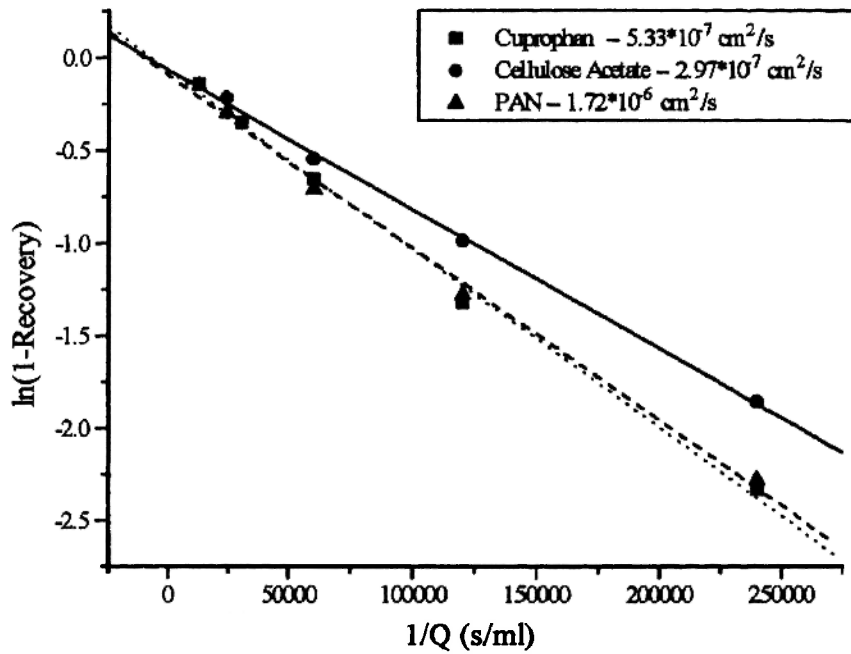


Figure 7. Permeability plots of hydroquinone through PAN, cellulose acetate and cuprophan membranes.

[Lightfoot, 1974]. Since 0.211 cm/s is much lower than these physiologically relevant velocities, the membrane is the limiting factor in mass transport in these systems at velocities greater than 0.211 cm/s and not diffusion through the sample.

Table I. Mass-transfer coefficients at different flow velocities.

Flow Rate ($\mu\text{l}/\text{min}$)	Linear Velocity (cm/s)	10^6 slope (cm^3/s)	10^4 k (cm/s)
7500	1.58	7.54	2.53
5000	1.05	7.65	2.57
1000	0.212	7.55	2.53
250	0.053	7.20	2.42
100	0.021	6.93	2.32
25	0.005	5.79	1.94
10	0.002	5.31	1.78
0	0.0	5.32	1.78

2.3.3 Permeability Determinations

The permeability of the membranes have been determined according to Equation 2 from the slopes of the plots shown in Figure 8. The permeability of hydroquinone through the membranes used is shown in Table II. These values are all lower than the free solution diffusion coefficient for hydroquinone, which was determined to be $0.85 \times 10^{-5} \text{ cm}^2/\text{s}$. This is further evidence that the membrane limits mass transport in a hydrodynamic situation. The permeability varies greatly between

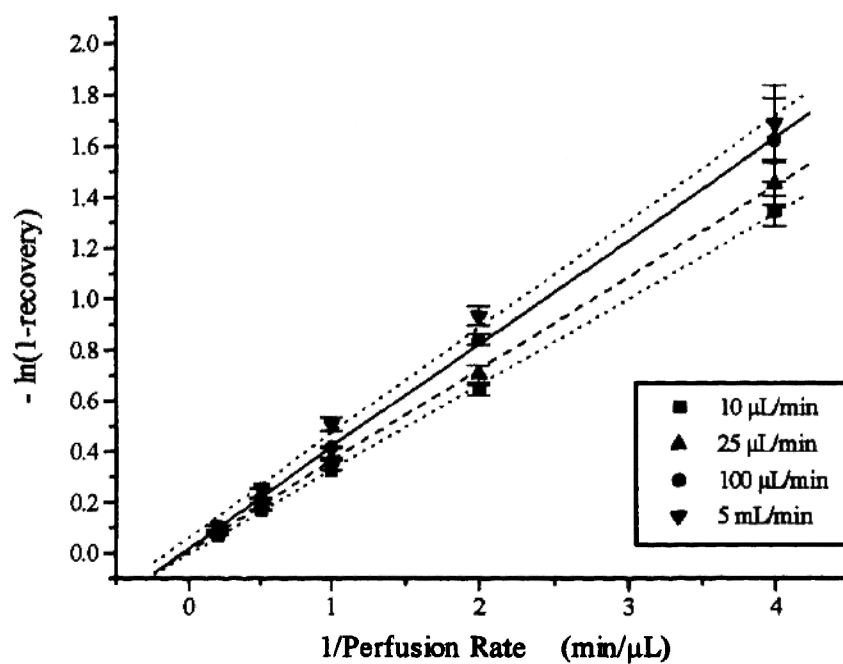


Figure 8. Plot of the determination of the mass-transfer coefficients for hydroquinone at various flow rates around a PAN fiber.

Table II. Membrane permeability of hydroquinone in dialysis fibers.

Membrane	Slope	Regression	Permeability (cm ² /s)
PAN	1.282	0.99	1.72*10 ⁻⁶
Cuprophan	1.365	0.99	5.33*10 ⁻⁷
Cellulose Acetate	1.801	0.99	2.97*10 ⁻⁷

Table III. Permeabilities of methylxanthine compounds in PAN membrane.

Analyte	Permeability (cm ² /s)
Theophylline	1.37*10 ⁻⁶
Theobromine	1.18*10 ⁻⁶
Caffeine	0.97*10 ⁻⁶

the membranes because of the different chemistry and porosity of the various fibers. Because the permeabilities differ through these membranes, the rate of mass transport through these membranes will be different. Ultimately it is the permeability and the surface area of the dialysis membrane that affects the amount of material recovered in a hydrodynamic microdialysis experiment. This was determined experimentally for three similar methylxanthines, theobromine, theophylline, and caffeine for a PAN membrane as shown in Table III. From Table III it can be seen that the permeabilities vary for the three methylxanthines. This is interesting as theophylline and theobromine have the same molecular formula and thus the same molecular weight and caffeine has only an extra methyl group. Additional observations on the variability of diffusion properties for set of neutral, cationic and anionic compounds has been described by Zhou and Lunte [Zhou and Lunte, 1995].

It may be expected that the sample velocity needed to decrease the diffusion layer such that diffusion through the membrane is limiting would vary among the different membranes. However, the recovery data shown in Figure 4 indicates that the difference in the permeabilities as well as the differences in the outer radius of the membranes do not cause a significant difference in the hydrodynamic behavior. Essentially, the permeability affects the value of the probe recovery but not the recovery's dependence on sample flow. This means that in physiologically relevant experiments using microdialysis sampling in a hydrodynamic system such as sampling intravenously, the membrane is the limiting factor in mass transport and that an *in vitro* determination of recovery in a stirred solution at 37°C should be valid *in vivo*.

2.3.4 Permeation Through the Membrane

Because the membrane permeability is defined as the product, $D_{\text{mem}}K$, an approximate value of the partition coefficient, K , in Equation 1 would be desirable. An approximate value of K would then allow for calculation of D_{mem} . The

approximate volume percent of the PAN and Cuprophan membranes has been experimentally determined as 57 and 65 percent [Collins and Ramirez, 1979]. This indicates that for the PAN membrane that the value of K for hydroquinone is approximately one as the value of the D_{mem} can be determined as the product of $\phi_{mem}D_{aq}$. However, the use of the volume fraction of space does not explain the order of magnitude difference between the Cuprophan and Cellulose Acetate membranes. Initial experiments using hydroquinone with only a few membrane fibers indicated that K must be one as there seemed to be little uptake of material. However, to test this further, more membrane fibers were used as described above in the methods section.

Because of the difficulties in determining the true volume of these membranes, an approach was used based on weight differences. Volume measurements of membranes are performed by wetting the membrane and determining the amount of water taken up by the membrane. This is performed by shaking or drying excess water off the hollow fiber. One can imagine the experimental error that would be incorporated into these measurements due to the uncertainties in shaking and drying. Therefore only the dry weights were used in these experiments. For these experiments phenacetin was used for convenience (current *in vivo* experiments were utilizing phenacetin) with cellulose acetate membranes. The results for three different samples are shown in Table IV. The concentration of phenacetin in the sample vials was lower than the control vials immediately after contact with the cellulose acetate membrane and this initial drop did not change over the 48 hour period. Permeation into these membranes was expected to exhibit equilibrium behavior and the initial decrease was unexpected. This immediate drop in concentration seems indicative of an adsorption phenomenon rather than an equilibrium. However, the data indicate that the same mass of phenacetin was taken up by each membrane despite the differences in the weight of the membranes in the vials. Phenacetin is a hydrophobic molecule

so it is possible that it adsorbed to the membrane. It should be noted that 0.1 g of membrane would be enough membrane to make more than 500 five mm dialysis probes. Therefore, the effect of possible adsorption onto the membrane on the results of a microdialysis study is unknown.

Table IV. Uptake of phenacetin into cellulose acetate membranes.

weight (mg)	uptake ($\mu\text{mol/g}$)		
	0 hours	24 hours	48 hours
0.174	1.02	0.98	0.83
0.266	0.68	0.74	0.66
0.328	0.62	0.59	0.51

To confirm these findings it would be useful to test a few model compounds with the membranes that are used in microdialysis experiments. Additional experiments such as the possible determination of a Langmuir isotherm should be determined for a selected class of compounds which the author would suggest below. The following because of their acid/base and steric effects (MW) are useful readily available compounds and can be easily quantitated by LC-UV methods: dopamine, DOPAC, acetaminophen, and acetaminophen glucuronide (available from Sigma).

Another useful data gathering exercise would be to determine the membrane diffusion coefficients for the various compounds mentioned above and compare that with their in vitro solution diffusion coefficients. The author suggests that these experiments continue to determine if any of the compounds used routinely in microdialysis sampling exhibit any permeation into the membrane. These experiments would be useful in continued development of membrane materials for microdialysis

as well as for various biosensor applications that utilize the same membranes used in microdialysis experiments.

2.4 Conclusions

It has been shown that the mass transport to a microdialysis membrane is affected by the velocity of the fluid flowing around the membrane. This fluid flow will cause a diffusion boundary layer to form which will affect the rate of mass transport to the dialysis membrane. As the linear velocity of the fluid increases the diffusion layer collapses, thus causing mass transport to be limited by the membrane rather than the sample solution. These observations are important because they indicate that an *in vitro* calibration may be performed for applications which involve a flowing solution such as the blood or bile.

2.5 References

- Bard, A.J.; Faulkner, L.R. *Electrochemical Methods: Fundamentals and Applications*; John Wiley and Sons: New York, 1980; p.292.
- Buttler, T.; Nilsson, C.; Gorton, L.; Marko-Varga, G. Membrane characterization and performance of microdialysis probes intended for use as bioprocessor sample units. *J.Chromatogr. A* **1995**, in press.
- Chen, A.; Lunte, C.E. Microdialysis sampling coupled on-line to fast microbore liquid chromatography. *J. Chromatogr. A* **1995**, *691*, 29-35.
- Church, W.H.; Justice, J.B. Jr. Rapid sampling and determination of extracellular dopamine *in vivo*. *Anal. Chem.* **1987**, *59*, 712-716.
- CMA/Microdialysis AB *Library of Microdialysis: Bibliography*. CMA/Microdialysis AB: Stockholm, 1994.
- Collins, M.C.; Ramirez, W.F. Mass transport through polymeric membranes. *J. Phys. Chem.* **1979**, *88*, 2294-2301.

Cussler, E.L. *Diffusion. Mass Transport in Fluid Systems*; Cambridge University Press: Cambridge, 1984, p.306.

Hsiao, J.K.; Ball, B.A.; Morrison, P.F.; Mefford, I.N.; Bungay, P.M. Effects of different semipermeable membranes on in vitro and in vivo performance of microdialysis probes. *J. Neurochem.* 1990, 54, 1449-1452.

Jacobson, I; Sandberg, M.; Hamberger, A. Mass transfer in brain dialysis devices -a new method for the estimation of extracellular amino acids concentration. *J. Neurosci. Methods* 1985, 15, 263-268.

Johnson, R.D.; Justice, J.B. Model studies for brain dialysis. *Brain Res. Bull.* 1983, 10, 567-71.

Kehr, J.; Ungerstedt, U. Fast HPLC estimation of gamma-aminobutyric acid in microdialysis perfusates: Effects of nipecotic and 3-mercaptopropionic acids. *J. Neurochem.* 1988, 51, 1308-1310.

Kolthoff, I.M.; Orlemann, E. The use of the dropping mercury electrode as an indicator electrode in poorly poised systems. *J. Am.Chem. Soc.* 1941, 63, 664-667.

Kuipers, R.A.; Korf, J. Flow resistance characteristics of microdialysis probes in vitro. *Med. & Biol. Eng. & Comput.* 1994, 32,103-107.

Levich, V. *Physicochemical Hydrodynamics*; Prentice-Hall Inc.: Englewood Cliffs, NJ, 1962; p.59.

Lightfoot, E.N. *Transport Phenomenon and Living Systems: Biomedical Aspects of Momentum and Mass Transport*; John Wiley and Sons:New York, 1974; p. 83.

Marko-Varga, G.; Buttler, T.; Gorton, L.; Grönsterwall, C. A study of the use of microdialysis probes as a sampling unit in on-line bioprocess monitoring in conjunction with column liquid chromatography. *Chromatographia* 1993, 35, 285-290.

Mulder, M. *Basic Principles of Membrane Technology*. Kluwer Academic Publishers: Dordrecht, The Netherlands, 1991.

Newton A. P.; Justice J. B.. Temporal response of microdialysis probes to local perfusion of dopamine and cocaine followed with one-minute sampling. *Anal.Chem.* 1994, 66, 1468-1472.

Ruggeri M., Zoli M., Grimaldi R., Ungerstedt U., Eliasson A., Agnati L. F., and Fuxe K. Aspects of neural plasticity in the central nervous system - III. Methodological studies on the microdialysis technique. *Neurochem. Int.* **1990**, *16*, 427-435.

Sakai K. Determination of pore size and pore size distribution 2. Dialysis membranes. *J. Membrane Sci.* **1994**, *96*, 91-130.

Scott, D.O.; Lunte, C.E. In vivo microdialysis sampling in the bile, blood and liver of rats to study the disposition of phenol. *Pharm. Res.* **1993**, *10*, 335-342.

Steele, K.L.; Scott, D.O.; Lunte C.E. Pharmacokinetic studies of aspirin in rats using *in vivo* microdialysis sampling. *Anal. Chim. Acta* **1991**, *246*, 181-186.

Zhou, Y; Lunte, C.E. *Anal. Chim Acta* 1995, in press.

Chapter 3

Development and Analysis of Mechanistic Models to Describe the Extraction Efficiency in Microdialysis Experiments.

3.1 Development of Models to Describe Microdialysis Experiments

This chapter presents methods that will be used to describe mathematically the fundamental processes that affect microdialysis experiments. Two approaches will be used to model microdialysis experiments: analytical and numerical. Analytical methods are used when a general description about a particular process is desired. An analytical model will describe why a response is affected by the input variables in a particular manner. An example would include the exponential expression that is used to describe radioactive decay, $C(t)=C_0e^{-kt}$. The output concentration at a specific time, $C(t)$, is related to the input variables which includes the initial concentration, C_0 , the decay rate, k , and time. Numerical methods on the other hand give a specific answer to a complex set of equations. Numerical methods become necessary when the equations used to describe a physical process become too complex to be solved by analytical methods. For the microdialysis sampling case, the equations become complex due to the system of partial differential equations that is necessary to describe the physical process of microdialysis. Other examples of complex terms include time-varying or spatially-varying parameters or non-linear kinetic terms such as Michaelis-Menten kinetics or Langmuir isotherms.

Mathematical modeling of physical processes can aid microdialysis research in a number of ways [Box et al., 1978]. First, modeling forces the researcher to identify the variables and parameters that affect the system being studied. Second, it provides a means of making progress through basic understanding of the system. For example the interaction of the various parameters that influence microdialysis sampling such as diffusion coefficients and kinetic rate constants can be predicted.

Third, the gain in understanding may suggest further experiments thus providing a way to confirm and if necessary to improve the model. In the words of the famous analytical chemist, I.M. Kolthoff, the approach is "to allow theory to guide, but experiments to decide" [Christian, 1995]. Fourth, mechanistic models that have been tested can provide a basis for extrapolation of values near the boundary conditions. This type of extrapolation is questionable when used with empirical models based on polynomial fits of the data. Fifth, a mechanistic model can be used to estimate parameters. Sixth, a mechanistic model is more parsimonious than models obtained empirically. A parsimonious model would predict the experimental results using as few variables as possible. In the radioactive decay model mentioned above, the mechanistic model using the exponential would be more parsimonious than a polynomial fit of the decay data.

Chapter 1 provided introductory details about modeling the three different mass transport systems in microdialysis. Assumptions about these processes can be made such that simplified analytical expressions can be obtained. These analytical expressions will provide a basic insight into how the diffusion coefficient and kinetic rate constant parameters will affect microdialysis sampling. After presentation of the analytical methods, the development of the numerical methods used to model microdialysis sampling will be presented. A discussion of the assumptions and limitations of the numerical model will be presented.

3.2 Analytical methods

An important aspect of modeling is to facilitate understanding and enhance prediction capabilities. A simplified approach to modeling the microdialysis sampling process is derived in Appendix 2. Only the equations which are pertinent to this chapter are presented here.

3.2.1 Analytical assumptions

Several assumptions are necessary to model the microdialysis sampling process through the use of analytical methods. The derivation in Appendix 2 uses the following assumptions. 1) The microdialysis probe is assumed to be a cylinder with a defined outer radius, r_o , as shown in Figure 1. Although the linear probe geometry is shown here, a cannula design can also be used. 2) At r_o , a constant amount of material is released from the cylinder, C_{max} . 3) The substances emanating from the cylinder diffuse only in the radial direction, r , and not in the axial direction, z . This is because the length is assumed to be greater than the radius to force the solution into cylindrical terms. For most microdialysis experiments this is true except for probes with membrane lengths of 1 mm or less. For shorter probes, it becomes necessary to use a spherical geometry approach. 4) The analyte moves through the tissue by diffusion, concentration gradient driven mass transport, but not convection, fluid flow (pressure) driven mass transport. 5) Kinetic processes such as metabolism or uptake terms are included as one lumped kinetic term. These terms are also considered to be first order. This is because these processes are additive and thus need to be summed. These uptake processes are assumed to occur homogeneously in the tissue space. For the simple case that will be considered, that of delivery, these processes are assumed to only be uptake processes and not generation processes. 6) The diffusion coefficient is constant throughout the tissue medium. This ignores the possibility of the molecule diffusing through cell membranes and having a different affinity through the cell membrane. 7) A value for the volume fraction, ϕ_{ecf} is not included. Although this term is necessary to describe the physical process of diffusion and reaction through a tissue medium, it only serves to reduce the parameters by the fraction number. For example the diffusion coefficient, D_{ecf} , would just be reduced to $\phi_{ecf}D_{ecf}$. 8) The system is at a steady-state.

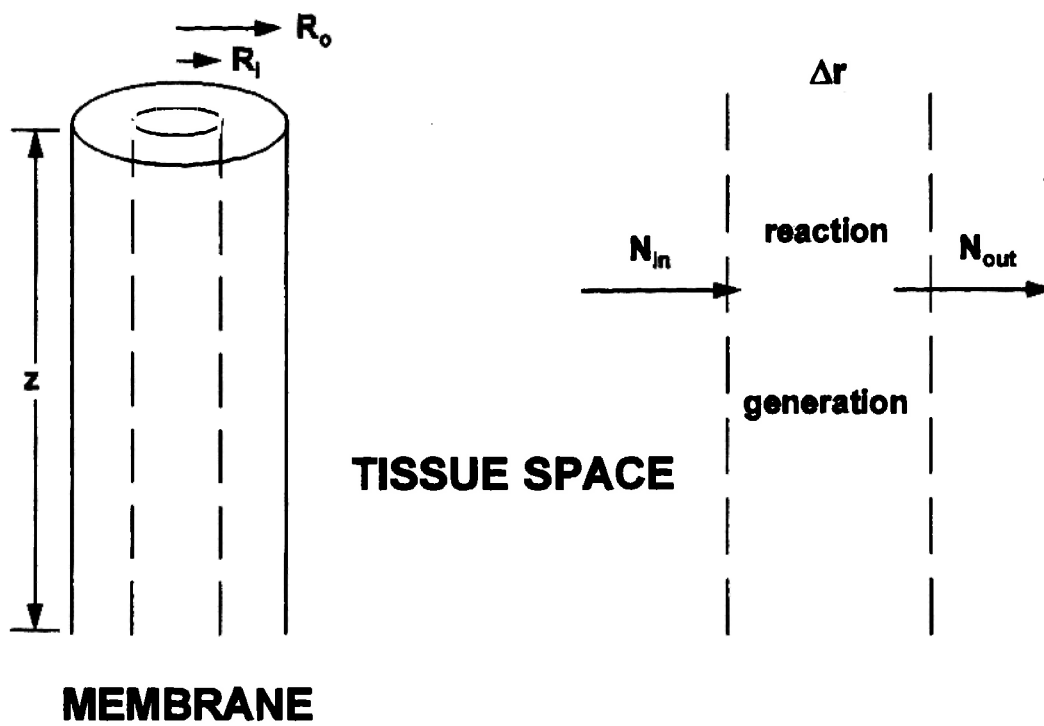


Figure 1. Control Volume of the tissue space used in microdialysis and the mass-balance.

3.2.2 Analytical Solution

By using the assumptions given above and solving the appropriate mass balance, Equation 1 is obtained.

$$\frac{dC_{ECF}}{dt} = D_{ECF} \frac{1}{r} \frac{d}{dr} \left(r \frac{dC_{ECF}}{dr} \right) - kC_{ECF} = 0 \quad (1)$$

Because the probe is assumed to be a cylinder the $(1/r)$ dependence is necessary for the diffusion part of the expression [Cussler, 1984]. Through expansion of the derivative, it is noticed that the equation fits that for a generalized Bessel function solution that can be found in mathematics textbooks [Mickley, et al., 1957]. The Bessel function is a series function that is used to solve some types of differential equations. The value of these functions for specific arguments can be found by looking them up in mathematical handbooks [Abramowitz and Stegun, 1964], by calculation through a numerical method using Fortran or some other programming language, [Press et al., 1992] or by using a common spreadsheet program such as Microsoft Excel. Bessel functions appear to be exponential in nature with increasing values of the argument as shown in Figure 2.

Equation 1 is solved using the following boundary conditions. 1) $C_{ecf} = 0$ as $r \rightarrow \infty$. 2) $C = C_{max}$ at $r = r_o$, where C_{max} is the concentration at the outer radius, r_o . The solution of Equation 1 gives Equation 2, which can be used to describe the concentration profile away from the probe.

$$C_{ECF} = C_{max} K_o \left(\sqrt{\frac{k}{D_{ECF}}} r \right) / K_o \left(\sqrt{\frac{k}{D_{ECF}}} r_o \right) \quad (2)$$

This concentration profile is dependent upon the diffusion of the substance away from

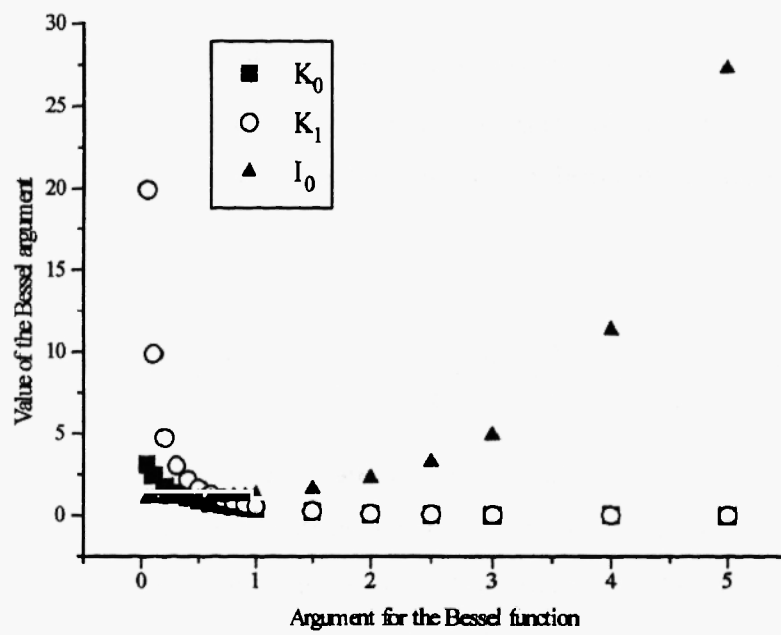


Figure 2. Values for arguments using the Bessel functions I_0 , K_0 , and K_1

the cylinder, D_{ECF} , and consumption of the substance in the tissue space, k .

Figure 3 shows the values obtained by using Equation 2 for various values of the kinetic rate constant, k , and for a fixed diffusion coefficient of $7.5 \cdot 10^{-6} \text{ cm}^2/\text{s}$. From this simplified equation it can be seen that the concentration profile away from the cylinder will become steeper with increasing values of the kinetic processes. This is expected when diffusion is combined with reaction [Cussler, 1984]. These steeper values will in turn reflect an increased flux from the probe.

Flux is defined as the amount of material removed from the dialysis membrane per unit area and per unit time. The general expression for flux is $J = -D \text{ dC/dr}$. For the case of a cylinder this is found by taking the derivative of Equation 2 which gives

$$J = \sqrt{D_{ECF}k} C_{\max} K_1 \left(\sqrt{\frac{k}{D_{ECF}}} r \right) / K_0 \left(\sqrt{\frac{k}{D_{ECF}}} r_0 \right) \quad (3)$$

As the values of the kinetic rate constant increases or the diffusion coefficient decreases, K_1 and K_0 will approach a value of one. In these cases the value of the flux, J , will approach the square root of the product of the diffusion coefficient, the kinetic rate constant. For the diffusion coefficient value considered above of $7.5 \cdot 10^{-6} \text{ cm}^2/\text{s}$ the limiting cases described above would occur when the kinetic rate constant exceeds 10 min^{-1} . Whether this is faster than biological rates found *in vivo* is unknown.

3.2.3 Addition of Membrane Diffusion

Diffusion through the membrane can be added to modify the derivation. The microdialysis literature states that only the tissue plays a role in limiting the flux of

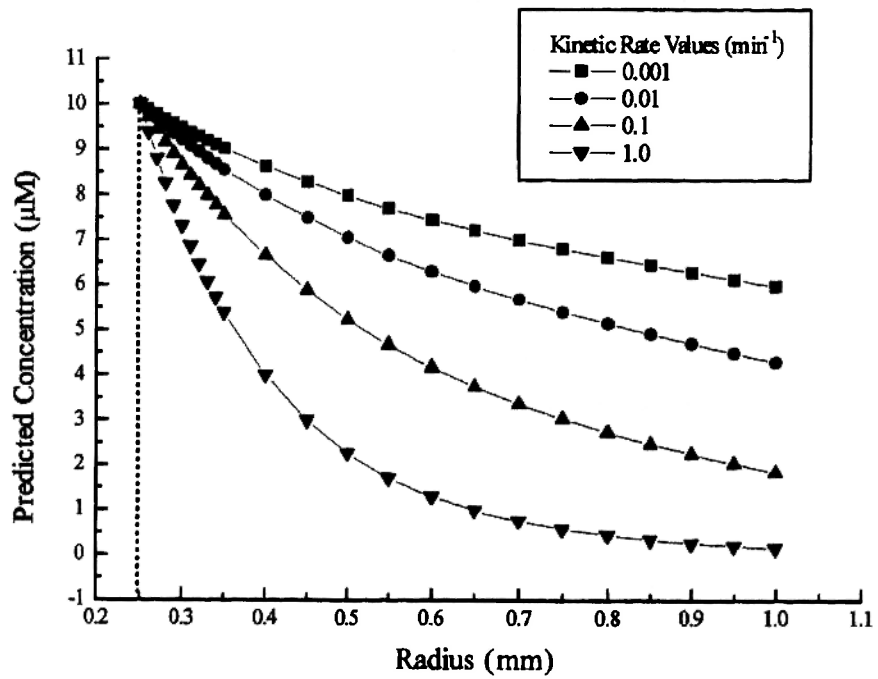


Figure 3. Predicted tissue concentrations for the simple analytical model for various values of kinetic rate constants.

a substance through the microdialysis membrane [Morrison et. al., 1991, Hsiao et al., 1991]. In the brain tissue this assumption has been shown to be valid for acetaminophen and a few acid metabolites of dopamine, DOPAC and homovanillic acid [Hsiao et al., 1991]. However, for other tissues such as liver or even other compounds in the brain such as the neurotransmitter dopamine [Smith and Justice, 1994] this assumption may not be valid. In these cases, the membrane may become more limiting. Solving for a mass balance that includes diffusion through the membrane as well as through the tissue yields the equation that describes the flux of a substance at the outer radius of the cylinder.

$$J = D_m \left(\kappa \frac{C_i}{(D_m/r_o) + \kappa \ln(r_o/r_i)} \right) \frac{1}{r_o} \quad (4)$$

In Equation 4, D_m is the effective membrane diffusion coefficient for the analyte, r_o is the outer radius, and r_i is the inner radius of the cylinder. In this expression, κ , is defined as shown in Equation 5.

$$\kappa = \sqrt{D_{ECF} K} \frac{K_i (\sqrt{K/D_{ECF}} r_o)}{K_o (\sqrt{K/D_{ECF}} r_o)} \quad (5)$$

One useful practice with analytically derived equations is to evaluate the equation at the limits of the equation. For thin membranes, as r_o approaches r_i as in the case for a Cuprophan membrane ($r_o = 106 \mu\text{m}$, $r_i = 100 \mu\text{m}$), the value of r_o/r_i approaches 1 and thus the natural logarithm approaches zero (for this particular Cuprophan membrane, the value of $\ln(r_o/r_i)$ is 0.058). In this case, the flux through the tissue becomes the predominant factor in determining the flux from the probe. For thicker membranes such as PAN or the CMA/polycarbonate the value of r_o/r_i will be greater than one, and the natural logarithm of r_o/r_i will be about 0.35, for the PAN

which has $r_o = 170$, $r_i = 120$. In this case the membrane may provide a greater resistance to the mass transport which could influence studies used to determine which tissue processes are dominant in microdialysis sampling. For low values of the kinetic rate constants, values of the concentration obtained using Equation 4 will approach the values for the ECF space only approximation in Equation 3.

The approximate value for the delivery of a substance can be calculated by considering the dialysate flow to be fast enough that the amount lost from the inner fiber lumen is small. This approximate value will depend on the membrane type and length, but practical experience suggests that perfusion flows greater than $5\mu\text{l}/\text{min}$ could be used. In general, perfusion flows greater than $5\mu\text{l}/\text{min}$ will give delivery values of 10 percent or less, indicating that less than 10 percent is lost from the probe. Figure 4a shows that for thicker walled membranes, the membrane resistance affects the delivery as the kinetic rate constant, k , approaches 1.0 min^{-1} . In situations which have rapid kinetic processes, the membrane resistance and the tissue resistance will both contribute to the amount of material extracted from the probe. Figure 4b shows that for thinner walled membranes, the rate constant in the tissue needs to increase to 10 min^{-1} before the membrane resistance has an effect on mass transport. This finding indicates that if microdialysis is to be used for determining the values of different parameters such as the *in vivo* diffusion coefficient or the kinetic rate constants, then a thinner walled membrane with a lower mass transport resistance should be used.

3.3 Numerical Methods

The use of the analytical method described above can be a practical tool for understanding and predicting how microdialysis experiments may behave *in vivo*. In order to evaluate the transient behavior of the probe and to begin inclusion of the flow regime it is necessary to use numerical methods. Because these equations form the

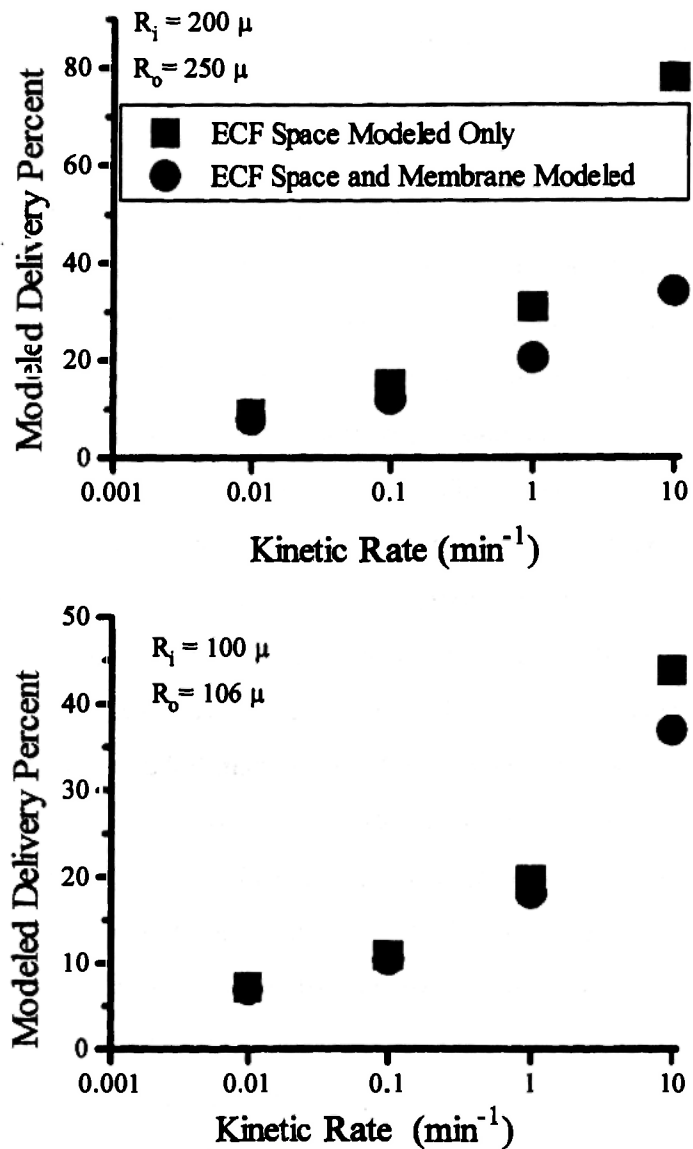


Figure 4. Analytical model predictions for a microdialysis experiment with a perfusion speed of 5 μ l/min for the membrane dimensions given.

bulk of this dissertation, they will be derived here. The following sections derive the necessary mass-balances used for this model. As the mathematical model forms the body of this work, it has not been placed into an appendix. Readers who are not interested in the mathematical development are encouraged to read through the assumptions needed to develop the model as well as the limitations of the model.

3.3.1 Numerical Method Assumptions

Many of the assumptions that were made for the analytical solution still hold here and are only briefly described again. 1) The microdialysis probe is a cylinder and is assumed to have intimate contact with the surrounding tissue. No liquid layer, fibrotic layer or interferences with other substances such as protein adsorption onto the outer membrane are considered. 2) The concentration at the outside of the probe is not a constant, but rather a function of the three mass-transfer resistances encountered by a molecule. 3) Only diffusion away from the cylinder in the radial direction is taken into account. Axial diffusion, although physically possible in a microdialysis experiment, is assumed to be negligible as the length of the cylinder is greater than the radial diameter of the cylinder. Moreover, the inclusion of an axial diffusion component would add another complexity to an already complex analysis. 4) Mass transport by diffusion only is considered, i.e., convective processes are not included in the model development. 5) Metabolism and uptake terms are separated so that they can be modified by the user of the model. 6) The diffusion coefficient remains constant throughout the tissue space. 7) A volume fraction and tortuosity through which diffusion and reaction occur must be considered. Diffusion for some substances is generally considered to be through the ECF space only which reduces the effective diffusion coefficient to $\phi_{ecf}D_{ecf}$, where ϕ_{ecf} is the volume fraction in the ECF space. The diffusion through the tissue is tissue specific. In the brain most substances do not cross cell membranes through passive diffusion [Cooper et al., 1991], whereas in the liver uptake occurs because the hepatocyte is highly fenestrated

thus facilitating the uptake of substrates by diffusion through the cell membrane [Goresky and Schwab, 1988]. 8) The system is allowed to behave transiently. Assumptions that are needed in addition to the modification of the simplified version are as follows. 9) The blood capillaries are considered to be evenly spaced in the tissue space. This allows for the microvasculature efflux term to be constant at all radial points. 10) Metabolic processes are equally spaced. 11) Metabolic and microvasculature uptake processes are considered only to be first order or linear, i.e. saturable metabolism is not considered. For systems in which the concentration of substrate is well below the Michaelis constant, K_m , this is valid. Since for most cases this assumption will not be true in general, the inclusion of saturable metabolism or higher order terms would need to be considered. However, the inclusion of saturable metabolism in the numerical model will require extensive computation effort. A later section discusses how saturable metabolism affects microdialysis sampling. 12) Because the model is already somewhat parameter laden, binding to plasma or cellular proteins is not included in the model. These processes however, can be included into the FORTRAN code provided in Appendix 4. For many of the compounds used in microdialysis, separate experiments would be necessary to determine the extent of binding to proteins.

3.3.2 Solution of the Numerical Equations

3.3.2.1 Tissue Space

A partial differential equation (Equation 6) is obtained after solving the mass

$$\begin{aligned} \frac{\partial C_{ecf}(r, z, t)}{\partial t} = & \phi_{ecf} D_{ecf} \frac{1}{r} \frac{\partial}{\partial r} \left(r \frac{\partial C_{ecf}(r, z, t)}{\partial r} \right) \\ & - K_x \phi_{icf} k_{imet} C_{ecf}(r, z, t) - \phi_{ecf} k_{emet} C_{ecf}(r, z, t) \\ & + \phi_{ecf} k_{pe} C_D(t) - \phi_{ecf} k_{ep} C_{ecf}(r, z, t) + k_{gen} C_{gen}(r, z, t) \end{aligned} \quad (6)$$

balance [Bird, et al., 1960] in the tissue space for the diffusion and reaction processes. This equation is found from Morrison's model [Morrison et al., 1991] and thus the term names are kept the same. This equation states that the change in concentration in the extracellular fluid space, C_{ecf} with respect to time is a function of the following parameters: ϕ_{ecf} , the volume fraction of the ECF space typically considered to be 0.2 for most tissues; ϕ_{icf} , the volume fraction of the intracellular space which is defined for this model as $(1-\phi_{ecf})$; D_{ecf} , the *in vivo* diffusion coefficient of the substance, and the various rate processes in the tissue such as k_{imef} , the intracellular rate constant; k_{eme} , the extracellular rate constant; k_{pe} , the plasma to extracellular fluid space exchange rate across the microvasculature; k_{ep} , the extracellular to plasma space exchange rate; and k_{gen} a generation rate constant associated with the concentration of the species that is being generated, C_{gen} . K_{π} is a partition coefficient that describes the intracellular, C_{icf} , and extracellular concentrations, C_{ecf} , of the dialyzed substances and is defined as C_{icf}/C_{ecf} . K_{π} is set as 1 in the mathematical model described here. This value can be adjusted when more is known about the nature of the uptake of substances in the ECF space. Further experimentation such as the use of autoradiography [Dykstra et al., 1992, 1993] or fluorescence microscopy would be needed for verify the assumption of unity for K_{π} for each analyte modeled.

The following boundary and initial conditions are needed for the ECF space. The initial condition for recovery is that at $t = 0$; $C_e(\text{all } r) = C_{\text{known}}$, where C_{known} is either zero for a pharmacokinetics experiment or the known concentration value for an endogenous species. The initial condition for a delivery is at $t=0$, $C_d=C_{\text{enter}}$, where C_{enter} is the concentration of the substance in the entering perfusate. The boundary conditions are: 1) $r = \infty$, $C_e = C_{\infty}$, where C_{∞} is calculated by an analytical equation described in Appendix 3 for the pharmacokinetic recovery experiment, or is zero for a delivery experiment. 2) $r=r_{\text{out}}$; $C_e(r_o) = C_m(r_o)$.

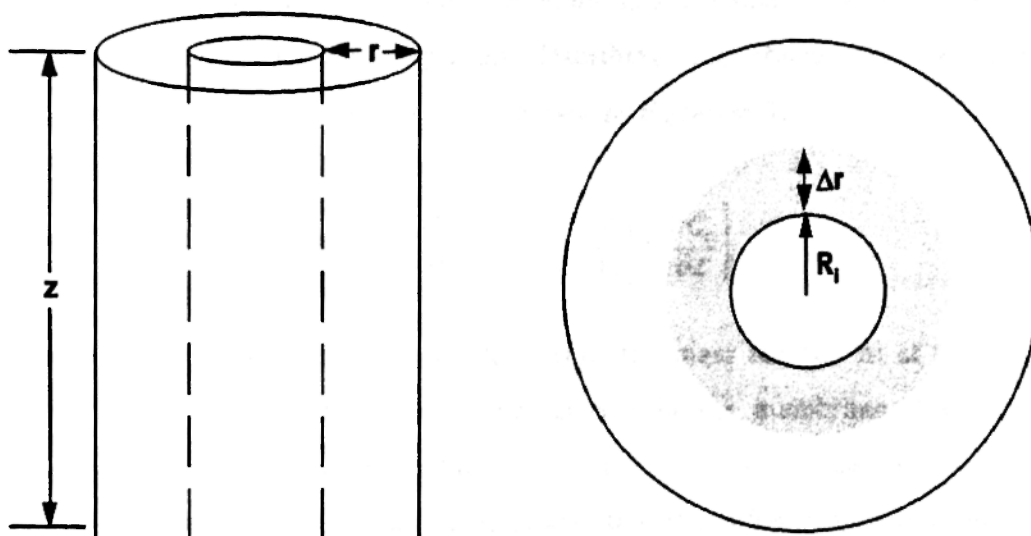


Figure 5. Diagram of the control volume used for the membrane with inner radius, R_i , and length, L .

3.3.2 Membrane mass balance

The mass balance through the membrane is depicted in Figure 5. The assumptions that apply to the membrane mass balance are: 1) Mass transport through the membrane occurs by diffusion. The diffusion coefficient describing this mass transport assumes that diffusion occurs through the water space in the membrane [Sakei, 1994]. 2) Diffusion only occurs in the radial direction and not in the axial direction giving an axial average of the concentration through the membrane at all radial points. 3) No reaction processes occur in the membrane. Unlike Morrison's model, in this work, the role of the membrane is accounted for in the solution of the equations. The differential equation describing the change in the membrane concentration as a function of time is shown in Equation 7.

$$\frac{\partial C_m}{\partial t} = D_m \frac{1}{r} \frac{\partial}{\partial r} \left[r \frac{\partial C_m}{\partial r} \right] \quad (7)$$

The initial condition used to solve the membrane mass balance is: at $t=0$, $C_m = 0$, where C_m is the concentration of the analyte in the membrane. Two boundary conditions are necessary and include at $r = R_o$, $C_m = C_o(r_o)$ and at $r = R_i$, $C_m = C(\text{average})_d(z,t)$. The boundary conditions state that when the dialysis experiment begins the membrane is free of material. At the outer radius, the value of the concentration of the membrane is equal to that in the ECF space at the interfacial point. Similarly for the dialysate the inner membrane radius is averaged as having a value equal to the average concentration of the dialysate leaving the probe. These boundary conditions greatly simplify the mathematics in that they assume that the concentration values are an axial average. This allows the problem to be 1-dimensional in nature rather than two dimensional. However, these assumptions of the 1-D nature may break down at slow flow rates or with long probes, which will have a large variation in the concentration in the axial direction.

3.3.3 Dialysate mass balance

Finally, the third system which must be considered is the perfusion of fluid through the dialysis fiber lumen. In this case, the fluid flows through the fiber lumen at a set perfusion rate generally between 0.5 and 2.0 $\mu\text{l}/\text{min}$. The fluid itself is actually taken as one piece and the concentration at individual points are averaged as done by Bungay et al. [Bungay, 1990]. It is assumed that the membrane is short enough that the fluid can be considered to be well-stirred or at least moving fast enough that back diffusion into the tissue space does not occur.

Figure 6 depicts the mass balance control volume for the dialysate. In the steady-state balance for a delivery experiment, analyte enters the system through convection (flowing fluid) through the lumen and leaves the system by convection and diffusion through the membrane in an axial increment defined as Δz . Note that the system is radial and thus diffusion occurs at all points across the membrane. The steady-state mass-balance is described and derived by the following sets of equations using the following assumption: 1) Diffusion occurs only in a radial direction and not in the vertical (z) direction.

$$Q_d \frac{\partial C_d}{\partial z} - 2\pi R_l D_m \frac{\partial C_m(r_l, z)}{\partial r} = \frac{\partial C_d}{\partial t} = 0 \quad (8)$$

This partial differential equation requires an initial condition and 2 boundary conditions in order to be solved. The initial condition is that at $t=0$, $C_d = C_{in}$, where C_{in} is the concentration of the substance that enters the dialysis probe. The boundary conditions are 1) at $z = 0$, the inlet to the probe, $C_d = C_{in}$, and 2) a condition exists

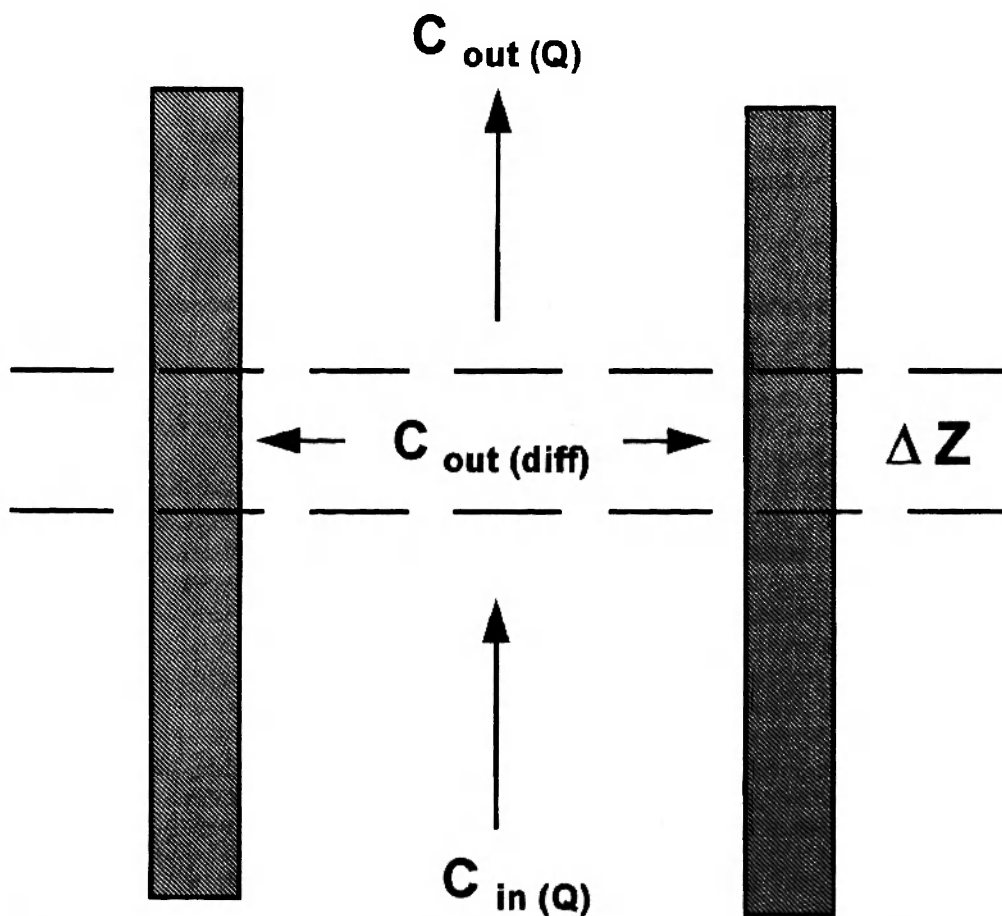


Figure 6. Control volume used for the determinations of the mass-balance equations for the dialysate.

such that the flux across the membrane is proportional to the concentration difference between the membrane and the dialysate [Bungay et al., 1990]. This boundary condition is described by Cussler as:

$$N = k (C_{1i} - C_1) \quad (9)$$

where k = a mass transfer coefficient (mass/time); C_{1i} = the concentration at the interface; and C_1 = the concentration in bulk solution. Flux for diffusion across the membrane is described in Equation 10 [Crank, 1975]

$$N = -D_m \frac{dC_m}{dr} \quad (10)$$

The right hand side of Equation 9 can be approximated by using a mass transfer coefficient approach [Cussler, 1984, pg. 300]. This approach is based on the assumption of simple mass transport through a hypothetical film [Cussler, 1984], in this case the dialysate. This is described as

$$\frac{kL}{D} = 1 \quad (11)$$

where k is the mass transport coefficient, cm/s, L is the length through which mass is being transported (the radial distance in dialysate), cm, and D is the diffusion coefficient of the substance through the hypothetical film, cm²/s. Transformed into the dialysate case the length of the path, L , simply becomes the inner radius of the fiber lumen, r_i . The inner radius is chosen rather than the diameter of the membrane

because there exists an equality of flux such that there is no change in mass concentration across the midline of the dialysate perfusion fluid. By using this

$$D_m \frac{\partial C_m(x, z, t)}{\partial x} \Big|_{x_i} = \frac{D_d [C_m(x_i, z, t) - \bar{C}_d(z, t)]}{x_i} \quad (12)$$

approximation Equation 9 is transformed into Equation 12 and is used in the finite difference solution of these equations. The assumption of the hypothetical film works well as incorporation of another mass transfer expression for laminar flow found after development gave similar answers as outputs from the model. This alternative mass-transfer correlation is described by as [Cussler, 1984, p.230]:

$$\frac{kd}{D} = 1.86 \left(\frac{dv^o}{D} \right)^{0.8} \quad (13)$$

where d is the cylinder diameter and v^o is the average velocity in the cylinder.

3.4 Solving the system of equations for microdialysis

Complex partial differential equations can be solved by a variety of methods. These methods include: finite difference methods [Carnahan et al., 1969 and Chapra and Canale, 1986], method of lines [Schiesser, 1991], and finite element methods [Chapra and Canale, 1986]. The method of lines suffers from the inability to couple several different equations together. For the microdialysis case, the role of the membrane resistance would have to be excluded in the solution process. The finite element method is typically used for complex geometries. For a simple geometry the finite difference method can be easily described in terms of FORTRAN code and is the method that was chosen to solve the microdialysis equations.

Differential equations solved by finite difference methods can be described either explicitly or implicitly [Carnahan et al., 1969]. The solution begins by defining

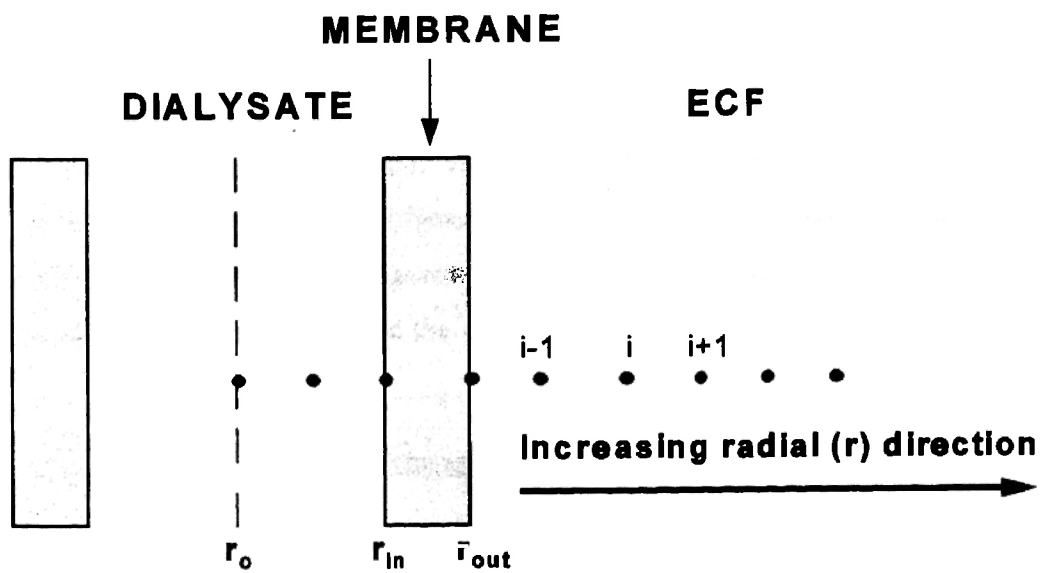


Figure 7. A grid system depicting the finite difference scheme through the membrane and the tissue space.

a grid for the system to be solved. An example of a grid for the microdialysis equations can be seen in Figure 7. In this case, the vertical (z) direction is considered negligible and is averaged. The finite difference method is derived from a Taylor's series expansion of the function. It assumes that in the direction of change in the function is a very small increment and that the function remains continuous in that increment. A Taylor's forward series expansion can be defined as:

$$f(x_{i+1}) = f(x_i) + f'(x_i) h + \frac{f''(x_i)}{2} h^2 + \dots \quad (14)$$

where h stands for the incremental step taken along the function curve. In the Taylor's series, if h is chosen to be small enough the higher order terms can be truncated [Chapra and Canale, 1986]. Equation 18 then can be solved for the derivative. For the partial differential equation describing the mass-balance in the ECF of the microdialysis experiment the finite difference equation is described in Equation 15 for diffusion and the rate constants.

$$\frac{C_{i,j+1} - C_{i,j}}{\Delta t} = \phi_{ecf} \frac{D_{ecf}}{r} \left(\frac{C_{i+1,j+1} - C_{i-1,j+1}}{2\Delta r} + \frac{C_{i+1,j+1} - 2C_{i,j+1} + C_{i-1,j+1}}{(\Delta r)^2} \right) \quad (15)$$

$$- k_{met} K_n C_{i,j+1} - k_{oi} C_{i,j+1} - k_{ie} K_n C_{i,j+1} - k_{ep} C_{i,j+1} + k_{pe} C_p + k_{gen} K_n C_{i,j+1}$$

where, $C_{i,j+1}$ is the concentration at the (i)th position in radial space volume element and the (j+1)th time point, i.e. the next incremental time point. In this equation a forward divided difference is used for the time derivative and a centered divided difference is used for the first partial in the equation. In this case the equation is written implicitly. Implicit finite difference equations require that all the radial steps be solved at one time. An explicit solution would require that only the next time point at a particular point in space be solved. Although the explicit finite difference method is well-described in the field of electrochemistry [Feldberg, 1969, Maloy,

1986, Bartlett and Pratt, 1993], it is not practical for solving the microdialysis equations.

The principal shortcoming of the explicit finite difference method is that for stability the solution diffusion coefficient, $D\Delta t/(\Delta r)^2$, λ needs to be less than 0.5 [Carnahan et al., 1969]. The explicit finite-difference approximation also has stability problems when the concentration changes in certain volume elements are rapid. Unlike electrochemical events which occur on the millisecond or lower time scale, microdialysis is bounded by the sampling interval time. Although interfaces such as capillary electrophoresis allow for shorter sampling intervals due to the nanoliter volumes necessary, the sampling performed in this thesis was on the order of minutes. In order for λ to be less than 0.5 in the microdialysis equations, the value used for Δt must be very small or the value used for Δr needs to be large. For a diffusion coefficient of $5 \cdot 10^{-6}$ cm²/s and a five minute time period, Δt , the value of Δr would have to be 547 microns or larger in order to satisfy the stability requirement. This value is larger than the membrane wall thickness which indicates that it is not suitable. Use of a small Δt greatly increases the computational time to solve the equations. Therefore the use of an implicit method is a better choice for solving the microdialysis equations.

Equation 15 describes the ECF mass-balance in terms of an implicit finite difference equation. The implicit finite difference method varies from the explicit method in that in the explicit method the solution is solved by marching forward from space point to space point and from time point to time point. In the implicit scheme, all the space points are solved simultaneously thus requiring the use of linear equation solvers. The system of equations that must be solved for is unique in that a tridiagonal matrix is formed which can be readily solved using the Thomas algorithm [Carnahan, et al., 1969] on the matrix set shown in Equation 16, where A,B,C are

coefficients derived from rearrangement of the finite difference equation in terms of the space points $i-1, i, i+1$ and also include the boundary conditions.

$$\begin{bmatrix} B & C & & & & & & & \\ A & B & C & & & & & & \\ & A & B & C & & & & & \\ & & A & B & C & & & & \\ & & & A & B & C & & & \\ & & & & A & B & C & & \\ & & & & & A & B & C & \\ & & & & & & A & B & C \\ & & & & & & & A & B \\ & & & & & & & & A & B \end{bmatrix} \begin{bmatrix} R1 \\ R2 \\ R3 \\ R4 \\ R5 \\ R6 \\ R7 \\ R8 \end{bmatrix} = \begin{bmatrix} C1 \\ C2 \\ C3 \\ C4 \\ C5 \\ C6 \\ C7 \\ C8 \end{bmatrix} \quad (16)$$

3.5 Specifics Needed for the FORTRAN code

Solution of the dialysate concentration and concentration profile from the dialysis membrane out into the ECF space begins by determining what the far field concentration is in the ECF space. The far-field concentration (∞) for a pharmacokinetics experiment is determined by using Equation 17, which is derived

$$C_e^\infty(t) = \frac{k_{pe}^x C_o e^{(-\lambda t)}}{(k_{ep}^x + k_{met} - \lambda)} + \frac{k_{pc}^x C_o}{e^{(k_{ep}^x + k_{met}) t} (k_{pc}^x + k_{met} - \lambda)} \quad (17)$$

in Appendix 3. In Equation 16, the far-field concentration in the ECF fluid space

after an i.v. infusion is a function of the initial concentration, C_0 , in the plasma, the elimination rate from the plasma, λ , and the transport and metabolism rates in the tissue space which have been defined above. Note that for a delivery experiment this far-field concentration is usually set to a value of zero.

The program begins by setting a percentage guess of the far-field concentration as the outflow dialysis concentration. Typically this guess is less than one percent of the far-field concentration for a recovery experiment. For the delivery experiment the guess is based on an incremental one percent loss from the dialysate. By using this value the program then utilizes the analytical solution of the dialysate concentration to determine the flux into or out of the fiber lumen. The program then solves for the membrane concentrations based on the boundary condition that the flux is based on a concentration difference between the membrane and the dialysate as shown in Equation 18. At the membrane/dialysate interface and the membrane/ECF interface a condition holds that the flux across these two boundaries is equal and is shown below:

$$D_m \frac{dC_m}{dr} = \frac{D_d (C_m |_{R_i} - C_d)}{R_i} \quad D_m \frac{dC_m}{dr} = D_e \frac{dC_e}{dr} \quad (18)$$

The program compares these two flux values and determines whether or not they meet a minimum tolerance (1 percent) and if not, the program increases the percentage of the guess and continues until the answer is obtained through relaxation. [Press et al., 1992]. A copy of the FORTRAN code is attached in Appendix 4 of this document.

A feature used to save computational time and space is the inclusion of a logarithmic step increase originally described by Feldberg [Feldberg, 1981]. This

logarithmic step increase was necessary as these equations were solved using Microsoft FORTRAN, which seemed to have a memory limitation that would not allow the arrays to be greater than 700. Because the Taylor's series approximation is assumed in the finite difference approximation, small values of Δr are necessary to achieve an answer closer to the 'true' value. For large values of the far-field radius, the number of radial spaces could exceed 700. The logarithmic approximation used in the solution of these equations is shown in Equation 19

$$\Delta r = \Delta r_o e^{\beta(i-1)} \quad \beta \leq 0.5 \quad (19)$$

where i is the space step and β is a tolerance. The logarithmic approximation allows the values Δr to stay small near the membrane, where the greatest rate of change in the concentration will occur. Feldberg found that for most cases this equation worked fairly well for $\beta < 0.5$. For the microdialysis model, $\beta = 0.005$. In Figure 8, the effects of various tolerances is depicted. Table 1 shows the differences in the outflow concentrations and calculated deliveries for the various values of β that were shown in Figure 8. There is a 2.0% absolute error difference in the predicted dialysate percent delivery using $\beta=0.005$ versus $\beta=0.0$. Although a lower beta will give a lower error this has to be weighed with the memory that can be lost with the computer as well as the computational time involved with the calculation. In the program the default Δr is the difference between the inner and outer membrane divided by 10. Since the model will be used in conjunction with analytical data obtained *in vivo* it is suspected that the data obtained would not have an error associated with it of less than 2.0 %.

The program initially had a time instability with the early data points. This was solved through the use of the subroutine RAMP described in the FORTRAN code

in Appendix 4. RAMP is used to get numerical values into the concentration vectors. This gives more accuracy in the first time step as then the values don't go from a zero value to another value.

3.6 Adaptations to the Original Program

The solutions to the equations above fit well with similar solutions from the program of Morrison. There are a few advantages of using the complete numerical approach. The first is that the analytical approach of Morrison reduces the role of the membrane in the equation solution. With the finite difference approach the membrane's diffusivity is always included in every microdialysis calculation. The present program can be modified to include different types of microdialysis experiments such as euthanasia or metabolite recovery after a delivery of a parent compound. In a euthanasia situation, it could be envisioned that k_{ep} , the microvasculature permeability rate constant falls to zero. In a recovery of metabolites from a local delivery, the boundary conditions near the dialysis probe would require modification.

3.6.1 Euthanasia of the Animal

For the effect of euthanasia, the initial condition must be modified. In this case, the initial concentration of the substance being dialyzed is no longer zero or a fixed concentration, but rather the concentration gradient of that substance prior to death. This change in the initial condition is easily incorporated into the main program. The parts of the program that are different than the main program entitled 'DIALYSIS.FOR' are shown in Appendix 5 for the program 'DEADDIAL.FOR'. With this the outflow concentration of the dialysate can be modelled over time and its decay can be approximated.

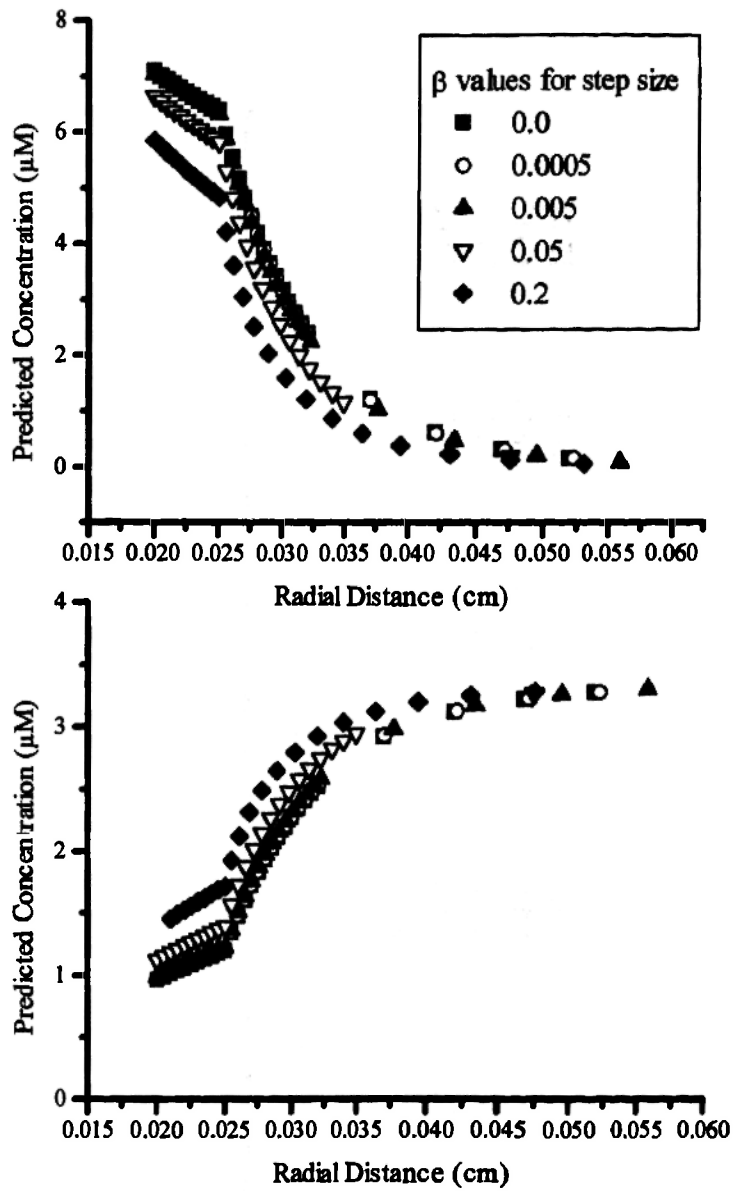


Figure 8. Effect of the tolerance β on the predicted concentration profile from the mathematical model 'DIALYSIS.FOR'.

Table 1. Error associated with the value of β in the exponential step function.

Beta	# Steps	predicted [outflow]	% Delivery	% Error	% Error [outflow]
0.0	462	7.822	21.77	-	-
0.0005	417	7.817	21.82	0.22	0.063
0.005	248	7.779	22.21	2.02	0.56
0.05	75	7.469	25.30	16.21	4.51
0.2	35	6.883	31.16	43.17	12.01

3.6.2 Metabolite formation

An interesting use of the microdialysis model would be to use it in conjunction with metabolite studies and thus determine the concentration of metabolites that could be generated. This is especially useful in conjunction with the experiments, which are described in Chapter 4 indicating that at least in the liver, blood flow dominates the kinetic processes *in vivo*. This means that from a single recovery or delivery experiment the value of the rate constants are non-parsimonious, that is the values could be a combination of a variety of values. However, the value of the metabolic formation for specific metabolites may be obtainable. Here the initial concentration will be a function of the metabolic rate constant in the tissue space. The file DATAFILE.DAT needs to be modified and the program runs under METAB.FOR. An example of the output is shown in Figure 9.

3.6.3 Non-linear kinetics in microdialysis

Biological reactions that involve metabolism or receptor uptake are described by the use of non-linear kinetics. For enzyme metabolism, this is termed Michaelis-Menten kinetics. Since microdialysis samples from tissue which will contain enzymes, it is possible that these kinetic rates are not linear as assumed above for the development of this microdialysis model. In these cases the diffusion and kinetic rates can be expressed in a concise manner as shown in Equation 20

$$\frac{dC(r)}{dt} = \frac{D_{ecf}}{r} \frac{d}{dr} \left(r \frac{dC(r)}{dr} \right) - \left(\frac{k_{cat} C(r)^n}{K_m + C(r)^n} \right) = 0 \quad (20)$$

where k_{cat} is the turnover number for the enzyme, and n is the Hill coefficient which

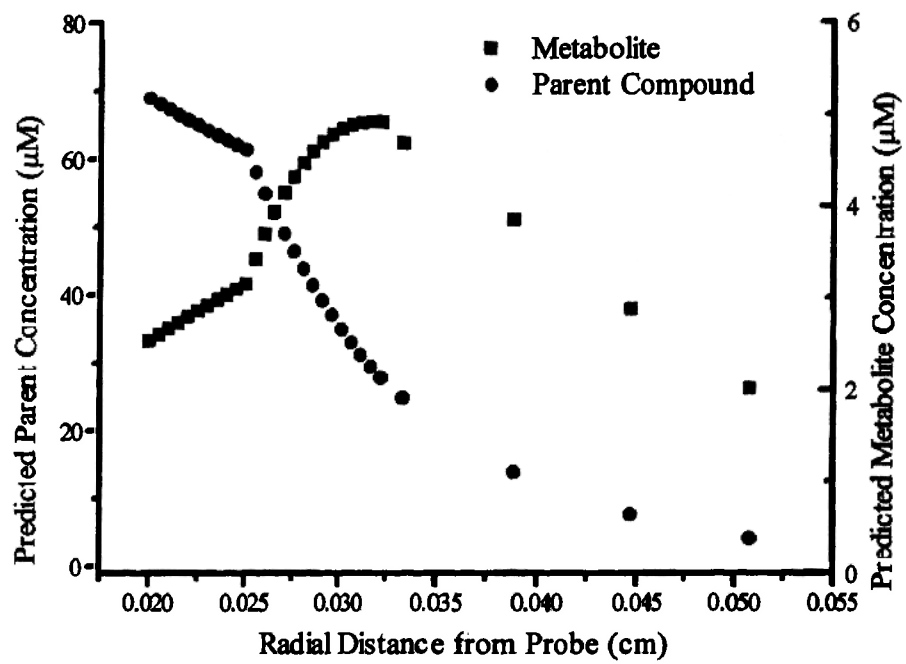


Figure 9. Predicted metabolite concentration profile after local infusion of a parent substance using 'METAB.FOR'

can have a non-integer value of 1 or greater. Equation 20 assumes that the amount of enzyme is constant. Considering the case for when material is delivered, the highest concentration of material will be nearest to the dialysis probe. If this concentration is greater than one tenth of the value of the Michaelis constant, K_m , then the kinetics in that region would be non-linear. However, further away from the probe, the kinetics would approach the linear limit as the concentration decreases away from the probe. The argument for the recovery case is the opposite, the kinetics near the probe will approach the linear limit whereas at a distance from the probe, the kinetics would be non-linear.

The non-linear term was added to the analytical equation derived at the beginning of this chapter, Equation 1, and a solution was obtained for the kinetic rate constants depicted in Figure 10. The inset shows that the concentration profile near the dialysis probe matches that of the linear limit shown, 0.5 min^{-1} . However, further away from the probe, the concentration profile approaches the other limit of 1.0 min^{-1} . The flux out of the probe will depend upon the concentration profile near the probe, thus it will be approximated by the lower limit of 0.5 min^{-1} . Therefore, using the numerical model described above with the linear kinetic terms at the lower limit will best approximate the non-linear terms without further extensive computation. However, the non-linearities may affect the recovery and delivery terms. This indicates that when Michaelis-Menten kinetics describe the rates in the tissue, the values of *in vivo* recoveries may not match *in vivo* deliveries.

3.7 Strengths and limitations of the model

The mathematical model derived here has several advantages and disadvantages. Several of these points have already been mentioned by Morrison et al. [Morrison et al., 1991]. If the kinetic rate values are known along with the *in vivo* diffusion coefficient, then the model can be used in lieu of a calibration method such

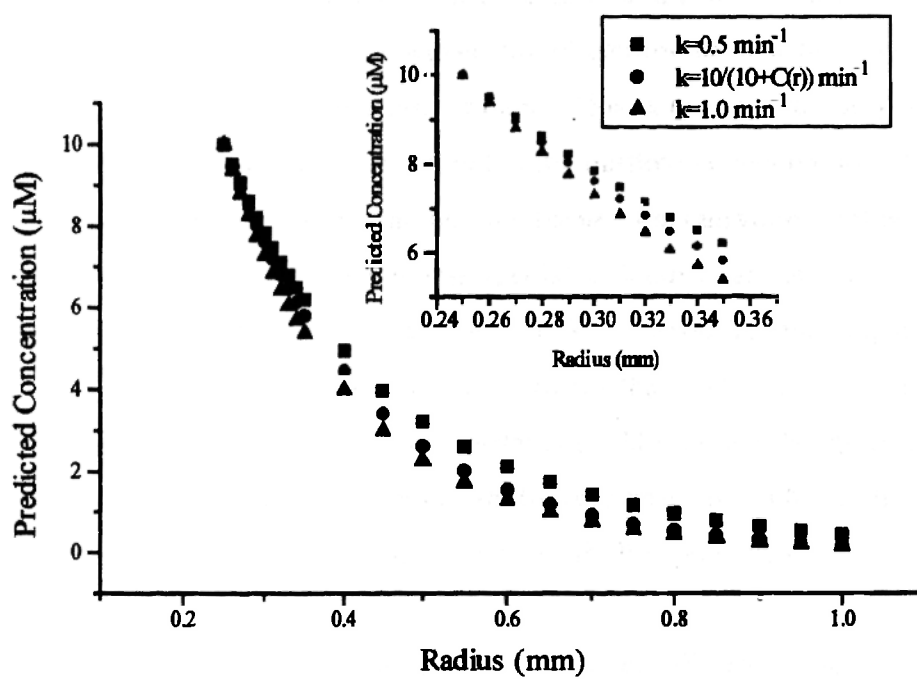


Figure 10. Predicted concentration profile away from a hypothetical cylindrical probe using linear and Michaelis-Menten kinetics.

as the Lonroth no-net-flux method. However in many cases the values of the *in vivo* diffusion coefficient are not known and therefore the value must be scaled from *in vitro* values. Rice et al.[Rice et al., 1986] have pointed out that this can lead to a discrepancy in the diffusion coefficient of an order of magnitude for cationic substances such as dopamine and norepinephrine.

This model does allow the researcher to determine which factors, such as the kinetic rate constants, the diffusion coefficient, or the membrane, will affect the microdialysis values the most. However model confirmation with experimental data will be limiting for this microdialysis model. This is because the only value that is measured in the microdialysis experiment is the outflow concentration. This outflow concentration profile is dependent on the tissue concentration profile around the dialysis probe which is unknown unless special techniques are employed such as the use of autoradiography [Dykstra et al., 1992, 1993]. Therefore matching model output with experimental data is a poor way to confirm the model as any combination of diffusion coefficients or reaction rate constants could produce the model output. For this reason, the use of the model in metabolic recoveries is useful as the metabolism values will be the same for the parent and metabolite generation.

An essential part of model-building is model discrimination and parameter estimation [Box and Hunter, 1962, 1965]. These concepts also illustrate more of the limitations with the microdialysis model. Model discrimination is difficult because multiple mechanistic models have not been created. Additionally the problems of confirmation with only one experimental output readily measurable (outflow concentration) make it difficult to try to improve the microdialysis model. Since the microdialysis model has not be truly confirmed through experimental data, parameter estimation may not provide the 'true' results for the kinetic rate constants and *in vivo* diffusion coefficients. Additionally if parameter estimation is a goal of the

microdialysis model, then sensitivity analyses will be necessary [Seinfeld and Lapidus, 1974, Koda et al., 1979]. Sensitivity analyses are necessary to determine the amount of error that would be obtained in the output as a result of error in the parameter estimation. For analytical diffusion-reaction models, there are set methods available to determine the sensitivity of the model to errors [Koda et al., 1979]. However for the microdialysis model described here, the sensitivity analysis may need to be performed one variable at a time due to the coupling of the non-linear equations. It may be possible to apply statistical methods such as partial least squares regression (PLS) to the microdialysis model to obtain a sensitivity analysis. However intuitively, it should be realized that errors in the value of the perfusion fluid flow rate and the volume fraction of the ECF will affect the output of the microdialysis model the most.

3.8 References

- Abramowitz, M.; Stegun, I.A. (Eds.) *Handbook of Mathematical Functions*, National Bureau of Standards: Washington, D.C., 1964.
- Bartlett, P.N.; Pratt, K.F.E. Modelling of processes in enzyme electrodes. *Biosensors Bioelectronics* 1993, 8, 451-462.
- Bird, R.B.; Stewart, W.E; Lightfoot, E.N. *Transport Phenomena*, John Wiley & Sons: New York, 1960.
- Box G. E. P.; Hunter W. G. A useful method for model-building. *Technometrics* 1962, 4, 301-318.
- Box, G.E.P.; Hunter, W.G. The experimental study of physical mechanisms. *Technometrics* 1965, 7, 23-42.
- Box, G.E.P.; Hunter, W.G.; Hunter, J.S *Statistics for Experimenters: An Introduction to Design, Data Analysis, and Model Building*, John Wiley & Sons: New York, 1978.
- Bungay, P.M.; Morrison, P.F.; Dedrick, R.L. Steady-state theory for quantitative microdialysis of solutes and water in vivo and in vitro. *Life Sci.* 1990, 46, 105-119.
- Carnahan, B.; Luther, H.A.; Wilkes, J.O. *Applied Numerical Methods*. Robert E.

Krieger Publishing Co.; Malabar, Florida, 1990.

Chapra, S.C.; Canale, R.P. *Numerical Methods for Engineers, 2nd Edition*, McGraw-Hill, Inc.:New York, 1988

Christian, G.D. Evolution and revolution in quantitative analysis. *Anal. Chem.* **1995**, *67*, 532A-538A.

Crank, J. *The Mathematics of Diffusion, 2nd Edition*. Clarendon Press: Oxford, 1975.

Cooper, J.R.; Bloom, F.E.; Roth, R.H. *The Biochemical Basis of Neuropharmacology, 6th edition*. Oxford University Press: New York, 1991.

Cussler, E.L. *Diffusion: Mass Transfer in Fluid Systems*. Cambridge: Cambridge University Press. 1984

Dykstra K. H., Hsiao J. K., Morrison P. F., Bungay P. M., Mefford I. N., Scully M. M., and Dedrick R. L. Quantitative examination of tissue concentration profiles associated with microdialysis. *J. Neurochem.* **1992**, *58*, 931-940.

Dykstra K. H., Arya A., Arriola D. M., Bungay P. M., Morrison P. F., and Dedrick R. L. Microdialysis study of zidovudine (AZT) transport in rat brain. *J. Pharmacol. Exp. Ther.* **1993**, *267*, 1227-1236.

Feldberg, S.W. Digital simulation: A general method for solving electrochemical diffusion-kinetic problems. in A.J. Bard, ed. *Electroanalytical Chemistry: A Series of Advances, Vol. 3*. Marcel Dekker, Inc.; New York, 1969.

Feldberg, S.W. Optimization of explicit finite-difference simulation of electrochemical phenomena utilizing an exponentially extended space grid: Refinement of the Joslin-Pletcher algorithm. *J. Electroanal. Chem.* **1981**, *127*, 1-10.

Goresky, C.A.; Schwab, A.J. Flow, cell entry, and metabolic disposal: Their interactions in hepatic uptake. In *The Liver Biology and Pathobiology, Second edition* I.M. Arias, W.B. Jakoby, H. Popper, D. Schachter, eds. Raven Press Ltd.: New York 1988.

Hsiao, J. K., Ball, B. A., Morrison, P. F., Mefford I. N., and Bungay P. M. Effects of different semipermeable membranes on in vitro and in vivo performance of microdialysis probes. *J. Neurochem.* **1990**, *54*, 1449-1452.

Koda, M.; Dogru, A.H.; Seinfeld, J.H. Sensitivity analysis of partial differential equations with application to reaction and diffusion processes. *J. Comp. Phys.* 1979, 30, 259-282.

Maloy, J.T. Digital Simulation of Electrochemical Processes in P.T. Kissinger and W.R. Heineman, eds. *Laboratory Techniques in Electroanalytical Chemistry*, Marcel Dekker, Inc.: New York, 1984, 417-460.

Mickley, H.S.; Sherwood, T.K.; Reed C.E. *Applied Mathematics in Chemical Engineering, 2nd edition*, McGraw-Hill Book Company: New York, 1957, 163-200.

Morrison, P.F.; Bungay, P.M.; Hsiao, J.K.; Mefford, I.V.; Dykstra, K.H.; Dedrick, R.L. Quantitative microdialysis. In *Microdialysis in the Neurosciences*. T.E. Robinson and J.B. Justice Jr., eds. Elsevier: Amsterdam, 1991, 47-80.

Press, W.H.; Flanner, B.P.; Teukolsky, S.A.; Vetterling, W.T. *Numerical Recipes in FORTRAN: The Art of Scientific Computing, 2nd edition*; Cambridge University Press: Cambridge, 1986.

Rice, M.E.; Gerhardt, G.A.; Hierl, P.M.; Nagy, G.; Adams, R.N. Diffusion coefficients of neurotransmitters and their metabolites in brain extracellular fluid space. *Neuroscience* 1985, 15, 891-902.

Sakai K. Determination of pore size and pore size distribution 2. Dialysis membranes. *J. Membrane Sci.* 1994, 96, 91-130.

Schiesser, W.E., *The numerical method of lines, Integration of partial differential equations*. Academic Press, Inc., San Diego, 1991.

Seinfeld J. H.; Lapidus L. *Mathematical methods in chemical engineering. Volume 3. Process modeling, estimation, and identification*; Prentice-Hall, Inc.: Englewood Cliffs, New Jersey, 1974.

Smith A. D.; Justice J. B. The effect of inhibition of synthesis, release, metabolism and uptake on the microdialysis extraction fraction of dopamine. *J. Neurosci. Methods* 1994, 54, 75-82.

Chapter 4

Liver microdialysis: Identification of processes that contribute to the flux from the probe using model compounds phenacetin, antipyrine, and acetaminophen.

4.1 Introduction

The liver is a highly complex organ that is devoted to many special tasks including endocrine production, gluconeogenesis and metabolism of xenobiotics. Metabolism in any specific site in the liver is difficult to study as the blood flow pattern through the organ creates metabolic zones which differ in oxygen tension and drug metabolism ability [Thurman and Kauffman, 1985, Pang et al. 1994]. In addition to the metabolic complexity the liver is difficult to study *in vivo* due to its anatomical attachment. For example, in the brain it is easier to locate the same position from one experiment to the next with the use of a stereotaxic unit. Because of the structure of the brain, the implantation point of the microdialysis probe can be verified by comparison with an atlas. Since a stereotaxic atlas for the liver does not exist, placement of a probe in the same area from one experiment to the next is difficult to achieve. *In vitro* techniques such as the use of microsomal fractions, isolated hepatocytes, and perfused liver preparations, which were discussed in Chapter 1, have been developed to study the liver and its function. Although the use of these *in vitro* techniques can provide useful information concerning metabolism and uptake of drugs, they disturb the physiology of the animal. These techniques also by their means of disrupting the physiology, also disrupt processes which may be interconnected such as the blood flow rate and the uptake of compounds into the hepatocytes. A technique which can be used *in vivo* and not disrupt the normal physiology of an animal is desirable to study drug effects quantitatively in the liver.

This chapter presents experiments that were performed to determine how metabolism and uptake rates affect the flux of a substance from the microdialysis

probe. In particular, the change in the flux (amount of a substance delivered) of specific compounds from the microdialysis probe after selective inhibition experiments was studied. If the flux of the microdialysis probe changes in animals with inhibited metabolism, then the mathematical model developed in Chapter 3 could be applied to approximate the values of the rate constants that were inhibited. In the liver, it is expected that the major contributions to the microdialysis flux include the permeability of the substance across the sinusoids, k_{sp} (in the model), and the metabolism, k_m of the substance. If the flux does change with the inhibition of metabolism, then microdialysis in conjunction with a mathematical model could provide an alternate method to determine kinetic rate constant values as compared to difficult isolated perfused liver studies [Gores et al., 1986].

4.1.2 Inhibition Studies

Phenacetin and antipyrine were chosen to study the effect of inhibition on the microdialysis flux. These test drugs were chosen for several reasons. 1) They have been well-characterized *in vivo* in rat liver and there exists a large body of knowledge concerning these drugs. 2) Both of these compounds are metabolized through the cytochrome P450 isozymes, which will allow for easier inhibition than substances that undergo conjugation such as acetaminophen. The cytochrome P450 enzyme system can be inhibited through entities such as suicide substrates which block the binding and electron transport system of the cytochrome. Generally for enzymes that conjugate compounds, the best way to block those enzymes is to include a substrate that rapidly utilizes most of the co-factor necessary for the conjugation reaction rather than through inhibition of the enzyme [Hanzlik, 1991]. 3) Phenacetin is a high-clearance drug and antipyrine is a low-clearance compound. In metabolic terms this means that the metabolic rates associated with phenacetin are more rapid than that for antipyrine. A high clearance compound is defined as a compound which is removed more than 70 percent from a first pass through an isolated perfused liver preparation.

A low clearance compound is defined as one in which less than 30 percent is extracted after first pass metabolism [Gibaldi and Perrier, 1982]. Phenacetin is *o*-deethylated in the rat by CYP 1A2 [Seasardic, 1990a,1990b] and antipyrine is oxidized by three different rat P450's. Figures 1 and 2 depict the metabolic pathways for phenacetin and antipyrine.

An animal can be made cytochrome P450 deficient by using cobalt protoporphyrin IX [Drummond and Kappas, 1982, Spaethe and Jallow, 1989; Muhuberac et al., 1989]. Cobalt Protoporphyrin IX (CoProto IX) represses δ -aminolevulinate synthase, which is the rate limiting enzyme of heme biosynthesis. CoProto IX also potently induces microsomal heme oxygenase, which is the rate limiting enzyme of heme catabolism. These two effects cause the cytochrome P450 levels to decrease in the liver. Cobalt chloride can also be used for this purpose, but has some disadvantages. Cobalt chloride produces a short lived suppression of the heme oxygenase levels (48-72 hours versus the protoporphyrin's 2-10 days), and it causes an increase in the levels of hepatic glutathione, an enhancement of acetaminophen glucuronidation, and a suppression of acetaminophen sulfation. Cobalt Protoporphyrin IX was used for some initial experiments in this chapter. A problem with this compound was that it caused the rats to lose weight and hair. It was then decided that although the CoProto IX was documented in the primary literature as a means to make an animal P450 deficient, it would be more appropriate on ethical and scientific grounds to use a different inhibitor.

The antidepressant drug fluvoxamine was found to be a CYP 1A2 inhibitor [Brøsted, 1993] and could be used as a means of inhibiting phenacetin metabolism. Fluvoxamine was given as a systemic dose for some experiments. In other experiments, it was co-perfused with phenacetin. Initially no change was observed and disagreements from the manufacturer proved that it would be difficult to obtain

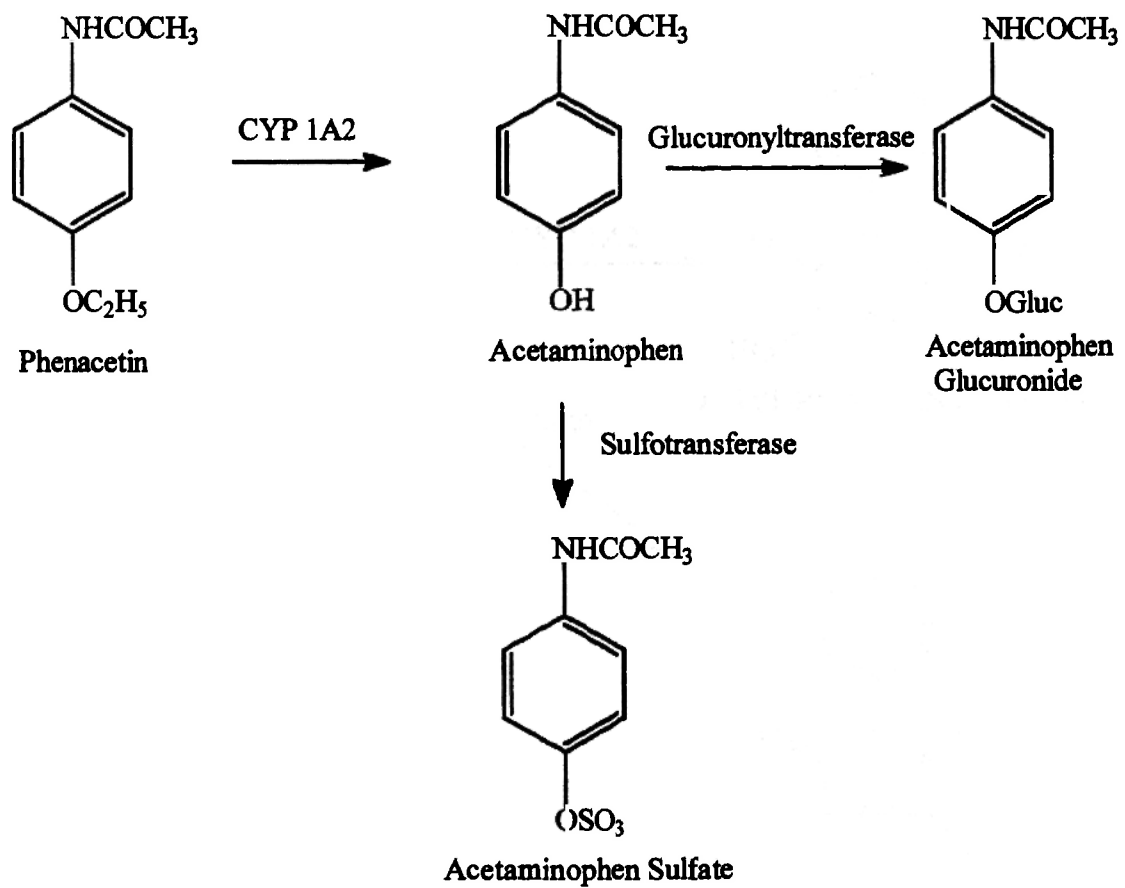


Figure 1. Metabolic disposition of phenacetin and its metabolite acetaminophen.

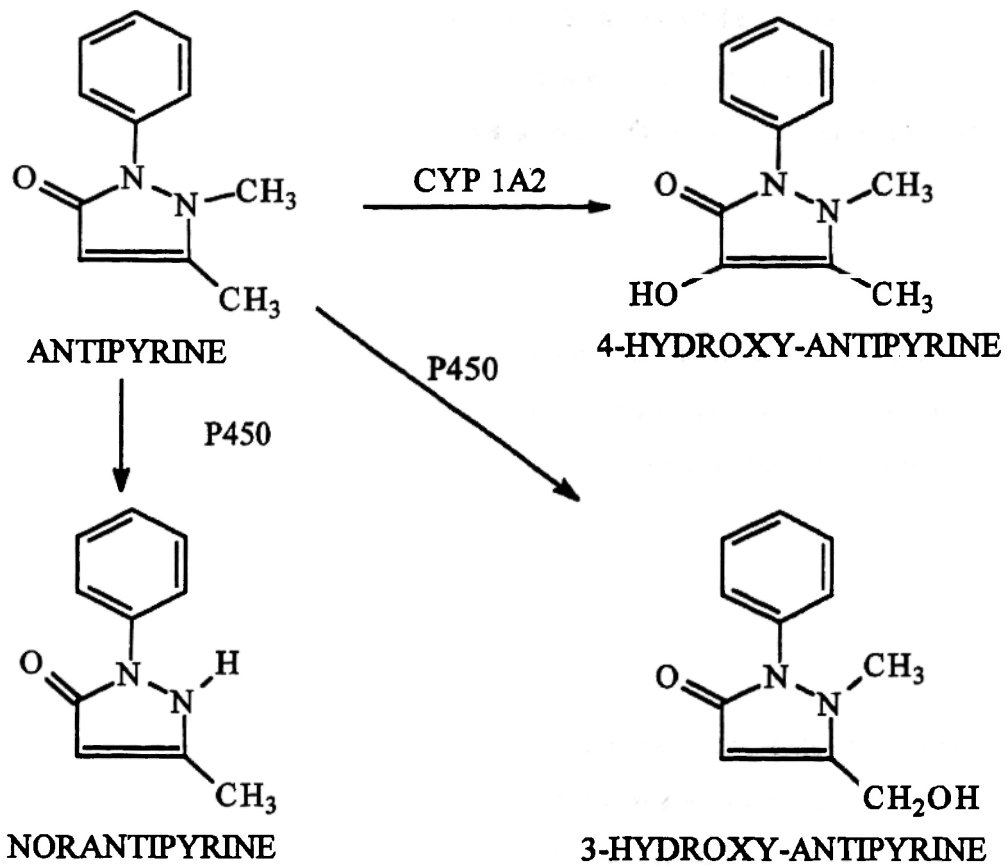


Figure 2. Antipyrine metabolic schme.

enough to continue the studies with this drug.

Since CoProtoIX could not be used to inhibit cytochrome P450 because of the ethical considerations and fluvoxamine became unavailable, the suicide substrate 1-aminobenzotriazole (1-ABT) was chosen. 1-ABT is a suicide substrate for CYP 1A2 [Mico et al, 1987,1988]. A suicide substrate is a substance that binds irreversibly to the cytochrome thus causing it to lose activity [Ortiz de Montellano, 1983]. 1-ABT has the advantage that the effect is short term because heme synthesis replaces the destroyed heme which causes the content of the active CYP 1A2 to increase after 48 hours.

4.1.3 Metabolite Studies

For metabolite studies phenacetin and acetaminophen were used. Again these compounds were chosen because of the extensive body of knowledge in the literature and because the metabolic rates for these compounds are greater than the antipyrine metabolic rate [Houston, 1994].

4.2 Materials and Methods

4.2.1 Materials

A CMA-10 microdialysis probe with a 4 mm polycarbonate membrane, (CMA/Microdialysis AB Stockholm, Sweden or CMA/Microdialysis Acton, MA) with 20 cm of FEP inlet tubing and 3 cm of FEP outlet tubing was used and was prepared according to the instructions given by the manufacturer. Briefly this initial preparation involves rinsing and flushing the probe with ethanol to remove the glycerol used in the manufacturing process. After the flushing period, the probe is ready for use.

Phenacetin, antipyrine, acetaminophen, acetaminophen glucuronide, 1-aminobenzotriazole, and cobalt protoporphyrin IX were obtained from Sigma (St.Louis, MO). Acetaminophen sulfate was a gift from the McNeil Consumer Products Company (Ft. Washington, PA) Fluvoxamine was a gift from Docent Leif Bertilsson at the Department of Clinical Pharmacology, Huddinge University Hospital, Huddinge, Sweden. Halothane and Ringer's solution were obtained from Apoteksbolaget at the Huddinge University Hospital, Huddinge, Sweden. Ketamine and Xylazine were obtained from the local animal care facility at the University of Kansas. Sprague-Dawley rats were obtained from ALAB (Sollentuna, Sweden) and were allowed at least 24 hours to accommodate to the animal facility prior to use. Sprague-Dawley rats used at the University of Kansas were obtained from a local breeding colony.

4.2.2. Ethical Statements

All animal experimental procedures were approved by the local ethical committee at the Huddinge University Hospital and the local IUCUC at the University of Kansas.

4.2.3 *In Vitro* Experiments

In vitro samples were obtained by placing the dialysis probe in an *in vitro* stand attached to a CMA 102 syringe pump (CMA/Microdialysis AB Stockholm, Sweden). The probe is placed in a 2.0 ml microcentrifuge tube which contained Ringer's solution and was perfused with the drug of interest at a concentration of 5 μ M at flow rates of 0.5, 1.0 and 2.0 μ l/min. 10 μ l of dialysate was collected for LC analysis. These studies were performed to check probes removed from the package and to assess the performance of re-used probes.

4.2.4 *In vivo* Experiments

Surgical procedure: Male Sprague-Dawley rats weighing 220-280 grams were used. The rat was anesthetized using Halothane and was placed on its back with its tail facing the operator. For pharmacokinetic studies the left jugular vein was exposed by making an incision just above the animal's collar bone. In young rats, the jugular vein is clearly visible whereas in the heavier animals, fat tissue was removed through blunt dissection in order to locate the jugular vein.

The liver was exposed by making an incision perpendicular to the midline of the animal approximately one cm from the xyphoid process. The lower lobe (right) is then secured to the abdominal wall by preparing a suture through the skin on the left side of the incision and then by gently inserting the suture needle through the edge of the lobe (left side of the operator) and tightening it. On the right side of the incision, a second suture is passed through the abdominal wall to secure the microdialysis probe. A 23 gauge needle is used to gently pierce the outside of the liver tissue so that the dialysis probe can be inserted into the tissue. A small amount of blood will emerge from this puncture and the dialysis probe is then inserted carefully through this hole toward the animal's head and parallel to the midline of the animal. Note that the 23 gauge needle is only used to pierce the outside of the tissue and is not used to create a channel for the indwelling probe.

The FEP tubing connected to the syringe pump is then taped to the animal's body to prevent the probe from causing damage to the liver through movement. The cannula is secured to the skin by a third suture. This allows the probe to move with the animal's respiration. This is illustrated in Figure 3. This prevents the probe from moving excessively during the experiment. Normally this procedure does not cause any bruising around the dialysis probe. However on some animals a bruise was observed and thus that animal was not used and was euthanized. Finally a large piece

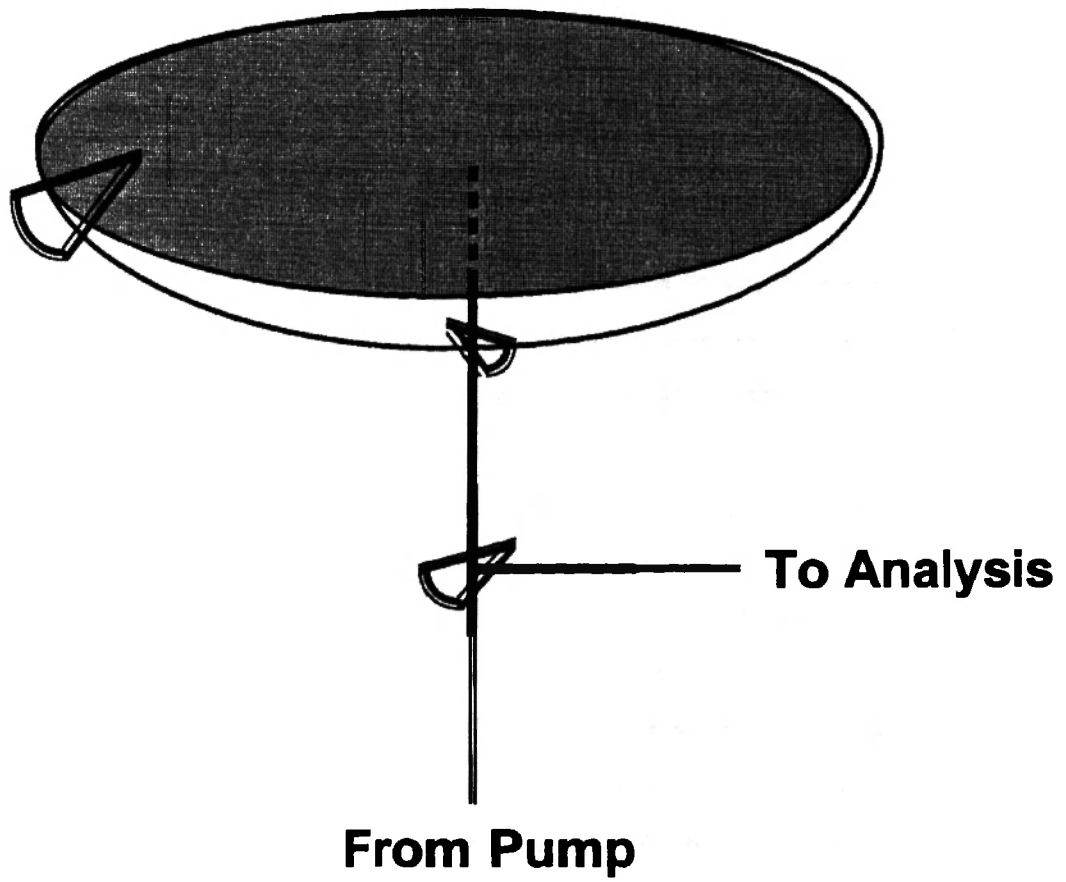


Figure 3. Implantation of CMA-10 probe into liver tissue.

of tape is used to cover the incision and to prevent the liver from becoming dehydrated.

The microdialysis probe was perfused with a 5 μM phenacetin Ringer's solution at a rate of 0.5 $\mu\text{l}/\text{min}$ or 1.0 $\mu\text{l}/\text{min}$ for the delivery studies and 2.0 $\mu\text{l}/\text{min}$ for the pharmacokinetic studies. Dialysates were collected for 50 minutes (two 25 μl samples) for the 0.5 $\mu\text{l}/\text{min}$ experiments and 45 minutes (three 15 μl samples) for the 1.0 $\mu\text{l}/\text{min}$ experiments to allow for equilibration. These dialysates were analyzed, but were not included in the calculation of the amount lost.

When pharmacokinetic experiments were performed after delivery of the drug, the probe was allowed to flush for 45 minutes prior to i.v. injection of the drug. With phenacetin, the animal was dosed at 5 mg/kg with a solution that contained 75/25 (v/v%) Ringer's solution/propylene glycol. A propylene glycol solution which contained 10 mg/ml was used to make the dilution with the Ringer solution. This was necessary as phenacetin has a water solubility of approximately 1 mg/1.3 ml H_2O [Merck Index]. Although phenacetin does dissolve in ethanol, this is not recommended as even small amounts of ethanol given i.v. to a rat will cause the blood alcohol concentration to reach intoxicating levels. For this reason propylene glycol is used as it is safe to inject i.v. and is converted to lactic acid *in vivo*. Pharmacokinetic samples were collected using a perfusion rate of 2.0 $\mu\text{l}/\text{min}$ in order to obtain the early time points on the kinetic curve.

1-ABT was dissolved in a saline solution. Animals were dosed at a level of 50 mg/kg with a 25 mg/ml solution of 1-ABT. This is approximately ten times the molar concentrations used for phenacetin and gave complete inhibition. One hour was allowed to pass before delivery samples were obtained or pharmacokinetic studies were begun.

In the metabolite studies, blanks without the phenacetin or acetaminophen in the Ringer's solution were necessary to identify possible interferences. After collection of Ringer's blanks at 1 μ l/min, an electronic syringe selector is used to switch to the sample syringe containing the substance to be perfused to prevent the introduction of air bubbles.

4.2.5 LC Analyses

A CMA/250 LC pump connected to a CMA/260 degasser (CMA Microdialysis AB, Stockholm, Sweden) was used with a Knauer fixed-wavelength UV photometer (Knauer, Germany). A Phenomenex C-8 spherex 3 μ m column (150 mm x 2.0 mm(i.d.)) (Torrence,CA) was used at a flow rate of 0.22 ml/min. Mobile phase conditions for the compounds studied were: phenacetin - 70/30 (v/v%) 0.05 M NaH_2PO_4 pH 2.7/acetonitrile, antipyrine - 75/25 (v/v%) 0.05 M NaH_2PO_4 pH 2.7/acetonitrile with 4 ml/liter tri-ethylamine, and acetaminophen and its metabolites acetaminophen sulfate and acetaminophen glucuronide - 97/3 (v/v%) 0.05 M NaH_2PO_4 pH 2.7/acetonitrile. An underfill injection of 7 μ l from the 10 μ l samples was performed manually with a Cheney adapter attached to a Hamilton HPLC syringe to provide greater reproducibility.

4.3 Results and Discussion

Microdialysis is an invasive technique. Upon insertion of a dialysis probe there will be damage to the local tissue site [Ungerstedt, 1991, Davies and Lunte, 1995]. This damage may include disruption of cell membranes and rupturing of capillaries. The disruption of cell membranes will release cellular components such as NADPH. This response can be observed in the blanks that are obtained prior to the collection of samples. The cellular species are usually hydrophilic and in a typical chromatogram for acetaminophen it can be seen that there is a large amount of material that elutes with or after the void response, which is an indication of a

hydrophilic material. The level of this void response decreases over time which is an indication that the liver is beginning to stabilize after the initial trauma associated with the insertion of the microdialysis probe. The void responses are shown in Figure 4 for post-surgical samples collected at 15 minutes (A), 30 minutes (B) and 45 minutes (C).

4.3.1 Inhibition Studies

Figure 5 shows the pharmacokinetic curves for control, cobalt protoporphyrin IX, fluvoxamine and 1-ABT treated animals. The half-lives and clearance values obtained from the CoProto IX and fluvoxamine inhibited animals were not different when compared to control values. The combination of poor inhibition of phenacetin and the difficulties with obtaining and using these two compounds provided a basis for rejecting their use in further experiments.

Figure 5 shows that 1-ABT increased the half-life of phenacetin clearance and Table I shows the pharmacokinetic parameters of the control animals and 1-ABT treated animals. A 90 percent inhibition of the phenacetin metabolism was obtained using 1-ABT. The percent inhibition of the phenacetin by 1-ABT was determined by using the method reported by Mico et al.[Mico et al. 1988]. Note that 1-ABT is a potent inhibitor as an accidental dose of only 5 mg/kg gave a two-fold increase in the elimination half-life of phenacetin. These experiments were performed in separate rats because it is difficult to maintain rats on halothane for longer than four hours. This is partly due to congestion that builds up in the animal's airway that causes the animal to have difficulty breathing. Atropine can be used to relieve the muscle spasms that may occur, but this does not always save the animal's life. The delivery experiments in conjunction with the clearance measurements require at least seven hours of anesthesia. This same problem occurs with the 1-ABT treated animals. Indeed, it may be argued that a better experimental design would have been to collect

Table I. Phenacetin pharmacokinetics in control and 1-ABT treated animals

	$t_{1/2}$ (min)	V_d (liter)	Clearance (l/min)
Controls	35.4	2.73	0.053
	30.7	1.53	0.034
	41.3	1.64	0.028
	43.2	1.44	0.023
Average	37.7	1.84	0.034
Std. Dev.	5.71	0.60	0.013
1-ABT treated	177.4	11.7	0.0046
	349.0	1.00	0.0020
	264.0	1.70	0.0044
Average	263.7	1.29	0.0037
Std. Dev.	85.8	0.36	0.0015

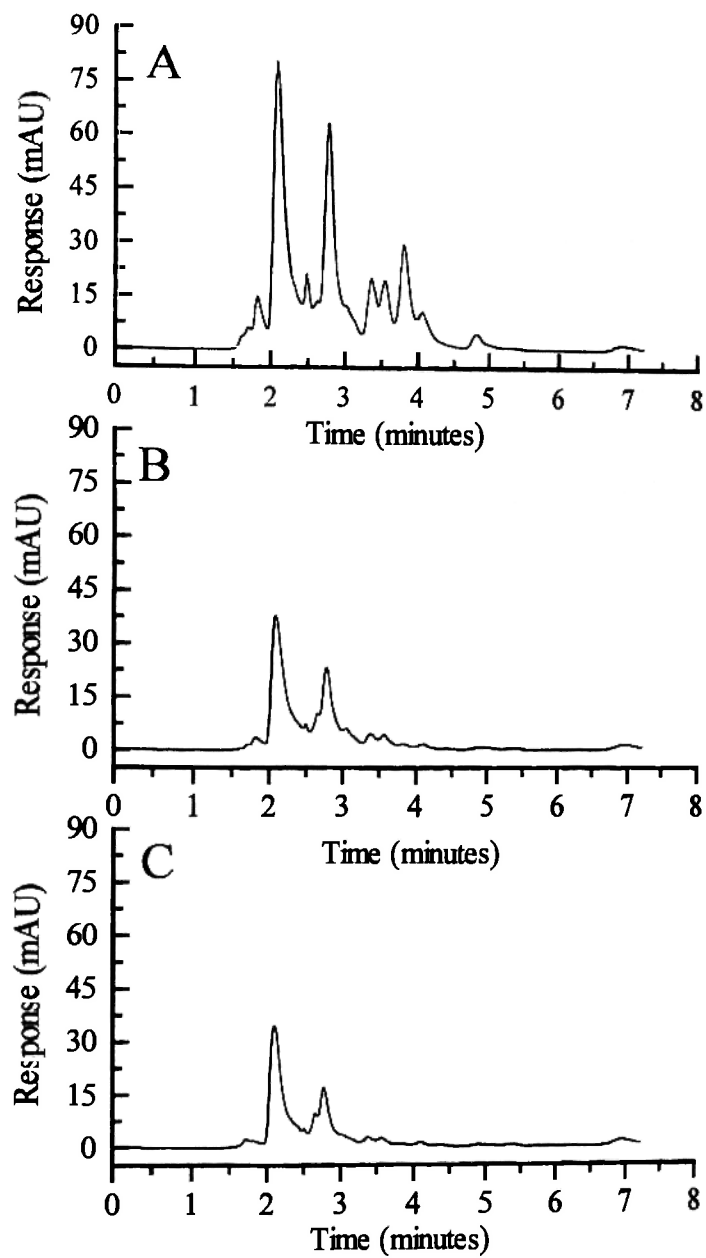


Figure 4. Chromatograms of blanks obtained from rat liver at 15, 30 and 45 minutes post-surgery.

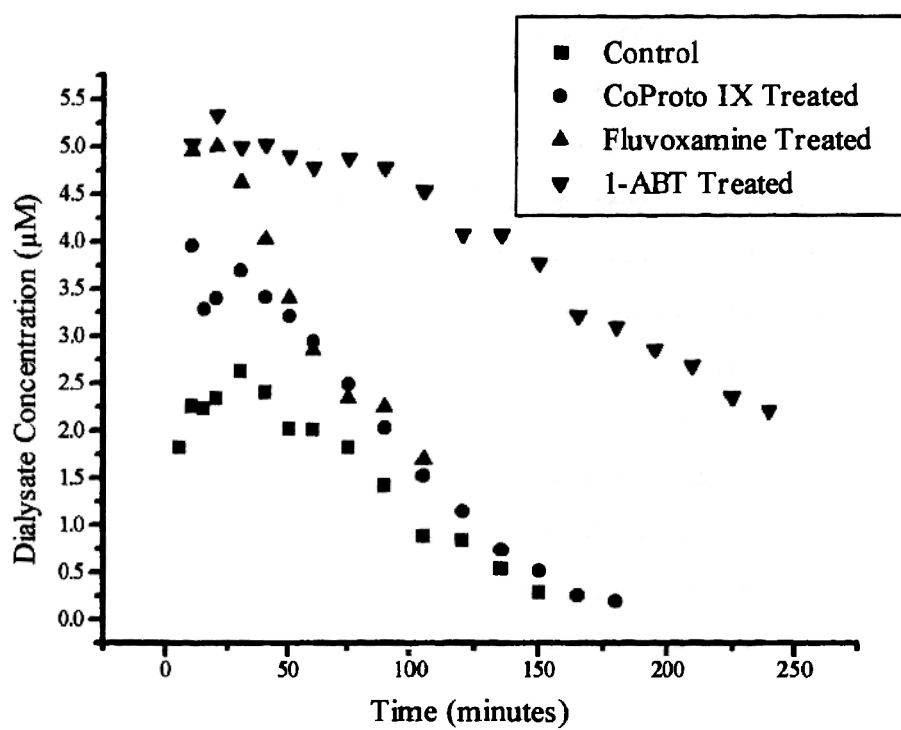


Figure 5. Pharmacokinetic curves of phenacetin in control and treated animals as indicated in the figure legend.

the control samples and then dose the animal with 1-ABT and collect the inhibited samples, however, this would have required at least six hours of sample collection thus the same problem with the halothane would have occurred. The delivery results for the inhibition of phenacetin and antipyrine are shown in Tables II and III.

Table II shows that there was no statistical difference between mean value for the delivery from the control animals and the 1-ABT treated animals with phenacetin. An ANOVA was performed to see where the most variation in the results occurred and it was determined that in the control animals there was significant animal to animal variation. With the treated animals this variation decreased and there was more variation from sample to sample. This can easily be attributed to operator experience with the surgical technique. In microdialysis it is of utmost importance to perform surgeries carefully as the results obtained from the experiments themselves can be related to the quality of the surgery performed. For example, a sloppy surgery will cause more damage to the tissue area in which the probe is inserted. The control animal experiments were performed first, shortly after the author had been trained to perform the surgical procedures necessary to insert the probe. For this reason eight animals were used. An example of the sample to sample variation in the phenacetin controls and 1-ABT treated phenacetin animals is shown in Figure 6 for all the animal experiments.

Initial scanning of the antipyrine results suggests an increase in the delivery values after 1-ABT treatment. To determine if the 1-ABT treatment had an affect on the delivery, the t distribution was applied to determine the probability of the results obtained. Using the t distribution as an approximation to the randomized distribution described by Box et al. [Box et al., 1978] the null hypothesis of no difference between the means was determined. The t value obtained can be used to find the tail probability for these observations which was 42 percent, which indicates that these

Table II. Phenacetin delivery to control and treated animals.

Controls			1-ABT		
Average (%)	Std. Dev.	n	Average(%)	Std. Dev.	n
63.2	2.4	5	70.3	2.2	5
77.3	0.9	5	69.3	3.0	6
69.5	4.5	5	69.2	1.7	6
74.8	4.7	4	71.7	3.4	6
72.9	4.4	5	73.4	2.0	6
74.3	2.4	4			
64.1	1.0	5			
68.0	4.1	5			

	Controls	1-ABT
Average (Delivery)	70.5	70.8
Std. Dev. (Average)	5.2	1.7
Pooled Variance	11.5	6.6
Grand Average	70.3	70.8
Between Animal Variance	26.8	3.1
F Ratio	2.3	0.5
F Distribution	0.04	0.76

* n denotes the number of dialysate samples taken to formulate the average.

Table III. Antipyrine delivery statistics for control and treated animals.

Controls			1-ABT		
Average (%)	Std. Dev.	n	Average (%)	Std. Dev.	n
55.9	4.3	4	54.6	1.6	6
54.9	3.1	5	49.5	1.9	6
42.1	4.3	5	55.5	1.4	5
44.8	6.5	5			
42.6	8.1	5			
37.8	4.8	5			

	Control	1-ABT
Average (Delivery)	46.35	53.25
Std. Dev. (Average)	7.35	3.23
t (null hypothesis)	0.198	
t distribution probability	42 %	

* n denotes the number of dialysate samples taken to formulate the average.

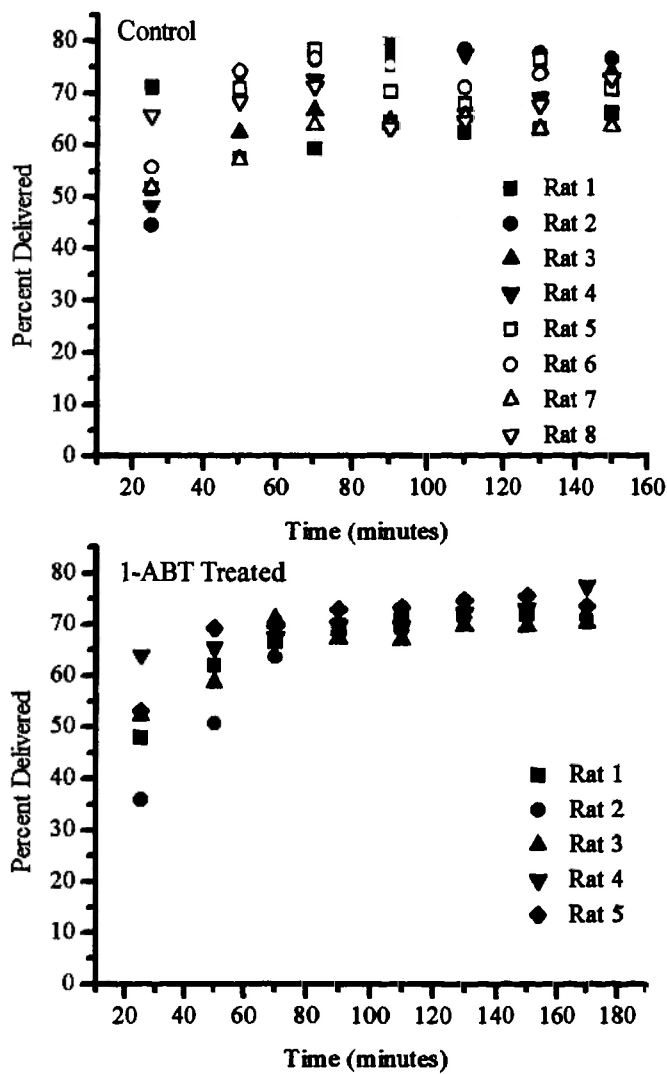


Figure 6. Delivery of phenacetin at 0.5 $\mu\text{l}/\text{min}$ to control and 1-ABT treated rats.

means are similar and that 1-ABT is without effect. It is not known why the control animals have lower values. These lower values (last two) were measured using a new probe from CMA. However, this fact alone does not exclude that data from the set as there were no experiments performed to test this hypothesis.

4.3.2 Euthanasia Studies

On several occasions after the collection of samples from control animals, the animal was euthanized using an overdose of halothane and then collection of the samples was continued. These values never approached a steady state convergence. Phenacetin seems to be reproducible, however, a steady-state value was not obtained indicating that the processes that allow for a 70 percent extraction of the phenacetin from the dialysis probe have ceased and that possibly only diffusion is driving the flux away from the probe. This is shown in Figure 7. The antipyrine data show more scatter. However in one case, the animal expired after the injection of 1-ABT and those results show a steady-state of approximately 20 percent delivery of antipyrine to the rat.

To verify that the liver wasn't being freely stirred, experiments were performed in the blood and the liver with two CMA-10 probes that were characterized as having similar delivery properties. The blood probe delivered more antipyrine than the liver probe as shown in Figure 8. Based on tortuosity and diffusion differences between the blood and the liver, it would be expected that the blood would extract more from the microdialysis probe. Figure 8 also depicts one of the many problems associated with microdialysis, i.e., probe to probe characterization. Although the surgical placement of a cannula type commercial probe into the liver is perhaps more difficult than that of using a linear probe design, the utilization of the same probe allowed for a more direct determination between the liver and the blood. However, upon death,

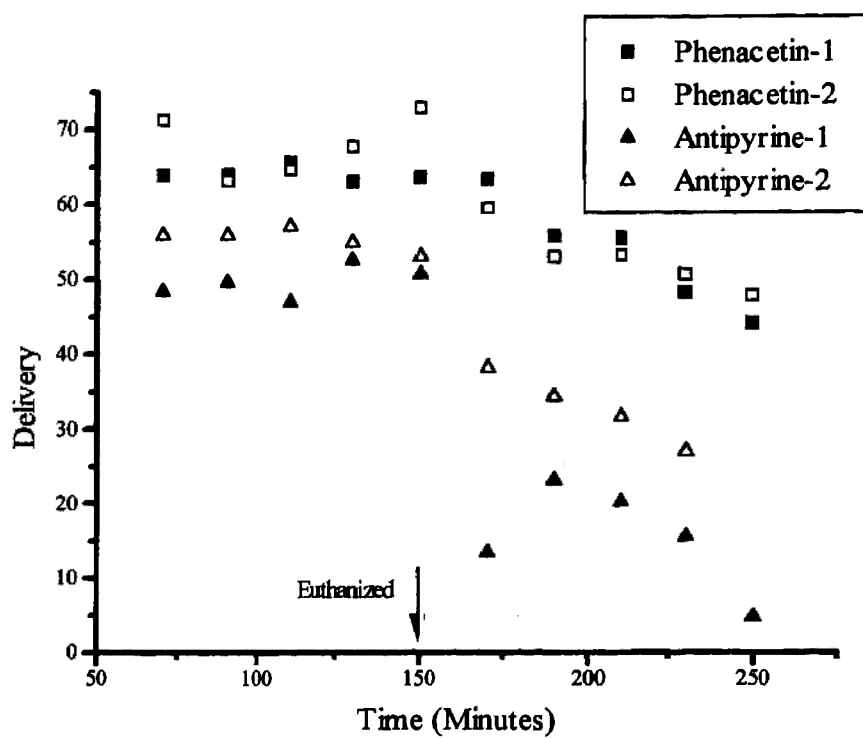


Figure 7. Delivery of phenacetin and antipyrine ($0.5 \mu\text{l}/\text{min}$) to normal rats that were euthanized at 150 minutes.

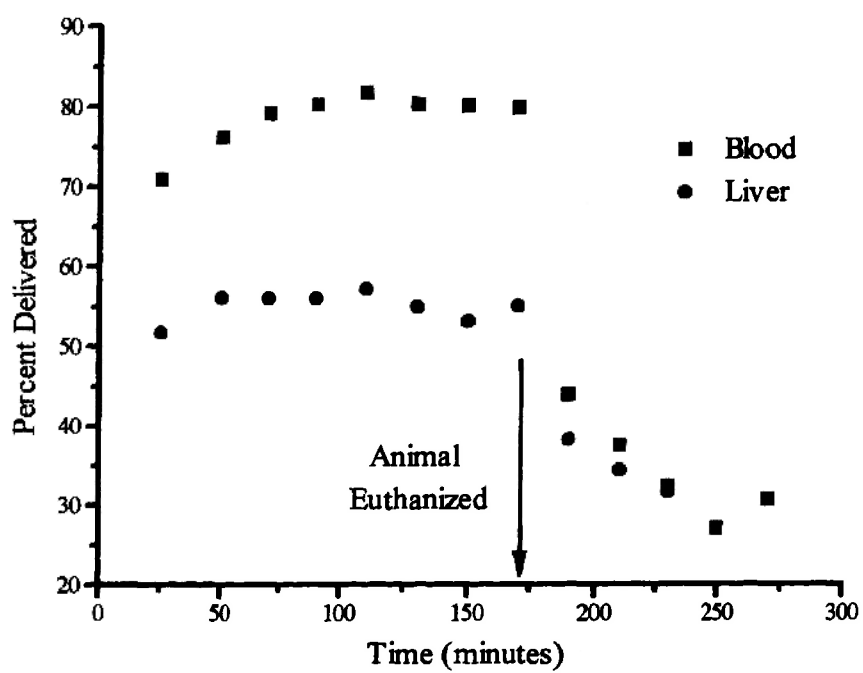


Figure 8. Antipyrine delivery ($0.5 \mu\text{l}/\text{min}$) to a normal rat using CMA-10 probes in the jugular vein and liver. The animal was euthanized at 170 minutes.

both values approached the same value, which could be an indication that around the blood probe, the antipyrine was diffusing through the vein.

The euthanasia studies do not match the mathematical modeling in that if metabolism continues, the probe should reach a steady-state shortly after euthanasia if the metabolism rates are as high as those reported in the literature. This is not due to the fact that the animal is dead, as the isolated perfused liver is obtained from a dead animal, liver slices have reported metabolic activity [Worboys, et al., 1995], and microsomes and hepatocytes remain viable after collection. A possible explanation to the rapid decline without convergence to steady-state is the high delivery values obtained are due to convection around the probe due to the animal's respiration. If there is convection around the probe, then the membrane rather than the tissue becomes the limit to mass transfer [Stenken et al., 1993]. This hypothesis is partially supported by the fact that *in vitro* characterization of the dialysis probes at room temperatures of 23° C at 0.5 μ l/min, give a delivery value close to 70 percent for phenacetin and antipyrine. The phenacetin *in vitro* delivery value matches its *in vivo* value. The *in vitro* value obtained for antipyrine does not match its *in vivo* value. It is possible that antipyrine has a diffusion coefficient *in vivo* that is reduced to a greater extent than for phenacetin. A lower *in vivo* diffusion coefficient due to hindered diffusion or possible protein interactions would cause lower *in vivo* delivery values. For phenacetin, the increased temperature, combined with a possible convective flow around the fiber due to the animal's respiration, may offset the delivery lowering effects of tortuous diffusion pathway and increased resistance in the tissue space.

Using estimated values from the literature for phenacetin and antipyrine, the mathematical model developed in Chapter 3 was applied to understand the inhibition results. Table IV shows the values used in the phenacetin simulation. Values for the

metabolism were scaled by using values for antipyrine and phenacetin obtained from the literature [Houston, 1994]. The microsomal clearance values of phenacetin and antipyrine reported by Houston are 33 and 3.6 $\mu\text{l}/\text{min}/\text{mg}$ microsomal protein. Houston reports that about 500 mg of microsomal protein is obtained from a rat of standard weight (250 g). Assuming that the density of liver tissue is about 1.5 the value for phenacetin approaches 1.8 min^{-1} . The value for the permeability of compounds across the sinusoidal space was taken to be 2.0 min^{-1} [Ichikawa et al., 1992]. Additionally it should be noted that the metabolic rate reported for antipyrine would be close to the inhibited rate of phenacetin. This is because phenacetin's metabolic rate is reduced by 90 percent upon inhibition by 1-ABT.

From Table V it is seen that values for the delivery do not change significantly with the reduction of capillary permeation for phenacetin because of the metabolic rate of phenacetin is high. For antipyrine, a reduction in the capillary permeation rate does affect its delivery. This is because the flux is affected by the addition of each kinetic process. Since the blood exchange rate is much greater than the metabolism rate, the changes in metabolism will not cause an effect in the levels of the flux from the probe. Additionally as was discussed in Chapter 3, as the kinetics increase the membrane becomes more limiting to mass transport, thus causing the flux to decrease little with changes in kinetic rate constant values. It should be noted that modeling results shown in this table do not match the experimental results. This may be due to several factors. The model does not account for convection and it is possible that convection around the probe due to the animal's respiration may occur. A second possible source of error may be in the model formulation. The capillaries may provide an additional sink volume that was not included in the original model formulation.

Table IV. Values used for Model Analysis of Phenacetin and Antipyrine

Inner Radius (cm)	0.020
Outer Radius (cm)	0.025
Diffusion Coefficient Dialysate (cm ² /s)	7.5*10 ⁻⁶
Diffusion Coefficient Membrane(cm ² /s)	7.0*10 ⁻⁶
Diffusion Coefficient Extracellular Fluid (cm ² /s)	5.0*10 ⁻⁶
Volume Fraction of ECF	0.3
Volume Fraction of the Membrane	0.6
Rate of Metabolism (intracellular) (min ⁻¹)	1.8
Rate of ECF/Plasma exchange (min ⁻¹)	2.0
Membrane Length (mm)	4.0
Flow Rate of Dialysate (μl/min)	0.5

Table V. Model predicted delivery values for phenacetin and antipyrine

	$k_{ep}=2.0$	$k_{ep}=1.0$	$k_{ep}=0.5$	$k_{ep}=0.001$
Phenacetin	52.8	52.6	51.0	50.3
Antipyrine	46.5	42.8	39.9	34.9

4.3.3. Portal Vein Ligation

Portal vein ligation in conjunction with microdialysis has proven to be difficult at the present time. Successful implementation will require an improved microsurgical technique. A change in delivery is expected, but the extent cannot be predicted easily except through modelling. The portal vein supplies 75 percent of the blood to the liver. Therefore, a reduction of the blood flow by 75 percent would be expected. If, however, the capillaries still provide good sink conditions with the lowered blood flow, then delivery will not change. A starting point for the surgery can be found in Brand et al. and Um et al. [Brand et al., 1995; Um et al., 1994].

4.3.4 Metabolite Studies

Other authors have reported the formation and collection of metabolites from microdialysis experiments in rat liver. Scott and Lunte [Scott and Lunte, 1993] reported obtaining over 20 μM phenyl-glucuronide after an infusion of 500 μM phenol of which 181 μM was lost across the probe. Van Belle et al. [Van Belle, 1995] observed a 18 percent oxidative conversion of carbamazepine at a 2 $\mu\text{l}/\text{min}$ flow rate after a local infusion.

Acetaminophen and phenacetin were used to determine the amount that could be obtained after a local infusion. In the acetaminophen case, only the sulfate was quantitated in the perfusion fluid. This is due to the location of the phenol sulfotransferases in the cytosolic space, whereas the glucuronyltransferases are located on the endoplasmic reticulum along with the cytochromes [Mulder, 1990]. It would be expected to obtain a greater amount of sulfated conjugates as the sulfates can be formed in the cytosol and diffuse or be transported out of the cell into the microenvironment sampled by the microdialysis probe. Whereas for the glucuronide, the glucuronyltransferases are located in the vicinity of the bile ducts and thus the metabolite, if it is formed, would be shunted into the bile more efficiently than be

transported back into the extracellular space. *In vitro* delivery values at 1 $\mu\text{l}/\text{min}$ for acetaminophen, acetaminophen sulfate and acetaminophen glucuronide were 47%, 42%, and 28%. Because of the lower delivery value for acetaminophen glucuronide, this compound would be extracted at a lower level than a sulfate conjugate.

Table VI shows the formation of acetaminophen sulfate after the infusion of various denoted concentrations of acetaminophen. The metabolite data obtained is in contrast to the observations by Scott and Lunte [Scott and Lunte, 1993], who reported collection of phenol-glucuronide after a local infusion of 500 μM phenol. No acetaminophen glucuronide formation was observed after the local infusion of acetaminophen in these experiments. The microdialysis data presented here is supported by phenacetin and acetaminophen data from Smith and Timbrell [Smith and Timbrell, 1974], Smith and Griffiths [Smith and Griffiths, 1976], and Pang et al. [Pang et al., 1985]. At the low concentrations of acetaminophen, 10 μM , approximately 9 percent of the amount removed from the probe was converted into the sulfate metabolite. Formation of a glucuronide conjugate was not observed. This is expected as a typical K_m value of the phenol sulfotransferase is given by Pang [Pang, 1990] as 10 μM and the K_m for the glucuronyltransferase is reported as 200 μM . The amount removed from the probe is well below both of these values at the 11 and 110 μM concentrations infused. A shift between sulfate conjugation and glucuronidation would be expected for the values between 10 and 50 μM for the acetaminophen as modeled by Morris and Pang for the isolated perfused liver [Morris and Pang, 1987]. Experimental results from Koster et al. exhibit the same behavior for phenol and other phenolic compounds [Koster et al., 1981]. As the concentration of acetaminophen was increased, a decrease in the percent of the acetaminophen sulfate was observed. This indicates that a process affecting the recovery of the acetaminophen sulfate across the microdialysis probe was perturbed. This may be

Table VI. Metabolite recovery from a local infusion of acetaminophen.

[APAP] μM	[APAP] μM	[APAP] μM	% of APAP-SO ₄
probe	lost (\pm std.dev)	gained (\pm std.dev)	gained from loss
11.9	3.73 \pm 0.46	0.04 \pm 0.026	10.82
11.9	3.43 \pm 0.07	0.22 \pm 0.12	6.25
11.0	1.75 \pm 0.21	0.16 \pm 0.02	9.53
119	35.6 \pm 4.9	2.34 \pm 0.03	6.59
119	27.4 \pm 2.0	1.56 \pm 0.06	5.69
110	18.9 \pm 1.5	1.03 \pm 0.15	5.44
238	61.4 \pm 6.0	3.54 \pm 0.14	5.77
238	52.14 \pm 5.2	2.88 \pm 0.2	5.54
220	49.8 \pm 4.4	1.57 \pm 0.55	3.17

Table VII. Phenacetin (59 μM) delivery to a rat. Recovery of the metabolites acetaminophen and acetaminophen sulfate.

[APAP-SO ₄] μM gained	[APAP] μM gained	[Phenacetin] μM	% metabolites gained from loss
0.38	1.06	43.6	3.3
0.79	1.58	35.4	6.7
1.29	1.42	30.3	8.9
0.99	1.59	31.3	8.3
1.21	1.51	29.9	9.1
1.06	1.89	33.5	8.7

saturation of the sulfotransferase or an inhibition of the active transport of acetaminophen sulfate out of the hepatocyte [Goresky et al.,1992].

After a local infusion of phenacetin the metabolites acetaminophen and acetaminophen sulfate were collected into the dialysate. The results of these experiments are described in Table VII. The K_m value reported for the high affinity site for phenacetin based on microsomal studies is approximately 5 μ M [Boobis et al., 1981]. Based on Michaelis constant values and maximum rate arguments, the formation of the sulfate seems reasonable as the sulfotransferases are known to be high affinity and low capacity enzymes whereas the glucuronyltransferases are low affinity and high capacity enzymes. This means that at low concentrations of the substrate the sulfotransferase will more readily convert the acetaminophen than the glucuronyltransferase.

Part of the problem with comparing these studies with studies in the isolated perfused liver is that it is not known to what extent the metabolite is lost across the tissue microvasculature. Van Belle et al. [Van Belle et al., 1995] discussed that microdialysis can be used in conjunction or as an alternative to the isolated perfused liver for metabolite conversion studies. However, in their experiments, they did not secure or verify the placement of the probe. In the dialysis experiment, part of the drug will be completely removed from the area through the sinusoids whereas another part may be taken up by the cells. It is unknown how 'good' a sink the microdialysis probe provides in contrast to the sinusoids in the isolated perfused liver.

4.4 Summary

From these studies it is seen that for microdialysis sampling applied in the liver, metabolism does not contribute greatly to the flux from the microdialysis probe. This was shown by the lack of change in the delivery after inhibition of cytochrome

P450 enzymes with the suicide substrate 1-ABT. Experiments with euthanized animals show that the blood flow is a large contributing factor to the amount of material removed from a microdialysis probe. The role of convection in microdialysis liver sampling is suggested as an additional factor that may attribute to the large flux values obtained in these experiments. *In vitro* delivery experiments suggest that the membrane may also contribute to the overall flux of phenacetin and antipyrine as the *in vitro* deliveries closely matched those *in vivo*.

Metabolic recovery after a local infusion of a parent compound may provide a way of utilizing the mathematical model formulated to determine metabolic rate constants. However, this procedure will be compound specific and will depend upon the transport properties of the dialysis probes.

A possible avenue of study would be the induction of the cytochrome P450 enzymes followed by an inhibition of the enzymes to determine if the increase of drug metabolizing enzymes would affect the flux. Sesardic et al. [Sesardic et al., 1990] have reported that CYP 1A2, the phenacetin o-deethylase, is highly inducible by using 3-methylcholanthrene. They reported a 30 fold increase in activity in microsomes (CYP 1A2 makes up about 4-6 percent of the overall cytochrome P450 pool). However, they also report a great variability in the induction from animal to animal.

Hepatic transport is an area that has undergone extensive work. There is tremendous complexity of transport and uptake for cationic as well as anionic drugs and their transport influence by protein binding [Meijer, 1987, Meijer and van der Sluijs, 1987]. Additionally the role of changes in metabolism as well as liver blood flow [Reichen et al., 1988, Buters et al., 1993] may be assessed by using microdialysis in animals induced with cirrhosis.

4.5 References

- Brøsen, K.; Skjelbo, E.; Rasmussen, B.B.; Poulsen, H.E.; Loft, S. Fluvoxamine is a potent inhibitor of cytochrome P4501A2. *Biochem. Pharmacol.* **1993**, *45*, 1211-1214.
- Boobis, A.R.; Kahn, G.C.; Whyte, C.; Brodie, M.J.; Davies, D.S. Biphasic o-deethylation of phenacetin and 7-ethoxycoumarin by human and rat liver microsomal fractions. *Biochem. Pharmac.* **1981**, *31*, 2451-2456.
- Box, G.E.P.; Hunter, W.G.; Hunter, J.S. *Statistics for Experimenters: An introduction to design, data analysis and model building*. John Wiley and Sons New York. 1978.
- Brand, M.I.; Kononov, A.; Vladisavljevic, A.; Milsom, J.W. Surgical anatomy of the celiac artery and portal vein of the rat. *Lab. Animal Sci.* **1995**, *45*, 76-80.
- Buters, J.T.M.; Zysset, T.; Reichen, J. Metabolism of antipyrine in vivo in two rat models of liver cirrhosis: Its relationship to intrinsic clearance in vitro and microsomal membrane lipid composition. *Biochem Pharmacol.* **1993**, *46*, 983-91.
- Davies, M.I.; Lunte, C.E. Microdialysis sampling for hepatic metabolism studies: Impact of microdialysis probe design and implantation technique on liver tissue. *Drug. Metab. Disp.* 1995, in press.
- Drummond, G.S.; Kappas, A. The cytochrome P-450 depleted animal: An experimental model for in vivo studies in chemical biology. *Proc. Natl. Acad. Sci. USA* **1982**, *79*, 2384-2388.
- Gibaldi M, Perrier D. *Pharmacokinetics, 2nd Edition*. Marcel Dekker, Inc.: New York, 1982.
- Gores, G.J.; Kost, L.J.; LaRusso, N.F. The isolated perfused rat liver: Conceptual and practical considerations. *Hepatology* **1986**, *6*, 511-517.
- Goresky, C. A.; Pang, K. S.; Schwab, A. J.; Barker, F. I., Cherry, W. F.; Bach, G. G. Uptake of a protein-bound polar compound, acetaminophen sulfate by perfused rat liver. *Hepatology* **1992**, *16*, 173-190.
- Houston, J. B. Utility of in vitro drug metabolism data in predicting in vivo metabolic clearance. *Biochem. Pharmacol.* **1994**, *47*, 1469-1479.

Ichikawa, M.; Tsao, S.C.; Lin, Tsu-H. et al. 'Albumin-mediated transport phenomenon' observed for ligands with high membrane permeability: Effect of the unstirred water layer in the Disse's space of rat liver. *J. Hepatol.* 1992, 16, 38-49.

Koster, H.; Halsema, I.; Scholtens, E.; Knippers, M.; Mulder, G.J. Dose-dependent shifts in the sulfation and glucuronidation of phenolic compounds in the rat in vivo and in isolated hepatocytes: The role of saturation of phenolsulfotransferase. *Biochem. Pharmacol.* 1981, 30, 2569-2575.

Meijer, D.K.F. Current concepts on hepatic transport of drugs. *J. Hepatol.* 1987, 4, 259-268.

Meijer, D.K.F.; van der Sluijs, P. The influence of binding to albumin and α_1 -acid glycoprotein on the clearance of drugs by the liver. *Pharm. Weekbl [Sci]* 1987, 9, 65-74.

Mico, B.A.; Federowicz, D.A.; Ripple, M.G.; Kerns, W. In vivo inhibition of oxidative drug metabolism by, and acute toxicity of, 1-aminobenzotriazole (ABT): A tool for biochemical toxicology. *Biochem. Pharmacol.* 1988, 37, 2515-2519.

Mico, B.A., Federowicz, D.A.; Burak, E.; Swagzdis, J.E. In vivo inhibition of phenacetin oxidation by suicide substrate 1-aminobenzotriazole. *Drug Metab. Dispos.* 1987, 15, 274-276.

Morris, M.E.; Pang, K.S. Competition between two enzymes for substrate removal in liver: Modulating effects due to substrate recruitment of hepatocyte activity. *J. Pharmacokin. Biopharm.* 1987, 15, 473-496.

Muhoberac, B.B.; Hanew, T.; Halter, S.; Schenker, S. A model of cytochrome P-450 centered hepatic dysfunction in drug metabolism induced by cobalt-protoporphyrin administration. *Biochem. Pharmacol.* 1989, 38, 4103-4113.

Mulder, G.J., ed. *Conjugation reactions in drug metabolism: An integrated approach*. London: Taylor and Francis, 1990.

Ortiz de Montellano, P.R.; Correia, M.A. Suicidal destruction of cytochrome P-450 during oxidative drug metabolism. *Ann. Rev. Pharmacol. Toxicol.* 1983, 23, 481-503.

Pang, K.S.; Kong, P.; Terrell, J.A.; Billings, R.E. Metabolism of acetaminophen and phenacetin by isolated rat hepatocytes: A system in which spatial organization inherent in the liver is disrupted. *Drug. Metab. Dispos.* 1985, 13, 42-50.

- Pang, K.S.; Sherman, I.A.; Schwab, A.J.; et al. Role of the hepatic artery in the metabolism of phenacetin and acetaminophen: An intravital microscopic and multiple-indicator dilution study in perfused rat liver. *Hepatology* 1994, 20, 672-683.
- Reichen, J.; Egger, B.; Ohara, N.; Zeltner, T.B.; Zysset, T.; Zimmermann, A. Determinants of hepatic function in liver cirrhosis in the rat: Multivariate analysis. *J. Clin. Invest.* 1988, 82, 2069-76.
- Scott, D.O.; Lunte, C.E. In vivo microdialysis sampling in the bile, blood, and liver of rats to study the disposition of phenol. *Pharm. Res.* 1993, 10, 335-342.
- Sesardic, D.; Cole, K.J.; Edwards, R.J.; et al. The inducibility and catalytic activity of cytochromes P450c (P450IA1) and P450d (P450IA2) in rat tissues. *Biochem. Pharmacol.* 1990, 39, 499-506.
- Sesardic, D.; Edwards, R.J.; Davies, D.S.; Thomas, P.E.; Levin, W.; Boobis, A.R. High affinity phenacetin o-deethylase is catalysed specifically by cytochrome P450d (P450IA2) in the liver of the rat. *Biochem. Pharmacol.* 1990, 39, 489-498.
- Smith, G.E.; Griffiths, L.A. Comparative metabolic studies of phenacetin and structurally-related compounds in the rat. *Xenobiotica* 1976, 6, 217-236.
- Smith, R.L.; Timbrell, J.A. Factors affecting the metabolism of phenacetin I. Influence of dose, chronic dosage, route of administration and species on the metabolism of (1-¹⁴C-acetyl)phenacetin. *Xenobiotica* 1974, 4, 489-501.
- Spaethe, S.M.; Jollow, D.J. Effect of cobalt protoporphyrin on hepatic drug-metabolizing enzymes: Specificity for cytochrome P450. *Biochem. Pharmacol.* 1989, 38, 2027-2038.
- Stenken, J.A.; Topp, E.M.; Southard, M.Z.; Lunte, C.E. Examination of microdialysis sampling in a well-characterized hydrodynamic system. *Anal. Chem.* 1993, 65, 2324-2328.
- Thurman, R.G.; Kauffman, F.C. Sublobular compartmentation of pharmacological events (SCOPE): Metabolic fluxes in periportal and pericentral regions of the liver lobule. *Hepatology* 1985, 5, 144-151.
- Um, S.; Nishida, O.; Tokubayashi, M.; Kimura, F.; Takimoto, Y.; Yoshioka, H.; Inoue, R.; Kita, T. Hemodynamic changes after ligation of a major branch of the

portal vein in rats: comparison with rats with portal vein constriction. *Hepatology* **1994**, *19*, 202-209.

Ungerstedt, U. Microdialysis - principles and applications for studies in animals and man. *J. Internal. Med.* **1991**, *230*, 365-373.

Van Belle, K; Sarre, S.; Ebinger, G.; Michotte, Y. Brain, liver, and blood distribution kinetics of carbamazepine and its metabolic interaction with clomipramine in rats: A quantitative microdialysis study. *J. Pharmacol. Exp. Ther.* **1995**, *272*, 1217-1222.

Worboys, P. D.; Bradbury, A.; Houston J. B. Kinetics of drug metabolism in rat liver slices: Rates of oxidation of ethoxycoumarin and tolbutamide, examples of high- and low-clearance compounds. *Drug Metab. Dispos.* **1995**, *23*, 393-397.

Chapter 5

The effect of acetylcholinesterase inhibition on the flux of ^{14}C -acetylcholine in microdialysis delivery experiments.

5.1 Introduction

Chapter 4 showed that for two model compounds, phenacetin and antipyrine, in the liver, metabolic rates did not affect the flux of these substances from a local delivery. This indicated that processes such as the microvasculature uptake rates, (k_{ep} in the model described in Chapter 3) contribute significantly to the overall sum of the kinetic processes in the liver. Since metabolism did not affect the delivery of compounds to the liver, a second tissue and analyte were explored to show that in specific cases metabolism will affect the flux in microdialysis experiments.

Acetylcholine esterase (AChE) is one of the most efficient enzymes known in terms of its catalytic efficiency, k_{cat} . AChE has a k_{cat} of $14,000 \text{ sec}^{-1}$, which means that it can convert 14,000 molecules of acetylcholine (ACh) into acetate and choline per molecule of AChE per second [Fersht, 1985]. Acetylcholine is unique as a neurotransmitter in that the only process that removes it from the extracellular fluid space is the degradation through AChE, unlike dopamine that can be taken back into the neuron through reuptake processes [Cooper et al., 1991].

Like most enzymes, AChE is heterogenous in its expression in the mammalian brain [Ogane et al., 1992]. There are several types of AChE that have been isolated from mammalian brain. The predominant forms in the mammalian brain include the globular tetrameric form, G_4 , and the monomeric G_1 form. The G_4 form in the membrane accounts for approximately 70 percent of the activity of AChE in membrane extracts and is known to be extracellular in nature, i.e, it faces the

extracellular space, which is the space that is sampled by microdialysis techniques. Therefore, this enzyme/substrate system serves as an ideal candidate for studying the effects of kinetic inhibition in microdialysis.

AChE can be inhibited by two different classes of inhibitors typically named reversible or irreversible [Taylor, 1990]. Reversible inhibitors, which include physostigmine and neostigmine, inhibit the acetylcholinesterase enzyme through carbamylation. The enzyme is then reactivated through hydrolysis of this carbamoylate bond. Irreversible AChE inhibitors, which include agricultural insecticides and chemical-warfare nerve gas agents, phosphorylate AChE. This is a stable process, which causes the enzyme to be inactive.

In this study, microdialysis probes were placed in the striatum of a rat to study the effects of inhibition on the loss of ^{14}C -acetylcholine through the microdialysis probe. Neostigmine was included in the perfusate in a cross-over design. This cross-over design allowed the comparison of ACh loss before and after pharmacological challenge with neostigmine.

5.2 Materials and Methods

CMA-12 microdialysis probes (CMA Microdialysis AB, Stockholm, Sweden) with a 4 mm membrane were used for all experiments. Probes were prepared according to the manufacturer's instructions which briefly state that probes need to be rinsed with ethanol prior to use to remove the glycerol that is used in the manufacturing process. After rinsing, the probes were ready for use.

^{14}C -acetylcholine chloride (50-60 mCi/mmol) was purchased from Amersham (Solna, Sweden) and was dissolved in Ringer's solution (Apoteksbolaget, Huddinge University Hospital, Huddinge, Sweden) to 2 μM prior to infusion. Neostigmine

bromide was obtained from Apoteksbolaget, Huddinge University Hospital and was prepared to a concentration of 100 μM prior to infusion with 2 μM acetylcholine.

Male Sprague-Dawley rats (225-275 g) were anesthetized with halothane and were maintained at 37° C through the use of a CMA-150 heating pad. Five rats were used. Each rat was placed in a Kopf stereotaxic frame, with the incisor bar set 3.3 mm below the interaural line. The skull was exposed and then trephined using a 1 mm diameter drill bit. The microdialysis probe was slowly inserted 0.2 mm anterior and 2.7 mm lateral to bregma, to a depth of 6 mm below the dura. These experiments were approved by the Animal Ethical Committee of the Huddinge University Hospital.

After insertion, the probe was allowed to flush at 1.0 $\mu\text{l}/\text{min}$ for one hour prior to the beginning of sampling. After one hour, four 15 minute samples were collected into scintillation vials and stored at ambient temperature until analysis, which occurred after the completion of the experiment (approximately 3.5 hours). After the control samples were obtained, cross-over to the syringe which contained 100 μM neostigmine and 2 μM C^{14} -acetylcholine occurred. The use of the syringe selector prevents the introduction of air bubbles into the microdialysis probe. To allow for the dead volume in the tubing, the probe was allowed to continue flushing for 15 minutes prior to the collection of the neostigmine inhibited samples. The dead volume of the tubing used and the probe together approaches 10 μl and would require at least 10 minutes for the dead volume to clear at a 1.0 $\mu\text{l}/\text{min}$ perfusion flow. Samples, which included neostigmine, were collected for another hour and then the perfusion fluid was switched back to the perfusion fluid which contained only ACh.

The 15 μl dialysate samples were mixed with 3 ml Optisolv scintillation fluid (DuPont) prior to counting. Standards were prepared by pipetting 15 μl from the solutions that were perfused through the microdialysis probes. Samples and standards

were analyzed using liquid scintillation counting. Deliveries were calculated by using the count ratio of $(\text{Counts}_{\text{stan}} - \text{Counts}_{\text{sample}}) / \text{Counts}_{\text{stan}}$, where $\text{Counts}_{\text{stan}}$ and $\text{Counts}_{\text{sample}}$ stand for the counts obtained for the standard and the sample respectively.

5.3 Results and Discussion

The percent of the ^{14}C -acetylcholine delivered is shown in Table 1. The same probe was used in rats number 4 and 5. The high delivery values obtained may indicate that this probe had a small micro-tear in the membrane, which would have caused a set amount of material to leak from the probe thus making the results appear higher when compared with the 15 μl standards.

Because the data are somewhat scattered due to animal-to-animal and sample-to-sample variation, the data were normalized to changes from the control values obtained within the first hour of sampling. These percent control values were calculated by taking the highest delivery percent from the initial ACh infusion and dividing the four samples by this value. This gives a value that is below 100 percent of control, but takes into account the sample-to-sample variation. This same procedure was performed for the perfusion that included neostigmine and the cross-back to acetylcholine. The bar graph depicting these values is shown in Figure 1. Table 2 shows the average percent lost, the standard deviation of the average and the probabilities that the treatments are the same based on a randomized t distribution.

By visual inspection it is clear that the cross-over back to the ACh after infusion with 100 μM neostigmine did not reach the original control value. However, the cross-over is statistically different from the neostigmine infusion and the controls. About a 30 percent reduction in the delivery was obtained through the use of infusion of neostigmine through the probe. The lack of greater increase after the cross back

Table I. Percent delivered of ^{14}C -acetylcholine \pm standard deviation for ACh and ACh/neostigmine treatments.

	ACh	ACh/NEO	ACh
Rat 1	13.0 \pm 1.0	7.6 \pm 2.1	11.0 \pm 3.4
Rat 2	17.4 \pm 1.6	13.0 \pm 1.7	15.0 \pm 0.9
Rat 3	20.0 \pm 1.9	15.5 \pm 0.7	17.0 \pm 1.3
Rat 4	40.8 \pm 2.3	26.8 \pm 0.9	36.5 \pm 0.9
Rat 5	43.2 \pm 0.8	24.6 \pm 1.4	27.2 \pm 0.8

Table II. Percent loss of ACh expressed as a control, standard deviation, and one tailed t probability for the null hypothesis.

Group	ACh (1)	ACh/NEO (2)	ACh(3)
Average	94.9	62.8	76.9
Standard deviation	2.7	7.6	8.7
Combination	t, tail area probability		
Group 1/2	1.0*10 ⁻⁵		
Group 2/3	0.012		
Group 1/3	0.0011		

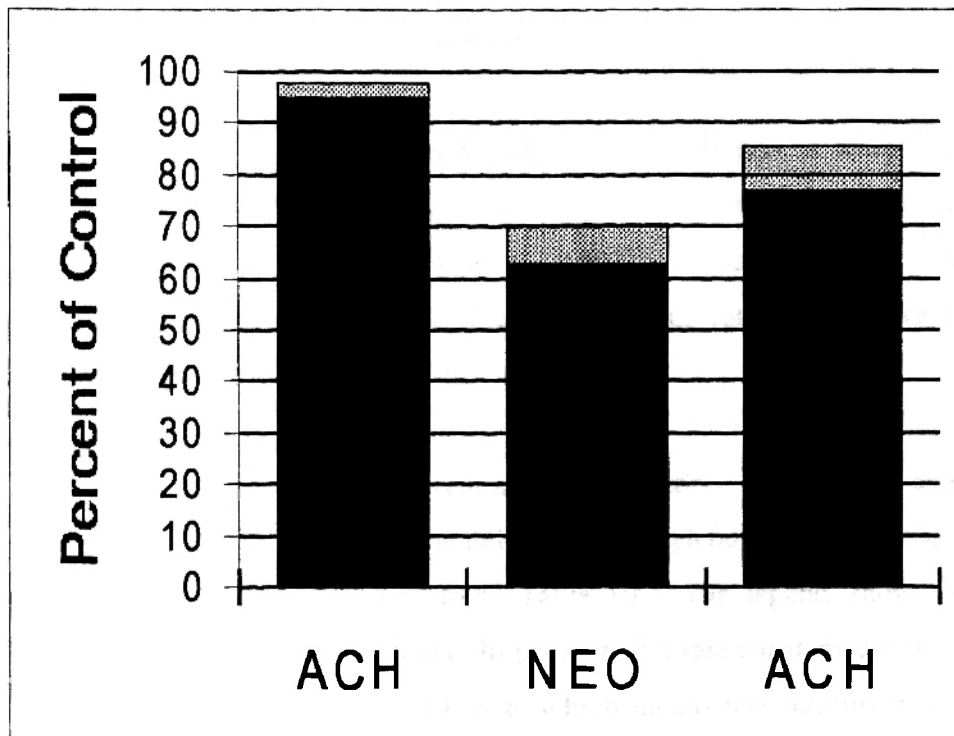


Figure 1. Acetylcholine delivery as a percent of control values, before, during and after neostigmine (NEO) treatment.

to the ACh perfusion fluid may be due to the presence of excess neostigmine in the area surrounding the probe. Additionally reversible inhibitors of AChE are known to have an effect that last approximately 3-4 hours *in vivo* [Taylor, 1990]. The area that is affected by the neostigmine relative to the acetylcholine is unknown. This is because the *in vivo* diffusion coefficient of neostigmine and the uptake rates are unknown compared to those for acetylcholine. Therefore neostigmine's effect at distances away from the probe may be different than those for acetylcholine and thus may affect the results of the cross-over back to acetylcholine.

Neostigmine has been previously reported to give a lower inhibition than physostigmine and unstable sample-to-sample results when used in concentrations greater than 50 μM [Messamore et al., 1993]. Although some sample-to-sample variation was observed in these studies, neostigmine consistently gave a reduction in the microdialysis delivery of ACh.

Figure 2 shows a theoretical approximation of how 50 and 90 percent inhibition to AChE may affect the delivery of acetylcholine *in vivo* after introduction of an inhibitor using the data from Table III. The legend shows what may be expected for inhibitions of 50 and 90 percent of a rate constant denoted as 1.0 min^{-1} . The pI_{50} of neostigmine on AChE is 8, which means that inhibition is 50 percent at 10^{-8} M or 10 nM [Cohen and Oosterbaan, 1963]. This value was exceeded assuming a 15 percent delivery of 100 μM neostigmine through the dialysis probe.

Figure 2 shows that for a 90 percent inhibition, a steady-state value should be reached after about 45 minutes. This was not observed experimentally *in vivo*. However, this drop to steady-state values only occurs over a 1 percent range of a predicted delivery value. If this did occur experimentally the phenomenon was probably lost in the experimental uncertainty.

Table 3. Parameters used for acetylcholine simulation

0.025	OUTER RADIUS OF THE MEMBRANE {cm}	(ROUT)
0.020	INNER RADIUS OF THE MEMBRANE {cm}	(RIN)
7.5e-6	DIFFUSION COEFFICIENT	(DDIAL)
7.0E-6	MEMBRANE DIFFUSION COEFFICIENT	(DMEM)
3.33e-6	ECF DIFFUSION COEFFICIENT (INCLUDES TORT)	(DECF)
0.2	Volume Fraction	(PHI)
0.6	Volume Fraction of the membrane	(PHIM)
1.0	Metabolism Rate Constant {min-1} ECF	(RMETAB)
0.0	Metabolism Rate Constant {min-1} ICF	(RICF)
0.0	Plasma to ECF exchange (min-1)	(XKPLEC)
0.0	ECF to Plasma exchange (min-1)	(XKECPL)
0.0	Production in the ICF	(GICF)
0.0	Production in the ECF	(GECF)
1.0	Ratio keix/kiex	(XKPI)
100.0	Total simulated time (min)	(TIME)
10.0	Number of time steps	(TMSTEP)
0.0	Plasma Conc	(CPLAS)
0.4	Length of the membrane (cm)	(XLEN)
1.0	Dialysis Flow Rate in $\mu\text{L}/\text{min}$	(QDIAL)
10.0	Perfusion Fluid Concentration	(CPERF)
0.0	Plasma decay constant	(xlam)

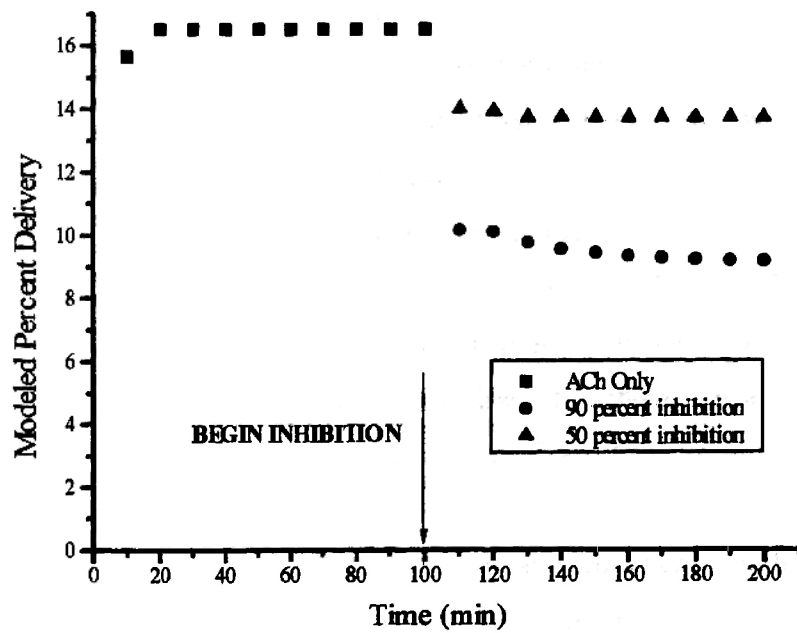


Figure 2. Model of acetylcholine delivery before and after various levels of inhibition of AChE.

5.4 Summary

This chapter shows that a reduction in the microdialysis flux can be obtained through a local inhibition of metabolism achieved by delivery of an enzyme inhibitor through the microdialysis probe. However, although a reduction in the delivery of ^{14}C -acetylcholine was observed, it is unknown if full inhibition of AChE was achieved. It may be possible to titrate the reduction in delivery through the use of varying combinations of concentrations of neostigmine and acetylcholine. It is unknown how much neostigmine was lost through the microdialysis probe. Assuming that its diffusion coefficient and uptake rate parameters are similar to acetylcholine then, the same percentage would be lost as acetylcholine. For these experiments this would be about 15 percent. This 15 μM loss of neostigmine would then be diluted in the tissue microenvironmental space. The microdialysis model can make approximate predictions about how far a molecule can diffuse through the microenvironment after diffusion through the microdialysis probe. However, these predictions would have to be confirmed in order to make further conclusions about the extent inhibition of AChE by neostigmine. For these reasons, it may be difficult to determine a metabolic rate for the uptake of neostigmine *in vivo*.

These results show that after a pharmacological challenge, such as the inhibition of an enzyme, the mass-transport dynamics to and from the probe may be changed and these changes need to be considered when interpreting microdialysis data. Fortunately for the inhibition case, the ACh levels in the brain not only rise, but the transport of ACh from the ECF space is lowered, therefore a decrease in the loss of ACh from the dialysate is expected. However, if it were possible to induce AChE, then the local levels of ACh in the ECF space would also change along with the probe dynamics due to a greater heterogenous rate constant. Dialysis data from this type of experiment should also be interpreted with caution. It should be noted that these

scenarios would not only hold true for microdialysis sampling, but for all *in vivo* sampling.

5.5 References

Cohen, J.A.; Oosterbaan, R.A. The active site of acetylcholine esterase and related esterases and its reactivity towards substrates and inhibitors. In *Cholinesterases and acetylcholinesterase agents*, Koelle, G ed. Berlin: Springer-Verlag, *Handbuch der Experimentellen Pharmakologie*, Vol. 15, 1963, pp. 299-373.

Cooper, J.R.; Bloom, F.E.; Roth, R.H. *The biochemical basis of neuropharmacology*, 6th edition. New York: Oxford University Press, 1991.

Fersht, Alan *Enzyme Structure and Mechanism*, 2nd. W.H. Freeman and Company, New York: 1985. p.152

Messamore E., Ogane N., and Giacobini E. Cholinesterase inhibitor effects on extracellular acetylcholine in rat striatum. *Neuropharmacology*, **1993**, *32*, 291-296.

Ogane, N; Giacobini, E.; Messamore, E. Preferential inhibition of acetylcholinesterase molecular forms in rat brain. *Neurochem. Res.*, **1992**, *17*, 489-495.

Taylor, P. Anticholinesterase agents. in Goodman Gilman, A.; Rall T.W.; Nies, A.S.; Taylor, P. *Goodman and Gilman's The Pharmacological Basis of Therapeutics*, 8th edition. New York: Pergamon Press. 1990.

Chapter 6

Determination of sub-cutaneous caffeine levels in a humans after voluntary caffeine ingestion.

6.1 Introduction

The chapter discusses the last experiment performed while working as a visiting scientist at the Karolinksa Institute in Stockholm. The experiment performed here does not directly relate to the mathematical model, but serves as a means to give the reader a flavor for some of the possible human uses of microdialysis. In humans, microdialysis probes are easily implanted into the subcutaneous fat. In this particular study, the dialysis catheter was used to study the dynamic changes of the caffeine levels as well as to see if the probe could be used to quantitate low levels of caffeine. This was a pilot study to determine if there is a certain level to which individuals dose themselves with caffeine.

Caffeine is one of the most widely used substances in the world. The human use and effects of caffeine have been widely studied [Starvic, 1992]. In Sweden the average daily ingestion of caffeine is 425 mg per day whereas in the United States the value is 211 mg per day [Spiller, 1984]. A consumption of over 250 mg per day of caffeine has been termed caffeineism [Somani and Gupta, 1988]. The reinforcing ability of caffeine has been debated and discussed in the literature [Griffiths and Woodson, 1988]. Studies have shown that physical dependence potentiates the reinforcing effects of caffeine [Griffiths et al., 1986]. Additional questions about the mode of action of caffeine and why it affects individuals differently has been called into question as well. Caffeine has several pharmacological effects. Effects that may be produced at physiological levels of caffeine obtained through ingestion from food or beverages include blockade of adenosine receptors and inhibition of cyclic-AMP

phosphodiesterase [Fredholm, 1980]. These effects and the dose at which they are obtained has been questioned [Nehlig and Debry, 1994]. Additional questions can be raised as to the inter-individual variability of caffeine metabolism [Caraco et al. 1990].

The purpose of this study was to use microdialysis sampling to follow the levels of caffeine in the subcutaneous fat of a human at regular time intervals while the subject participated in normal daily activities. Microdialysis sampling provides protein-free samples from the ECF space that can be directly analyzed without sample preparation. This is a distinct advantage over blood sampling methods which require sample clean-up prior to analysis. The author was chosen as a test subject because of her low ingestion of caffeine as compared to the native Swedes with whom she worked with for 10 months. Microdialysis sampling has been used in a previous study to determine the disposition of caffeine to male subjects after the ingestion of an oral dose of caffeine [Ståhle et al., 1991]. In those studies, caffeine was given in doses of 300 to 400 mg, which gave rather large dialysate outflow concentrations (20-80 μM). In this study the feasibility of determining levels throughout the day was investigated and if fluctuations and low levels could be obtained through the use of microdialysis sampling. This initial study may become part of a larger study to determine if there is a certain blood level to which individuals dose themselves between low level drinkers and higher level drinkers. This has not been addressed in the literature, as generally heavy-drinkers of caffeinated beverages are used [Griffiths et al., 1986] in caffeine related dosing studies, which ignores inter-individual variability in caffeine metabolism.

6.2 Materials and Methods

6.2.1 Microdialysis

A CMA Human dialysis catheter (CMA/Microdialysis AB, Stockholm, Sweden) was implanted 6 cm above the umbilical line after the application of a local anesthetic.

The probe was perfused at a rate of 0.5 $\mu\text{l}/\text{min}$ with a 0.9% saline solution by an infusion step-pump. All procedures were approved by the local ethical committee. The probe was implanted at 13:00 on day 1 prior to sampling the following morning. This allows any initial damage caused by the probe implantation to clear. Although sampling was to begin on day 2, difficulties with the LC system (the chromatography was still being optimized) and the absent-mindedness of the author (5 days and counting to departure from the country) caused several key time points to be missed throughout the day. On day 3, the analyses began. Samples were obtained every 30 minutes, if a deviation occurred in the sample changing time due to different circumstances this was noted in the lab book and 30 minute samples would continue from that time on. Dialysates were analyzed without any further sample clean-up or dilution. All dialysates were injected onto the LC column no more than 10 minutes after obtaining the sample. The afternoon of the first day was used to allow equilibration of the probe to occur. The second day was used to optimize the experimental procedures and thus the data is not presented as it was not collected continuously throughout the day. Although microdialysis is a continuous sampling technique, only discrete time point samples are obtained. For simplicity, the data are plotted as the single time point concentration outflow. It should be noted that each of these discrete dialysate samples contains the average caffeine concentration during the sampling interval.

6.2.2 Caffeine Consumption Procedure

The subject was allowed to ingest caffeine *ad lib*. The subject's normal coffee drinking behavior consisted of generally drinking only one cup of coffee at the 8:45 break and a half cup at the 14:45 break. On this day, out of curiosity's sake, a Coke Light® was consumed with lunch (12 noon), along with the normal cups of coffee.

6.2.3 LC Analyses

Caffeine was analyzed using liquid chromatography with UV detection. The system consisted of a Phenomenex C-8 column with a mobile phase of 0.05 M sodium acetate pH 5.0 and 15 % acetonitrile. The pump was a CMA-250 delivery system (CMA Microdialysis AB, Stockholm, Sweden) with a CMA/260 degasser. The flow rate was 180 μ l/min. The detection was performed using a fixed wavelength UV detector from Knauer (Germany). The system was calibrated between the ranges of 0.5 μ M and 10 μ M and was linear. The detection limit based on a S/N of 3 was 0.1 μ M. Caffeine eluted in 5 minutes and no interfering peaks were present in the human dialysate. A 1 ml aliquot of the caffeinated beverage consumed was saved for analysis of the dose. Caffeinated beverages were diluted 100 fold with 0.9% saline and injected onto the LC without any further sample clean-up.

6.3 Results and discussion

The main advantage of using microdialysis sampling versus blood sampling for drug disposition studies is that microdialysis sampling provides a clean sample. An example of this is shown in the chromatograms in Figure 1. Figure 1A is the chromatogram from a 7:30 am dialysate sample from the subject. Figure 1B is the 18:30 sample from the same subject after ingestion of caffeine throughout the day. The peak that elutes at approximately 3.50 minutes appears to be a metabolite of caffeine as it does not show up in the standards obtained from the beverages that were used to obtain the dose of caffeine as shown in Figure 2. This peak may be paraxanthine, which is caffeine's major metabolite that appears in the blood (Rall, 1990).

Figure 3 depicts the levels of caffeine obtained throughout the day. Prior to ingestion of the caffeine, a morning level of caffeine of approximately 1 μ M is present. For the caffeine ingested in the morning coffee break the caffeine level

rapidly rises and is detectable in the first sample obtained after ingestion of caffeine. Although caffeine was ingested with the noon meal the levels obtained do not seem to rise as much as the other two ingestion periods. The sharp rises in the caffeine concentrations after the morning and afternoon coffee breaks are most likely due to an increased absorption of caffeine because of an empty stomach. The maximum concentration obtained was 8.8 μM after ingestion of caffeine at the afternoon coffee break.

From this study it seems feasible to use microdialysis sampling to study the variation in caffeine after habitual ingestion even when caffeine is present in low levels. If microdialysis could be used in other studies of caffeine such as an alternative to the caffeine test used to determine the metabolic activity of CYP 1A2, which converts caffeine to paraxanthine, [Kalow and Tang, 1993] is unknown, but may be worthwhile to study.

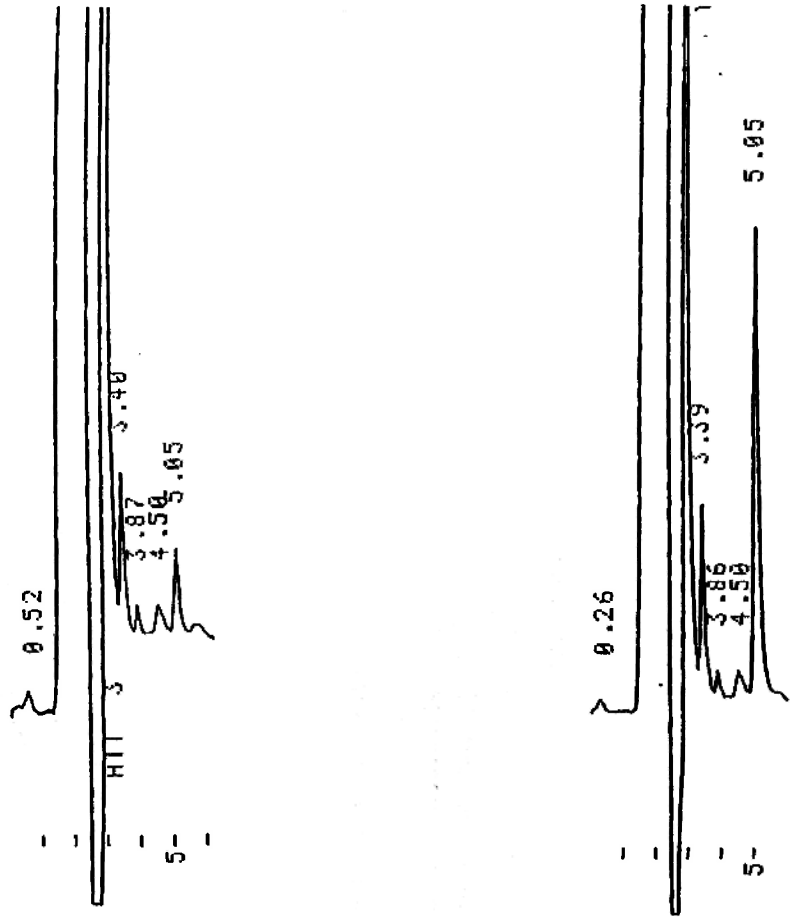


Figure 1. Chromatograms of human dialysate from 7:30 (left) and 18:30 (right). Caffeine elutes at 5.05 minutes.

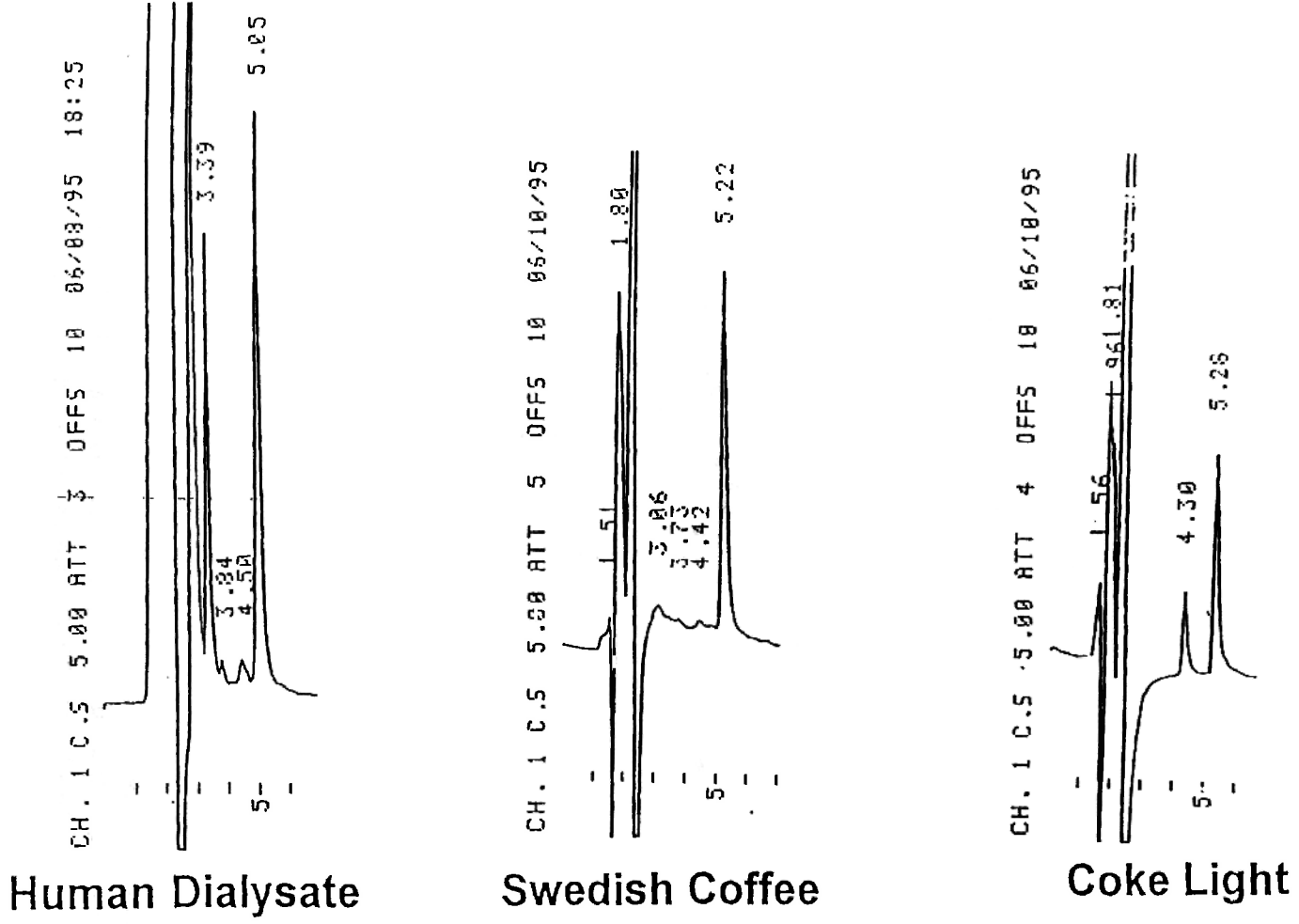


Figure 2. Chromatograms of human dialysate and samples of the beverages ingested. Caffeine elutes after 5 minutes.

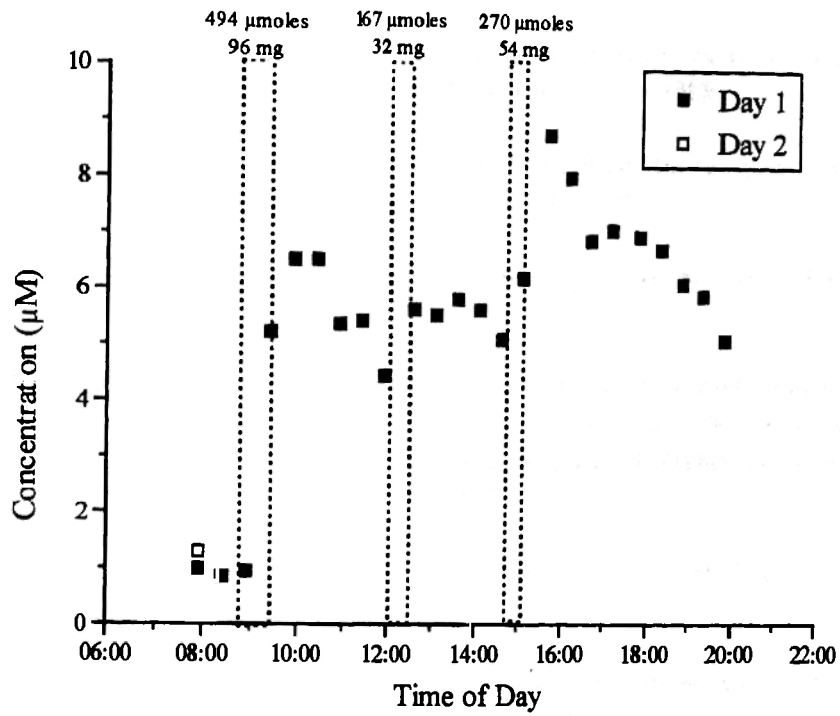


Figure 3. Caffeine concentration in human dialysate samples at the indicated discrete time points. The dose and the duration of time used to ingest the indicated dose are denoted by the boxes at 8:45, 12:00, and 14:45.

6.4 References

Caraco, Y.; Katz-Zylber, E; Granit, L.; Levy, M. Does restriction of caffeine intake affect MFO activity. *Biopharm. Drug Disp.* **1990**, *11*, 639-643.

Fredholm, B.B. Are methylxanthine effects due to antagonism of endogenous adenosine? *TIPS* **1980**, *2*, 129-132.

Griffiths, R.R.; Bigelow, G.E.; Liebson, I.A. Human coffee drinking: Reinforcing and physical dependence producing effects of caffeine. *J. Pharmacol. Exp. Ther.* **1986**, *239*, 416-425.

Griffiths, R.R.; Woodson, P.P. Reinforcing properties of caffeine: Studies in humans and laboratory animals. *Pharmacol. Biochem. Behav.* **1988**, *29*, 419-27.

Kalow W. and Tang Bing-K. The use of caffeine for enzyme assays: A critical appraisal. *Clin. Pharmacol. Ther.* **1993**, *53*, 503-514.

Nehlig, A; Debry, G. Caffeine and sports activity: a review. *Int. J. Sports Med.* **1994**, *15*, 215-223.

Rall, T.W. Drugs used in the treatment of asthma. The methylxanthines, cromolyn sodium, and other agents. in Goodman Gilman, A.; Rall T.W.; Nies, A.S.; Taylor, P. Goodman and Gilman's The Pharmacological Basis of Therapeutics, 8th edition. New York: Pergamon Press. 1990. pp. 618-637.

Somani, S.M.; Gupta, P. Caffeine: a new look at an age-old drug. *Int. J. Clin. Pharm. Ther Toxicol.*, **1988**, *26*, 521-533.

Spiller, G.A., ed. *The methylxanthine beverages and foods: Chemistry, consumption and health effects. Progress in Clinical and Biological Research, Vol. 158.* Alan R. Liss, Inc.: New York, 1984. p. 207.

Stavric, B. An update on research with coffee/caffeine (1989-1990) *Food Chem Toxicol.* **1992**, *30*, 533-555.

Stähle, L.; Arner, P.; Ungerstedt, U. Drug distribution studies with microdialysis. III: Extracellular concentration of caffeine in adipose tissue in man. *Life Sci.* **1991**, *49*, 1843-1852.

Chapter 7

Summary

The basic underlying principle that describes transport of substances to and from the microdialysis probe is diffusion. During a recovery experiment, material diffuses across the dialysis membrane into the inner fiber lumen in order to be sampled in microdialysis. The dialysis probe can also be used as a local infusion device in which analytes or enzyme inhibitors can be delivered. Although diffusion into the microdialysis probe may be a straight-forward concept, there are other factors that can affect diffusion to the microdialysis probe. These other factors will affect the separation efficiency of the microdialysis process.

Diffusive behavior of substances can be altered by a number of different processes including forced convection, homogeneous or heterogeneous reactions, tortuous pathways, solute-boundary interactions, and solute-solvent interactions. All of these processes should be considered when interpreting microdialysis data or any data obtained from an *in vivo* sensor that may include diffusion of an analyte through a membrane.

During microdialysis sampling, convection in tissues is ignored because it is assumed that diffusion is the dominant mass-transport process in tissues [Benveniste and Hüttemeier, 1990]. Chapter 2 has shown that at very low fluid velocities the flux of material to a microdialysis membrane changes as the velocity of the fluid is increased. For three different microdialysis membranes that are commonly used in our laboratory, a linear velocity of 0.025 cm/s or greater would cause the membrane to be the limit to diffusion when placed in a fluid sample. It is unknown what the values for linear fluid velocities in tissues would reach. For the brain, convection may not be a problem since the probe is secured to the skull in microdialysis experiments.

However for use in other tissues such as liver or muscle of rats, the convection may affect the recovery of a substance. In microdialysis experiments in muscle and liver, both tissues may be subject to movement, particularly in animals that are freely-moving. For liver, the question that should be considered is to what extent does the respiration of the liver play in the membrane separation. For muscle, a different question would be to what extent does local muscle contraction play in the recovery of substances.

Chapters 4 and 5 discussed how inhibition of metabolism affects the flux from the microdialysis probe. This is because diffusion through the membrane is defined by diffusion and reaction processes that occur in the tissue, which was discussed in Chapter 3. With reaction terms, the diffusive flux is increased, which results in a greater loss of material from the microdialysis probe. However, the kinetic processes that occur in a tissue are additive. If one kinetic term is much greater than another, then it is possible that the diffusive flux will not change significantly when the smaller term is removed through inhibition. This was shown in Chapter 4 from the experimental results and by using the model developed in Chapter 3. In the liver, inhibition of metabolism does not change the flux from the microdialysis probe. This can be attributed to one or two factors. The first is that the capillary permeability exchange rates are large enough that an inhibition would not significantly change the flux from the probe. This is supported by experiments that observed a drop in the flux of phenacetin and antipyrine after euthanasia of the animal. The second is that respiration of the animal cause some fluid convection around the membrane, which causes the membrane to be a limiting factor to mass-transport. The second factor is not completely supported by experimental evidence since the *in vitro* deliveries of antipyrine and phenacetin were the same, but *in vivo* deliveries were significantly different. The differences between the *in vivo* deliveries of antipyrine and phenacetin suggests that the tissue and not respiration affected the flux from the dialysis probe.

In Chapter 5, acetylcholine was used for inhibition studies because there exists only one kinetic reaction that removes it from the ECF. In this study, when metabolism was inhibited, a decrease was observed in the microdialysis flux of acetylcholine. These results and the results obtained from Chapter 4 indicate the importance of understanding the underlying physiology of the microdialysis process. Many researchers use microdialysis without appreciating how pharmacological changes affect the amount of analyte that is obtained. For brain studies, it seems relevant to proceed with caution when comparing results obtained from control and pharmacologically treated animals that obtain tissue concentrations by using *in vitro* calibrations, since tissue dynamics affect the flux to and from a microdialysis probe. In the liver, pharmacological studies will be easier to interpret since the microvasculature exchange rates dominate other kinetic rates in this tissue.

Although metabolism did not change the microdialysis flux, metabolites could be obtained in the dialysate after a local infusion in the liver. These types of experiments provide an alternate route to study metabolism with microdialysis. By perfusing the probe with varying concentrations of acetaminophen, it was found in Chapter 4 that saturable metabolism could be observed. This was seen as a decrease in the total percentage conversion of the parent compound, acetaminophen, into its metabolite acetaminophen sulfate. Additional studies with other substrates would be necessary to determine the feasibility of using microdialysis sampling as an alternative to liver perfusion studies for metabolite determination.

The results and the modeling presented in this dissertation show that diffusion coupled with microdialysis sampling can be affected by the various factors presented above. The factors presented are not meant to be the only factors that could affect microdialysis sampling. Other non-linear processes such as protein-binding and variation of diffusion coefficients through cells will also affect the microdialysis flux.

However, as was described in Chapter 3, models are made to be as parsimonious as possible. Inclusion of every possible interaction that could occur in a microdialysis experiment only leads to a model that would be parameter laden. Many of the parameters that are used in the model presented here are derived from other sources and have not been verified experimentally *in vivo*.

Benveniste, H.; Hüttemeier, C. Microdialysis-Theory and Application. *Prog Neurobiol.* **1990**, *35*, 195-215.

Appendix 1. Development of the membrane permeability equations for microdialysis.

The mathematical relationship used to determine the permeability of the

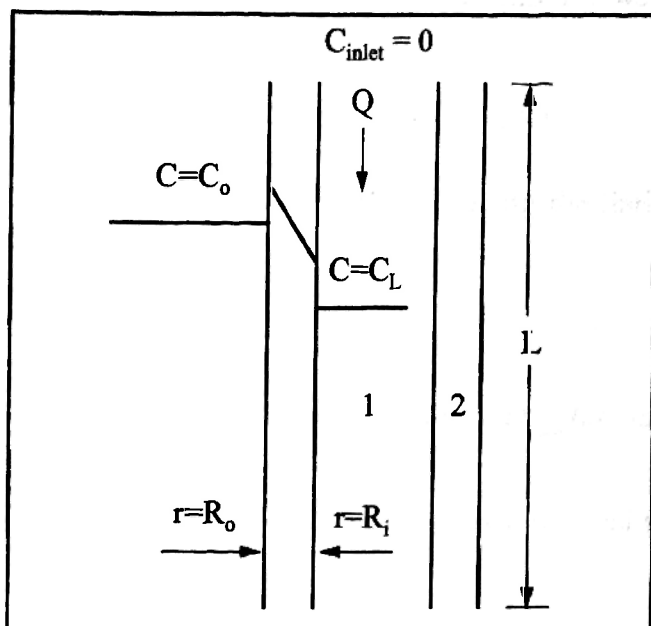


Figure 1. Schematic of the steady-state assumption. System 1 is the fluid in the probe lumen and system 2 is the membrane.

microdialysis probe membrane, Equation 1, is developed in this appendix. When the microdialysis probe is used as described in this paper, analyte diffuses from the surrounding fluid, across the probe membrane and into the flowing perfusion fluid, as shown schematically in Figure 1. For the mass balance around the probe membrane, a membrane with inner radius, R_i , and outer radius, R_o , is immersed in a solution containing a fixed concentration, C_o , of the analyte

of interest at high flow rate, so that the resistance of the external boundary layer is negligible. C'_o and C'_i are the concentrations of the analyte in the probe membrane at the inner and outer radii due to the partition coefficient, K , in Equation A1-1. Because the concentration at the inner radius is dependent on the partition coefficient, C'_o can be greater or less than the solution concentration C_o . The perfusion fluid flows through the probe at a fixed flow rate, Q . At the probe inlet, the analyte concentration in the perfusate, C_{in} , and is equal to zero in these experiments. At the probe outlet, the analyte concentration is C_L . The length of the probe exposed to the

dialysate fluid is L.

Analyte mass transport in the probe can be modelled mathematically by considering two "systems". System I consists of the flowing fluid within the probe. System II consists of the polymeric dialysis membrane that forms the wall of the probe. A mass balance around the membrane wall can be described as

$$0 = JA|_r \Delta t - JA|_{r+\Delta r} \Delta t \quad J = -D_{mem} dC'/dr \quad (A1.1)$$

Dividing equation A1 by $\Delta r \Delta t$ and taking the limit yields the following equation:

$$0 = -(d/dr)(-D_{mem}(dC'/dr)2\pi rL) \quad (A1.2)$$

Assuming no change with small changes in L and that D_{mem} is constant, Equation A1-2 may be written as

$$0 = -(d/dr)(r(dC'/dr)) \quad (A1.3)$$

Integration of Equation A1-3 two times yields

$$0 = C' + C_1 \ln r + C_2 \quad (A1.4)$$

This equation is subject to the following boundary conditions: at $r = R_o$, $C' = KC_o$ (C_o is the concentration outside of the probe); at $r = R_i$, $C' = KC_L$ (C_L is a function of the length and the concentration inside the probe).

In this case, K, the membrane partition coefficient is defined as

$$K = C'_o / C_o = C'_i / C_L \quad (\text{A1.5})$$

By using the above boundary conditions the constants C_1 and C_2 may be obtained and are as follows:

$$C_1 = K(C_L - C_o) \ln(R_i / R_o) \quad (\text{A1.6})$$

$$C_2 = \frac{K(C_o - C_L) \ln R_o}{\ln(R_o / R_i)} - KC_o \quad (\text{A1.7})$$

By using the boundary condition for R_o , Equation A4 becomes

$$C' = KC + \frac{K(C_o - C_L)}{\ln(R_o / R_i)} \ln(r / R_o) \quad (\text{A1.8})$$

Note that C_L will vary with distance along the length of the probe.

The second system, the dialysate mass balance around a unit surface area, dA , on the inside of the probe ($dA=2\pi R_i dx$) can be described as

$$0 = QC|_x - QC|_{x+\Delta x} + J\Delta A \quad (\text{A1.9})$$

By using the definition for flux from Equation A1-1, dividing by Δx , and taking limits, the mass balance becomes

$$0 = -Q(dC/dx) + 2\pi R_i D_{mem} (dC'/dr) \quad (\text{A1.10})$$

Taking the derivative of Equation A1-8 and substituting into Equation A1-10 yields Equation A1-11 upon rearrangement and integration becomes

$$\frac{dC}{dx} = \frac{2 \pi D_{mem} K}{Q \ln(R_o/R_i)} (C_o - C_L) \quad (A1.11)$$

$$-\ln(C_o - C_L) = \beta x + C_3 \quad \beta = \frac{2 \pi D_{mem} K}{Q \ln(R_o/R_i)} \quad (A1.12)$$

Equation A1-12 is subject to the entrance boundary condition, $C=0$ at $x=0$, and becomes

$$\frac{C_x}{C_o} = 1 - \exp\left(\frac{-2 \pi D_{mem} K}{Q \ln(R_o/R_i)} x\right) \quad (A1.13)$$

Rearrangement of equation A1-13 gives Equation 1 in the text of Chapter 2.

Evaluation of this equation at the probe outlet ($x=L$) relates the external bulk fluid concentration, C_o , the probe outlet concentration, C_L , and the geometry of the probe to the unknown permeability, $D_{mem}K$. The membrane permeability can then be determined experimentally by measuring C_L at various values of the perfusion flow rate, Q . The slope of the linear regression of $\ln(1-(C_L/C_o))$ vs $1/Q$ is proportional to the membrane permeability.

Several assumptions have been made in developing this equation: (1) The system is at steady state. (2) The analyte concentration just outside the probe (at $r = R_o$) is equal to the analyte concentration in the bulk external fluid. (3) Analyte transport across the probe membrane occurs by Fickian diffusion. (4) There are no radial gradients in concentration in the perfusion fluid (i.e., the fluid in the probe is well-stirred). The assumption that the system is at steady state (i.e., $dC_{outlet}/dt=0$) has been substantiated by experimental observation within 5 min of operation. Assumption 2 is equivalent to assuming that there is no resistance to analyte mass

transfer outside the probe. This is a reasonable assumption when the probe is immersed in a well-stirred liquid, as in these experiments, but may not apply to experiments performed in more resistant media such as tissue or agar. Assumption 3 is valid when hydrostatic and osmotic pressure gradients across the probe membrane are minimal, so that no significant convective mass transport occurs. Assumption 4 is likely the weakest of the four since radial concentration gradients will exist under the laminar flow conditions of these experiments. However, this assumption simplifies the mathematical modeling considerably. In addition, data presented in Chapter 2 suggest that this simple model describes the experimental results well.

Appendix 2. Development of Simplified Equations to Describe Microdialysis Flux

A.2.1 Flux From a Cylinder

This appendix derives the relationships that can be used to gain an approximate

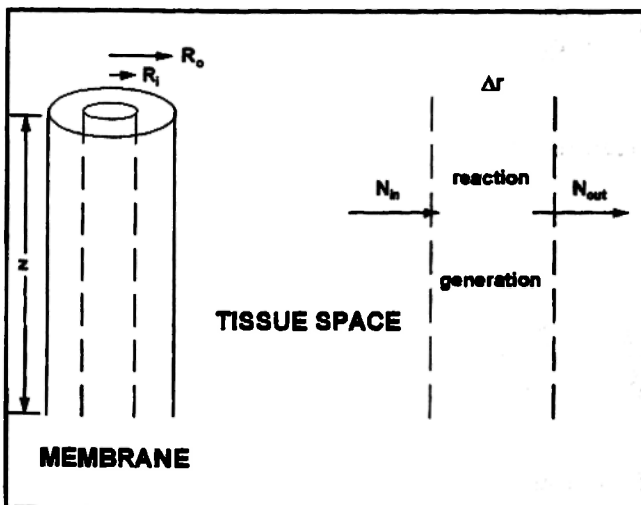


Figure 1. Dialysis membrane in a tissue space

understanding of the relative importance of the resistance from the extracellular fluid (ECF) space and the membrane to the microdialysis flux. These equations can then be used with varying approximations to determine the point at which kinetics and diffusion affect the microdialysis flux in the ECF space, and the combination of kinetic and diffusive values that

allow the membrane to begin to play more of a role in the overall mass-transport resistance of a molecule.

The approach used will first greatly simplify the microdialysis experiment so that an analytical solution for the flux away from the probe can be attained. The system to which equations will be developed is depicted in Figure 1. The dialysis membrane is a cylinder and therefore cylindrical coordinates will be used in the development of these equations. Step 1 assumes that the dialysis probe consists of a membrane cylinder that delivers a constant amount of material along the axial, z position. This would be analogous to a delivery (loss of analyte) experiment in microdialysis sampling terminology. This cylinder has an outer radius denoted as r_o .

The analyte is assumed to diffuse from the cylinder (probe) with a diffusion coefficient, D_t , and will react in the tissue space with a rate constant of k . Note that k could also be a generation constant, but here only consumption of material will be considered. The steady state ($dC/dt = 0$) equation for this process in cylindrical coordinates is described as

$$D_t \frac{1}{r} \frac{d}{dr} \left(r \frac{dC}{dr} \right) - kC = 0 \quad (\text{A2.1})$$

Upon expansion of the derivative and multiplication by the square of r , Equation A2.2 is obtained.

$$r^2 \frac{d^2C}{dr^2} + r \frac{dC}{dr} - \frac{k}{D_t} r^2 C = 0 \quad (\text{A2.2})$$

Equation A2.2 is a form of Bessel's equation that can be found in many standard mathematics textbooks as shown in Equation A2.3. [Mickley et al., 1957]

$$Ax^{2i} \frac{d^2y}{dx^2} + Bx^i \frac{dy}{dx} + Cx^k y = 0 \quad (\text{A2.3})$$

Determination of the constants in Equation A2.3 leads to the generalized form of the solution given in Equation A2.4.

$$C = c_1 I_0 \left(\sqrt{\frac{k}{D_t}} r \right) + c_2 K_0 \left(\sqrt{\frac{k}{D_t}} r \right) \quad (\text{A2.4})$$

The specific solution can be determined by using the boundary conditions at the radius and infinity: at $r = r_o$, $C = C_{\max}$ and at $r = r_{\infty}$, $C = 0$, where C_{\max} is the concentration of the material that is being released by the probe (cylinder).

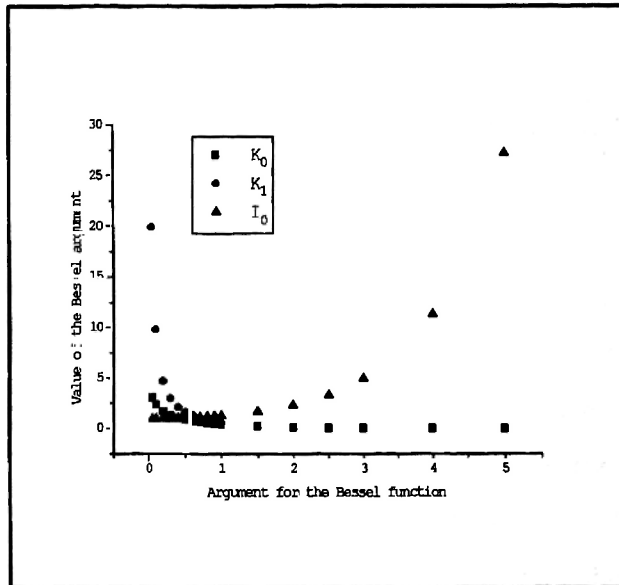


Figure 2. Values for arguments using the Bessel functions I_0 , K_0 , and K_1

The Bessel function I_0 approaches infinity with increasing values of r , and K_0 approaches zero as shown in Figure 2. Using the second boundary condition forces the value of C_1 to be zero. C_2 is found by using the first boundary condition giving the final solution shown in Equation A2.5.

$$C = C_{\max} K_0 \left(\sqrt{\frac{k}{D_t}} r \right) / K_0 \left(\sqrt{\frac{k}{D_t}} r_o \right) \quad (\text{A2.5})$$

The flux is defined as the amount of material removed per unit area and time and is described by Fick's law as:

$$J = -D_t \frac{dC}{dr} \quad (\text{A2.6})$$

The derivative of Equation A2.5 gives Equation A2.7 knowing that the derivative of the Bessel function K_0 is the Bessel function $-K_1$.

$$J = \sqrt{D_t k} C_{\max} K_1 \left(\sqrt{\frac{k}{D_t}} r \right) / K_0 \left(\sqrt{\frac{k}{D_t}} r_o \right) \quad (\text{A2.7})$$

The value Bessel functions K_0 and K_1 for the given values of the argument can be found by using tables found in handbooks [Abramowitz and Stegun], by writing a FORTRAN program [Press et al., 1986], or by using a common spreadsheet program such as Microsoft Excel, Version 4. Once the argument values are obtained the flux at the outer radius can be determined. Note that from Figure 2 that the quotient of K_1 / K_0 will approach one as the value of the argument increases, or for the same probe radius, for values of increasing rates of consumption or decreasing rates of diffusion as would be found with larger molecular weight substances. For these instances the flux reduces to the square root of the product of the tissue diffusion coefficient and the kinetic rate constant.

A2.2 Flux from the Membrane with Membrane Diffusion Included

The next step in the approximation of the factors that will affect the flux away from a microdialysis probe is to include the diffusion of substances through the membrane. By the inclusion of the membrane in the equations, it can be determined at what values of the diffusion coefficient in the tissue and the kinetic rate constants the membrane will play a limiting factor.

Equations A2.5 and A2.7 describing the flux from a cylinder will be used and incorporated into the flux derivation that includes flux through the membrane. For the diffusion through the membrane the mass balance is simply the diffusive flux through the membrane as was described in Appendix 1 for the equations used in Chapter 2.

$$0 = JA|_r \Delta t - JA|_{r+\Delta r} \Delta t \quad J = -D_m \frac{dC'}{dr} \quad (\text{A2.8})$$

Dividing by $\Delta r \Delta t$, taking the limit yields:

$$0 = -\frac{d}{dr} \left(-D_m \left(\frac{dC'}{dr} \right) 2\pi r L \right) \quad (\text{A2.9})$$

The length of the membrane, L , will remain constant and it is assumed that the diffusion coefficient also remains constant, i.e. no changes in temperature or viscosity across the membrane, allowing Equation A2.9 to be reduced to A2.10.

$$0 = -\frac{d}{dr} \left(r \frac{dC'}{dr} \right) \quad (\text{A2.10})$$

Integration two times yields,

$$C' = c_1 \ln r + c_2 \quad (\text{A2.11})$$

where c_1 and c_2 are the constants of integration and C' is the value of the concentration in the membrane. The boundary conditions are as follows: at $r = r_i$ (the inner radius) $C' = C_i$ and at $r = r_o$ (the outer radius) $J_m = J_i$. In words, these boundary conditions state that at the inner radius of the membrane, the concentration will be equal to a constant denoted as C_i . This assumes that the dialysate is flowing

fast enough to allow for minimal depletion of the substance through the dialysis fiber lumen. This could also be a well-stirred assumption that the concentration is constant across the fiber. An approximate value of this would be for flow rates greater than 2 $\mu\text{l}/\text{min}$. The value of the recovery is of course length dependent so an approximation would be no more than 10 percent loss from the dialysate fiber lumen. From this approximation the value of the C' would only range from say 10 μM at the beginning of the entrance of the dialysate to 9 μM at the outlet collection side of the dialysis probe. This rate of course would be dependent upon the kinetics of the tissue and the length of the membrane. Boundary condition 2 (BC 2) is an equality of flux equation that indicates that flux at the outer radius is the same as the flux through the tissue at that point. BC 2 will be used to couple the membrane equation with the tissue equation previously derived. From BC 1 it is clear that

$$c_2 = C_i - c_1 \ln r_i \quad (\text{A2.12})$$

By using the equation for c_2 and the membrane concentration equation, A2.11, the concentration at the membrane outer surface is shown in A2.13.

$$C_m = C_i + c_1 (\ln(r_o/r_i)) \quad (\text{A2.13})$$

C_m will be substituted for the term C_{max} from Equation A2.7. The flux at the membrane is described by using Fick's first law shown in Equation A2.8 and by taking the derivative of Equation A2.13.

$$J_{\text{mem}} = -D_m \frac{dC'}{dr} \quad \left. \frac{dC'}{dr} \right|_{r_o} = \frac{c_1}{r_o} \quad (\text{A2.14})$$

For continuity the flux into the tissue must equal the flux leaving the probe membrane. Utilizing Equations A2.7, A2.13 and A2.14 allows the determination of

the constant c_1 . To clean up the algebra the substitution κ is made to hold the Bessel functions is suggested as shown in Equation A2.15

$$\kappa = \sqrt{D_e k} \frac{K_1(\sqrt{k/D_e} r_o)}{K_0(\sqrt{k/D_e} r_o)} \quad (\text{A2.15})$$

After setting Equations A2.14 and A2.7 equal to each other and substituting Equation A2.7 for C_{\max} , the constant c_1 can be found.

$$c_1 = \frac{-\kappa C_i}{(D_m/r_o + \kappa \ln(r_o/r_i))} \quad (\text{A2.16})$$

An expression for the concentration in the membrane at any radial point, r , is shown in Equation A2.17.

$$C' = C_i - \left(\kappa \frac{C_i}{(D_m/r_o) + \kappa \ln(r_o/r_i)} \right) \ln(r/r_i) \quad (\text{A2.17})$$

Now the flux through the membrane at any radial point is found by taking the derivative of Equation A2.17 and inserting it into the expression provided by equation A2.14.

$$J = D_m \left(\kappa \frac{C_i}{(D_m/r_o) + \kappa \ln(r_o/r_i)} \right) \frac{1}{r} \quad (\text{A2.18})$$

Recall that κ approaches the value of one at high kinetic rates and low diffusion coefficients as would be found for larger molecular weight substances such as the neuropeptide substance P. Additionally the geometry of the membrane plays a role since for thinner membranes such as cuprophan that has a outer radius, r_o , of 222 μm

and an inner radius, r_1 , of 200 μm the value of the natural logarithm will approach unity.

A2.3 References

Abramowitz, M.; Stegun, I.A. (Eds.) *Handbook of Mathematical Functions*, National Bureau of Standards: Washington, D.C., 1964.

Mickley, H.S.; Sherwood, T.K.; Reed C.E. *Applied Mathematics in Chemical Engineering, 2nd edition*; McGraw-Hill Book Company: New York, 1957, 163-200.

Press, W.H.; Flanner, B.P.; Teukolsky, S.A.; Vetterling,, W.T. *Numerical Recipes in FORTRAN: The Art of Scientific Computing, 2nd edition*; Cambridge University Press: Cambridge, 1986.

Appendix 3. Development of the Far-Field Boundary Condition in a Recovery Microdialysis Experiment

The far-field boundary condition is described by the following differential equation:

$$\frac{dC_e^\infty}{dt} = k_{pe}^x C_o e^{-\lambda t} - (k_m + k_{tp}^x) C_e \quad (\text{A3.1})$$

This equation states mathematically that the change in the far-field tissue concentration, $C_e(\infty)$ is related to the initial concentration in the plasma, C_o , the local tissue concentration, C_e , the plasma elimination rate constant, λ the permeation rate constants between the tissue and the plasma compartments, k_{ep} , k_{pe} , and the local metabolism rate, k_m . The equation is a linear differential equation and can be solved by using integrating factors which is described in most standard textbooks on differential equations [Potter, 1978]. By combining the rate constants associated with C_e to give a new rate constant k_s , the solution can be obtained by the following general equation.

$$u(x) = \frac{1}{F(x)} \left[\int g(x) F(x) dx + C \right] \quad (\text{A3.2})$$

The general form of the equation is described as:

$$F(x) = e^{\int k_s dt} \quad (\text{A3.3})$$

By using the general solution the specific solution is then found to be:

$$C_e^\infty(t) = \frac{1}{e^{k_s t}} \left[\int (k_{pe}^x C_o e^{-\lambda t}) e^{k_s t} + C \right] \quad (\text{A3.4})$$

Integration of equation 4 yields:

The constant of integration, C , can be solved for by using the initial condition of $C_\infty=0$, when $t = 0$. The final solution that is used in the mathematical model

$$C_e^\infty(t) = \frac{k_{pe}^x C_o e^{(k_s - \lambda)t}}{e^{k_s t} (k_s - \lambda)} + \frac{C}{e^{k_s t}} \quad (\text{A3.5})$$

becomes:

$$C_e^\infty(t) = \frac{k_{pe}^x C_o e^{(-\lambda)t}}{(k_s - \lambda)} + \frac{k_{pe}^x C_o}{e^{k_s t} (k_s - \lambda)} \quad (\text{A3.6})$$

References

Potter, M.C. *Mathematical Methods in the Physical Sciences*. Prentice-Hall, Inc.: Englewood Cliffs, 1978.

Appendix 4. FORTRAN Code.

```

1 c      DIALYSIS.FOR
2
3 c      Julie Ann Stenken
4
5 c      Submitted with the Ph.D. dissertation in partial
6 c      requirements of the graduate school.
7
8 c      This FORTRAN program calculates the concentration profile
9 c      and the concentration outflow of a microdialysis
10 c     experiment given the parameters in the file DATAFILE.DAT.
11
12 c     The theoretical development of this model is given
13 c     in CHAPTER 3 of this dissertation. Additional information
14 c     concerning the steps taken to achieve a result are
15 c     also presented in Chapter 3.
16
17
18 c     The program can be used for the two typical modes
19 c     of operation in microdialysis -- recovery and delivery.
20
21 c     The program runs easily on an IBM compatible computer
22 c     with a 386 math co-processor or greater. The length of time
23 c     for the program to complete the calculations necessary is
24 c     dependent on the parameters inputted and the speed of the
25 c     computer, i.e., a 66 MHz 486 runs faster than a 33 MHz 486.
26 c     With the 486-66 MHz system the average time to completion
27 c     is approximately 3 minutes. This time to completion is also
28 c     dependent on the tolerances used in the final calculations.
29 c     The tolerances used for error are set, but could be
30 c     changed if the user only wishes for a rough answer to
31 c     a particular problem. The program would only need to
32 c     be recompiled using any FORTRAN compiler prior to use with
33 c     the new tolerances.
34
35 c     The program utilizes the finite difference approach to
36 c     solving the mass balance equations. This program does NOT
37 c     use any links to FORTRAN libraries such as the IMSL library.
38 c     This allows any individual to run and use this program as
39 c     the IMSL library is expensive and proprietary.
40
41 c     The program is made up of the following sub-routines
42 c     which are linked together and serve the functions briefly
43 c     mentioned here, but described in more detail in the code.
44
45 c     These subroutines are called in the following order. A
46 c     TOP-DOWN design indicates which subroutines call other
47 c     subroutines in the code.
48 c
49 c     1) INIT -- Subroutine INIT reads the file DATAFILE.DAT
50 c     and sets up all the initial values for the inputs
51 c     needed for the program
52
53 c     2) BCOND -- Subroutine BCOND sets up the initial arrays
54 c     of coefficients necessary for the solving of
55 c     the dialysis outflow concentration and the
56 c     concentration profile.
57
58 c     3) SOLVE -- This subroutine is sets up the arrays
59 c     needed for the other subroutines to perform their
60 c     job of solving the matrices which describe the
61 c     outflow concentration and the profile away from
62 c     the probe. SOLVE calls the following subroutine

```

63 c 3A) RAMP -- Subroutine RAMP is used as the
64 c finite difference methods are step methods
65 c in time and space. This subroutine gets
66 c values into the various arrays so that
67 c the computation in solve can be more
68 c stable. RAMP calls three other subroutines
69 c THOMEM and THOMECECF before calling DATOUT
70 c inorder to output the data.
71 c 3Ai) THOMEM -- Calculates the flux through the
72 c dialysis membrane. This routine uses the
73 c THOMAS algorithm found in basic numerical methods
74 c textbooks to solve the tri-diagonal matrices. This
75 c routine differs from THOMECECF because the number of
76 c equations necessary to solve the membrane matrices
77 c is fixed to the value of 10, whereas the THOMECECF
78 c routine uses the number of equations calculated
79 c the body of the program.
80 c 3Aii) THOMECECF -- Uses the same algorithm as above
81 c except that the number of equations is determined
82 c by the main program and the radius away from the
83 c dialysis membrane.
84 c 3Aiii) DATOUT -- This subroutine outputs the data
85 c into ASCII files which then can be read into any
86 c spreadsheet program for futher data analysis or
87 c plotting.
88 c
89 c 3B) THOMEM
90 c 3C) THOMECECF
91 c 3D) DATOUT

92
93 c VARIABLES USED IN THE PROGRAM

94
95 c *****
96
97 c ACOEFF(700) MATRIX OF COEFFICIENTS IN THE ECF IN "RAMP"
98 c BCOEFF(700) "
99 c CCOEFF(700) "
100 c CHI(700) Same as EPS except used in SUBROUTINE RAMP
101 c COEFFA(700) MATRIX OF COEFFICIENTS FOR THE ECF
102 c COEFFB(700) MATRIX "
103 c COEFFC(700) MATRIX "
104 c CMAX = CONCENTRATION AT A FAR RADIAL POINT USER INPUT
105 c DELCON = CONCENTRATION OF THE DIALYSATE
106 c DDIAL = DIFFUSION COEFFICIENT IN THE DIALYSATE (cm²/min)
107 c DECF = DIFFUSION COEFFICIENT IN ECF (CM²/MIN)
108 c DELTA = Delta of time (min)
109 c DELR = DELTA OF RADIAL DISTANCE (cm)
110 c DMEM = DIFFUSION COEFFICIENT IN THE MEMBRANE (CM²/MIN)
111 c ECFLAM(700) = MODEL DIFFUSION COEFFICIENT USED IN SUBROUTINE
112 c RAMP ...DIFFERENT TIME DEPENDENCE
113 c ECFT(700)= MATRIX OF NUMR VALUES AT TIME T
114 c ECFTP1(700)=MATRIX OF NEW VALUES AT T PLUS 1
115 c EPS(700) = A VALUE FOR THE COEFFICIENT OF C(i,j+1)
116 c FLUXRI = FLUX IN THE MEMBRANE AT INNER SURFACE
117 c GAMMA = APPROXIMATE DISTANCE OF THE CONCENTRATION PROFILE
118 c AT HALF THE CONCENTRATION MAXIMUM.
119 c See Morrison et al. Quantitative Microdialysis.
120 c TE Robinson and JB Justice Jr eds.in
121 c Microdialysis in the Neurosciences
122 c GICF = PRODUCTION (GENERATION) RATE IN THE ICF (min⁻¹)
123 c GECF = GENERATION RATE IN THE ECF
124 c LAMMEM = MODEL DIFFUSION COEFFICIENT IN THE MEMBRANE
125 c LAMECF(700) = MODEL DIFFUSION COEFFICIENT (DECF*DELTA/DELR²
126 c IN THE ECF
127 c MEMLAM = MODEL DIFFUSION COEFFICIENT IN THE MEMBRANE

```

128 C          DURING "RAMP"
129 C          PHI      = VOLUME FRACTION OF SPACE IN THE ECF
130 C          PHIM     = VOLUME FRACTION OF SPACE IN THE MEMBRANE
131 C          QDIAL    = DIALYSIS FLOW RATE mL/MIN
132 C          rmax     = USER INPUT OF MAX DISTANCE (cm)....7*GAMMA
133 C          RIN      = INNER RADIUS OF MEMBRANE (CM)
134 C          ROUT     = OUTER RADIUS OF MEMBRANE (CM)
135 C          RMETAB   = METABOLIC RATE IN ECF (min -1)
136 C          RICF     = METABOLIC RATE IN THE ICF (min -1)
137 C          TAU      = DELTA T/10.0 .....USED IN SUBROUTINE 'RAMP'
138 C          VOLICF   = VOLUME FRACTION IN THE ICF (1-PHI)
139 C          XKPI     = PARTITION COEFFICIENT BETWEEN ICF AND ECF
140 C          XKPLEC   = EXCHANGE RATE BETWEEN PLASMA TO ECF
141 C          XKECPL   = EXCHANGE RATE BETWEEN ECF AND PLASMA
142 C          XLEN     = LENGTH OF DIALYSIS FIBER IN CM
143
144 C          *****
145
146 C          Begin Program
147
148          REAL COEFFA(700), COEFFB(700), COEFFC(700), ECFT(700), ACOEFF(700),
149 &          BCOEFF(700), CCOEFF(700), LAMECF(700), ECFLAM(700), EPS(700),
150 &          CHI(700), DELR(700), RMAX, DELT, DECF, TIME, DMEM, XKPLEC, XKECPL,
151 &          CMAX, RMETAB, SUMKS, LAMMEM, TAU, MEMLAM, QDIAL, XLEN, DDIAL
152
153          INTEGER NUMR, NUMT
154
155 C          DATAFILE.DAT is a file which contains the necessary
156 C          microdialysis parameters such as diffusion coefficients,
157 C          rate constants etc.
158
159 C          All *.ASC files must be deleted prior to the start
160 C          of the program -- otherwise the program will not
161 C          run as the files cannot be opened and written over.
162
163
164 C          CONPROF.ASC is a created file of the concentration profile
165 C          away from the dialysis probe.
166 C          PLASMA.ASC is a file that outputs what the plasma
167 C          concentration is as a function of time..it can be deleted
168 C          if necessary.
169 C          OUTPUT.ASC is the concentration of the dialysis perfusion
170 C          fluid as a function of time.
171
172          OPEN(UNIT=15, FILE='DATAFILE.DAT', STATUS='OLD')
173          OPEN(UNIT=60, FILE='CONPROF.ASC', STATUS='NEW')
174          OPEN(UNIT=62, FILE='PLASMA.ASC', STATUS='NEW')
175          OPEN(UNIT=65, FILE='OUTPUT.ASC', STATUS='NEW')
176
177
178 C          THE PROGRAM FIRST INITIALIZES THE PARAMETERS AND READS
179 C          PARAMETERS FROM THE FILE 'DATAFILE.DAT'
180
181          CALL INIT(LAMECF, ECFLAM, EPS, CHI, DELR, RIN, DELT, DECF, DMEM,
182 &          MEMLAM, TIME, RMAX, XKPLEC, XKECPL, RMETAB, CMAX, LAMMEM, TAU,
183 &          ROUT, SUMKS, QDIAL, XLEN, DDIAL, RMULT, RUNIT, GICF, GECF, NUMR, NUMT)
184 C
185 C          The next call goes to subroutine bcond which will set up
186 C          the array for the boundary conditions. This
187 C          also includes the coefficients necessary to solve
188 C          the matrix implicitly.
189
190          CALL BCOND(COEFFA, COEFFB, COEFFC, ACOEFF, BCOEFF, CCOEFF,
191 &          ECFT, LAMECF, ECFLAM, EPS, CHI, MEMLAM, LAMMEM, RMULT, NUMR)
192

```

```

193 C      The next call goes to set up the matrix for the Thomas
194 c      algorithm. This solves the matrix at each time step.
195 c      This routine includes the call to the output also.
196
197      CALL SOLVE(ECFT, COEFFA, COEFFB, COEFFC, ACOEFF, BCOEFF, CCOEFF,
198 &      DELR, DELT, CMAX, SUMKS, ROUT, RIN, DMEM, DECF, QDIAL, XLEN, DDIAL,
199 &      TAU, XKPLEC, RUNIT, GICF, GECF, NUMR, NUMT)
200
201      CLOSE (UNIT=15, STATUS='KEEP')
202      CLOSE (UNIT=60, STATUS='KEEP')
203      CLOSE (UNIT=62, STATUS='KEEP')
204      CLOSE (UNIT=65, STATUS='KEEP')
205
206      print*, 'done'
207      END
208
209      SUBROUTINE INIT (LAMECF, ECFLAM, EPS, CHI, DELR, RIN, DELT, DECF, DMEM,
210 &      MEMLAM, TIME, RMAX, XKPLEC, XKECPL, RMETAB, CMAX, LAMMEM, TAU,
211 &      ROUT, SUMKS, QDIAL, XLEN, DDIAL, RMULT, RUNIT, GICF, GECF, NUMR, NUMT)
212
213      REAL LAMECF(700), ECFLAM(700), EPS(700), CHI(700), DELR(700), DELT,
214 &      DECF, TIME, RMAX, STEP, TMSTEP, RMETAB, XKPLEC, XKECPL, TAU, MEMLAM,
215 &      LAMMEM
216
217      INTEGER NUMR, NUMT
218
219 C      *****
220 C      PARAMETERS INTERNAL TO INIT
221 C      ++++++
222 C      RUNIT = SMALLEST POSSIBLE delta r
223 C      RMULT = A NUMBER TO SET THE COEFFICIENTS CORRECTLY AS
224 C      RIN.NE.0.0 ...THEREFORE NEED TO SET SPACE
225 C      DIMENSION CORRECTLY
226 C      SUMKS = THE SUM OF ALL THE RATE CONSTANTS
227 C      STEP = SIZE OF delta r
228 C      NSTEP = NUMBER OF POINTS IN THE MEMBRANE
229 C      SUMRAD = SUM OF THE RADIAL STEPS TO REACH RMAX (~COUNTER)
230 c      VOLICF = IS THE VOLUME IN THE ICF SPACE.
231 C      SMULT = THE EXPONENTIAL MULTIPLIER FOR THE SPACE STEP
232 C      *****
233
234 c      *****
235 c      3-14-94 Included the variable space step size from
236 c      Feldberg, J. Electroanal. Chem . 127(1981)1-10.
237 c      delx = delx*exp[beta*(i-1)] beta .LE. 0.5
238 c      The variable step size will only be included in the
239 c      ECF
240 C      *****
241
242 C      Purpose and function of subroutine INIT
243 c      -----
244 c      This subroutine initializes all of the values that
245 c      will be used in the program. It also sets up the delta r values
246 c      and the delta t values used in the program. There are two
247 c      different values that are used for delta t. The first is TAU
248 c      which is used for SUBROUTINE RAMP. TAU = DELT/10.
249 c      Then the program sets up the variables for the
250 c      model diffusion coefficients that include  $\delta t$  and  $\delta r$  dependence
251 c      and therefore need to be stored in the arrays LAMECF and
252 c      ECFLAM.
253 c
254 c      ++++++
255
256 C      Decf is in cm^2/sec. It will need to be converted to
257 c      CM^2/min

```

```

258 10      FORMAT(E10.4)
259          READ(15,10)ROUT
260          READ(15,10)RIN
261
262 C          The smallest radial unit (RUNIT) is defined as below:
263
264          RUNIT=(ROUT-RIN)/10
265          RMULT = RIN/RUNIT
266          READ(15,10)DDIAL
267          READ(15,10)DMEM
268          READ(15,10)DECF
269          READ(15,10)PHI
270          READ(15,10)PHIM
271          VOLICF = 1.0-PHI
272
273 c          Correct for the diffusion coefficient in terms of minutes and
274 c          in terms of volume fraction.
275
276          DDIAL = DDIAL*60.0
277          DECF  = (DECF*60.0)*PHI
278          DMEM  = PHIM*(DMEM*60.0)
279
280          READ(15,10)RMETAB
281          READ(15,10)RICF
282          READ(15,10)XKPLEC
283          READ(15,10)XKECPL
284          READ(15,10)GICF
285          READ(15,10)GECF
286          READ(15,10)XKPI
287
288 c          Change all the rates to reflect the dependence on the ECF
289 c          volume fraction
290
291          RMETAB = RMETAB*PHI
292          XKPLEC = XKPLEC*PHI
293          XKECPL = XKECPL*PHI
294          RICF   = RICF*XKPI*VOLICF
295
296 C          Note that the generation terms are concentration dependent ...if
297 c          the substance being modeled has zero order generation this
298 c          will need to be included in the matrix for the Thomas
299 c          algorithm..as is the case for the plasma to ECF term XKPLEC
300
301          GECF = GECF*PHI
302          GICF = GICF*VOLICF
303
304
305          SUMKS=(XKECPL+RMETAB+RICF)
306
307          RMAX = 0.5
308
309          STEP=(RMAX-RIN)/RUNIT
310          NSTEP = INT(STEP) + 1
311          READ(15,10)TIME
312          READ(15,10)TMSTEP
313          DELT=TIME/TMSTEP
314          TAU = DELT/10.0
315          LAMMEM=(DMEM*DELT)/(RUNIT**2.0)
316          MEMLAM=(DMEM*TAU)/(RUNIT**2.00)
317          NUMT = INT(TIME/DELT)+1
318
319          READ(15,10)CMAX
320          READ(15,10)XLEN
321          READ(15,10)QDIAL
322

```

```

323 C      Change QDIAL from ul/min to cm^3
324       QDIAL=QDIAL/1000.0
325
326       SUMRAD = RIN+(10*RUNIT)
327 c      SMULT is the multiplier for the exponential space step. 0.005
328 c      was determined 'experimentally' to be the best without
329 c      sacrificing disk space and computational time as well as FLUX
330 c      determination errors.
331
332       SMULT = 0.005
333
334 c      -----
335 C      The following loop is necessary for the correct 'model'
336 c      diffusion coefficient to be calculated. This coefficient
337 c      is based upon the length of delta r and hence must be stored
338 c      in an array that keeps this. When the RMAX has been passed
339 c      then the LOGICAL IF statement causes a jump out of the loop.
340 c      -----
341
342       DO 15 I=11,NSTEP
343         DELR(I)=RUNIT*EXP(smult*(I-11))
344         LAMECF(I+1)=(DECF*DELT)/(DELR(I)**2.00)
345         ECFLAM(I+1)=(DECF*TAU)/(DELR(I)**2.00)
346         EPS(I+1) = -1.0-(2.0*LAMECF(I+1))-(DELT*(SUMKS))
347         CHI(I+1) = -1.0-(2.0*ECFLAM(I+1))-(TAU*(SUMKS))
348         SUMRAD= SUMRAD+DELR(I)
349         IF(SUMRAD.GE.RMAX) THEN
350           GOTO 2
351         ENDIF
352 15      CONTINUE
353 2       NUMR=I+1
354
355       WRITE(60,163)NUMR
356 163    FORMAT(1X,'THE NUMBER OF STEPS =',I4)
357
358       RETURN
359       END
360
361
362       SUBROUTINE BCOND(COEFFA,COEFFB,COEFFC,ACOEFF,BCOEFF,CCOEFF,
363 & ECFT,LAMECF,ECFLAM,EPS,CHI,MEMLAM,LAMMEM,RMULT,NUMR)
364
365       REAL COEFFA(700),COEFFB(700),COEFFC(700),ACOEFF(700),
366 & BCOEFF(700),CCOEFF(700),ECFT(700),LAMECF(700),
367 & EPS(700),CHI(700),ECFLAM(700),MEMLAM,LAMMEM
368       INTEGER NUMR
369 C
370 c      *****
371 c      The purpose of BCOND is to set up the initial and
372 c      boundary conditions. It sets up all the coefficients
373 c      for the subroutine SOLVE and RAMP.
374 c      ++++++
375 c
376 C      Set the initial time conditions
377
378       DO 10 J=1,NUMR
379         ECFT(J)=0.00
380 10      CONTINUE
381
382 C      SET UP THE COEFFICIENT MATRIX
383
384 c      COEFF(11) is the membrane/ECF point and the 1,-1 account for
385 c      the equality of flux.
386
387         COEFFB(11) = 1.0

```

```

388          BCOEFF(11) = COEFFB(11)
389          COEFFA(11) = -1.0
390          ACOEFF(11) = COEFFA(11)
391
392 c          Points number 2-10 are all in the membrane
393
394          DO 15 I=2,10
395              ACOEFF(I)=MEMLAM-(MEMLAM/(2.0*(RMULT+(I-1))))
396              BCOEFF(I)= -1*(1.0 + (2.0*MEMLAM))
397              CCOEFF(I)=MEMLAM+(MEMLAM/(2.0*(RMULT+(I-1))))
398              COEFFA(I)=LAMMEM-(LAMMEM/(2.0*(RMULT+(I-1))))
399              COEFFB(I)= -1*(1.0 + (2.0*LAMMEM))
400              COEFFC(I)=LAMMEM+(LAMMEM/(2.0*(RMULT+(I-1))))
401 15          CONTINUE
402
403 c          Points 12 on are all in the ECF
404
405          DO 20 I=12,NUMR-1
406              ACOEFF(I)= ECFLAM(I)-(ECFLAM(I)/(2.0*(RMULT+(I-1))))
407              BCOEFF(I)= CHI(I)
408              CCOEFF(I)= ECFLAM(I)+(ECFLAM(I)/(2.0*(RMULT+(I-1))))
409              COEFFA(I)= LAMECF(I)-(LAMECF(I)/(2.0*(RMULT+(I-1))))
410              COEFFB(I)= EPS(I)
411              COEFFC(I)= LAMECF(I)+(LAMECF(I)/(2.0*(RMULT+(I-1))))
412 20          CONTINUE
413
414          RETURN
415          END
416
417
418          SUBROUTINE SOLVE(ECFT, COEFFA, COEFFB, COEFFC, ACOEFF, BCOEFF, CCOEFF,
419 &          DELR, DELT, CMAX, SUMKS, ROUT, RIN, DMEM, DECF, QDIAL, XLEN, DDIAL,
420 &          TAU, XKPLEC, RUNIT, GICF, GECF, NUMR, NUMT)
421
422          REAL ECFT(700), ECFTP1(700), COEFFA(700), COEFFB(700),
423 &          COEFFC(700), ACOEFF(700), BCOEFF(700), CCOEFF(700),
424 &          VALUE(700), DELR(700), DELT, CMAX, RIN, XKPLEC, sumks, TAU
425
426          INTEGER NUMR, NUMT, IPROG
427
428 c          The file 'ECFCON.DAT' is necessary for the auxillary
429 c          programs 'DEADDIAL.FOR' and 'METAB.FOR'
430
431          OPEN(UNIT=85, FILE='ECFCON.DAT', STATUS='NEW')
432
433          *****
434 c          PARAMETERS INTERNAL TO SOLVE
435 C          -----
436 C
437 C          PERCEN = A GUESS OF WHAT THE PERCENTAGE OF THE FAR-FIELD
438 C                   ECF VALUE WILL EQUAL THE OUTLET DIALYSATE CONC.
439 C          ARGUM  = A VALUE THAT CHECKS THE PERCENTAGE OF DIFFERENCE
440 C                   BETWEEN THE FLUX IN THE ECF TO THE MEMBRANE AND
441 C                   THE FLUX IN THE MEMBRANE.
442 C          ADUM   = A HOLDING VARIABLE TO CALCULATE CINFIN
443 C          CINFIN = CONCENTRATION VALUE AT THE FAR-FIELD ECF
444 C          PCNNEW = AN UPDATED VALUE OF PERCEN WHICH REFLECTS WHAT
445 C                   THE CONCENTRATION OF THE DIALYSATE SHOULD BE.
446 C          VALUE  = AN ARRAY THAT HOLDS THE VALUES NECESSARY FOR
447 C                   THE THOMAS COMPUTATION
448
449
450 c          For each time increment, a new matrix of values will have to
451 c                   be calculated. Once that matrix is set up then the program
452 c                   is ready to call the Thomas algorithm.

```



```

453 c      Start time loop
454 C          A percentage of the far-field concentration is
455 c          entered to get the program rolling.
456
457 c          *****
458 c          For the delivery case will use a percentage loss and
459 c          compare it with the various flux values.
460 c          *****
461
462          READ(15,*)CPERF
463          READ(15,*)XLAM
464
465
466 C          A set of integer flags called iprog to determine
467 c          initially if the program needs to be in recovery or
468 c          delivery mode.
469
470 c          IPROG = 1 denotes a recovery experiment
471 c          IPROG = 2 denotes a delivery experiment
472
473
474 c          The suroutine ramp is needed to just get values into the
475 c          arrays so that there is no lag in the curve due
476 c          to the time step jump. RAMP reduces the time step
477 c          to alleviate this lag problem. This was a rather
478 c          severe problem in the far-field concentration profile.
479 c          ...But did not seem to affect the dialysis
480 c          concentration. In order to make the program more
481 c          complete this sub-routine was included.
482
483
484 C          PERCEN is either the percentage lost or the percentage
485 c          gained of the far-field value CINF..USE 1.0 *(9-15-94).
486 c          For most applications this works well.
487
488          PERCEN = 0.001
489
490          CALL RAMP(ECFT,ACOEFF,BCOEFF,CCOEFF,DELR,CMAX,PERCEN,
491 & RUNIT,SUMKS,ROUT,RIN,DMEM,DECF,QDIAL,XLEN,DDIAL,TAU,XKPLEC,
492 & GICF,GECF,CPERF,XLAM,NUMR)
493
494          ARGUM = 0.0
495
496
497          DO 40 I=3,NUMT
498
499
500 c          Since the BC at the wall will be zero, then this moves
501 c          the indexing back one.
502 c          XLAM includes the decay in the blood.
503
504          CPLAS = CMAX*EXP(-XLAM*(REAL(i-1)*DELT))
505          TIME = REAL(I-1)*DELT
506          WRITE(62,368)TIME,CPLAS
507 368          FORMAT(1X,F10.6,3X,F10.6)
508
509          DENDUM = SUMKS-XLAM
510
511          ADUM= ((CPLAS*XKPLEC+GICF+GECF)/DENDUM)
512          BDUM = (XKPLEC*CMAX)/DENDUM
513          CINFIN=ADUM-(BDUM*EXP(-SUMKS*DELT*REAL(i-1)))
514          CPLAS = CMAX*EXP(-XLAM*(REAL(i-1)*DELT))
515          WRITE(60,367)CPLAS,cinfin
516 367          FORMAT(1x,F12.5,2x,f12.5)
517

```

```

518             IF (CPERF.GT.CINFIN) THEN
519                 IPROG = 2
520             ELSE
521                 IPROG = 1
522             ENDIF
523
524 C           5-9-94 HAD PROBLEMS WITH DIVIDE BY ZERO ERROR CHANGED THIS
525 C           TO A LOGICAL STATEMENT TO ALLEVIATE THE PROBLEM WITH
526 C           A REAL DELIVERY
527
528                 ADDER = 1.0E-4
529
530                 PCNNEW = PERCEN
531 c
532 c           Calculate the approx. value for DELCON (0.05*cinfin)
533 IARG = 1
534 369 format(1x,'DCNEW = ',f10.6)
535 18         IF (IPROG.EQ.1) THEN
536             AMTGN = PCNNEW*CINFIN
537             DCNEW = AMTGN + CPERF
538         ELSE
539             AMTLST = CPERF*PCNNEW
540             DCNEW = CPERF-AMTLST
541         ENDIF
542
543 C           Set up guess to determine the flux at the inner membrane
544 c           surface. See 3-5-94 development.
545 C           Use continuity equation to obtain guess
546
547             DELCON = DCNEW-CPERF
548             FLUXRI = (DELCON*QDIAL)/(2.0*3.14*RIN*XLEN)
549 c           ddial includes correction for flow (35/13)
550             CMEMRI = ((FLUXRI*RIN)/((35.0/13.0)*DDIAL))+DCNEW
551
552
553
554 C           Note VALUE only goes to 10 because the BC is
555 c           included.
556 C           Start with setting up the values to be solved for
557 c           in the matrix for the membrane.
558
559             ECFT(1) = CMEMRI
560             VALUE(1)=-ECFT(2)-COEFFA(2)*CMEMRI
561             VALUE(10)= (FLUXRI*(RIN/ROUT)*RUNIT)/DMEM
562             DO 45 K=2,9
563                 VALUE(K)=-ECFT(K)
564 45         CONTINUE
565
566 C           Call THOMAS calls the subroutine THOMAS to solve the
567 c           matrix of concentrations at each point.
568
569             CALL THOMEM(ECFTP1,COEFFA,COEFFB,COEFFC,VALUE)
570
571 C           Finish the rest of the ECF which includes the variable
572 c           time step. Value(12) is the first point in the
573 c           ECF. Value(numr-1) and Value(12) include the boundary
574 c           conditions.
575
576 C           Note VALUE only goes to NUMR-1 because the BC is
577 c           included.
578
579             VALUE(NUMR-1)=-ECFT(NUMR-1)-(XKPLEC*CPLAS*DELT)
580 &             -COEFFC(NUMR-1)*CINFIN
581             VALUE(12) = -ECFT(12)-(XKPLEC*CPLAS*DELT)
582 &             -((GICF+GECF)*DELT)-ECFTP1(10)*COEFFA(12)

```

```

583          DO 50 J=13,NUMR-2
584             VALUE(J)=-ECFT(J)-(XKPLEC*CPLAS*DELT)-((GICF+GECF)*DELT)
585 50          CONTINUE
586             ITHOM = 12
587             NUMEQ = NUMR-ITHOM
588
589 C           Call THOMAS calls the subroutine THOMAS to solve the
590 c           matrix of concentrations at each point.
591
592          CALL THOECF(ECFTP1,COEFFA,COEFFB,COEFFC,VALUE,NUMEQ,ITHOM,NUMR)
593 C
594 C           Now check the difference in the FLUXrout and FLUX ecf and
595 c           set an initial tolerance of 0.1 for the absolute value
596 c           of the difference between these flux values. Once the
597 c           the initial tolerance of 10 percent is encountered
598 c           then the program changes to slowly increment the values
599 c           in the dialysate so that a tolerance of 1 percent may be
600 c           obtained.
601
602             FLUXEC = ((ECFTP1(12)-ECFTP1(10))/RUNIT)*DECF
603             FLUXRO = FLUXRI*(RIN/ROUT)
604             DIFFLX = ABS(FLUXEC-FLUXRO)
605             ARGUM = ABS(DIFFLX/FLUXRO)
606             TOLER1 = 0.005
607             TOLER2 = 0.01
608             IF (IARG.EQ.7000) THEN
609                GOTO 38
610             ENDIF
611
612
613 C           The following sets of IF-THEN-ELSE statements are designed
614 c           to save a little computational time. Once the set tolerance
615 c           of 10% is reached the program shifts to a new set of IF-THEN-
616 c           ELSE statements to get the tolerance down to 1%. A problem
617 c           was encountered when the "true" answer was passed and the
618 c           concentration really needed to be lowered. This was observed
619 c           by noticing the increase in the differences between the old
620 c           arguments.
621
622
623             IF (ARGUM.GT.TOLER1) THEN
624                IARG = IARG+1
625                PCNNEW = PCNNEW + ADDER
626                ILOOP = 1
627                IFLAG = 1
628                GOTO 18
629             ENDIF
630
631 c           Update values in the membrane and in the ECF
632
633 28          DO 55 K=1,10
634             ECFT(K+1)=ECFTP1(K)
635 55          CONTINUE
636             DO 60 K=ITHOM,NUMR-1
637             ECFT(K)=ECFTP1(K)
638 60          CONTINUE
639
640
641          CALL DATOUT(ECFT,DELR,RUNIT,DELT,RIN,CINFIN,DCNEW,NUMR,I)
642
643 40          CONTINUE
644 38          print*, 'over tolerance level'
645
646 C           -----
647 C           10-8-94.....USED AS A TEST FOR EUTHANIZED ANIMALS NEED TO

```

```

648 C          SAVE THE CONDITIONS AND USE AS bc CONDITIONS IN THE
649 C          next program
650
651          DO 88 JJ=1,NUMR
652              WRITE(85,888)ECFT(JJ)
653 888          FORMAT(1X,F10.6)
654 88          CONTINUE
655
656          CLOSE(UNIT=85,STATUS='KEEP')
657 C          -----
658          RETURN
659          END
660
661          SUBROUTINE RAMP(ECFT,ACOEFF,BCOEFF,CCOEFF,DELR,CMAX,PERCEN,
662 & RUNIT,SUMKS,ROUT,RIN,DMEM,DECF,QDIAL,XLEN,DDIAL,TAU,XKPLEC,
663 & GICF,GECF,CPERF,XLAM,NUMR)
664 C          -----
665 c          The purpose of subroutine RAMP is to bring the initial values
666 c          in the matrix up. Because the finite difference program is a
667 c          step change a severe step change in the time domain can cause
668 c          instability in the routine.
669 c          RAMP takes the change in the time domain and divides it by
670 c          10 and then solves the implicit finite difference for all space
671 c          points at these early time points. The coefficients used are
672 c          defined for the smaller delta t above in the initializing
673 c          subroutine
674 c          -----
675
676          REAL ECFT(700),ECFTP1(700),ACOEFF(700),BCOEFF(700),CCOEFF(700),
677 & VALUE(700),DELR(700),CMAX,RIN,RUNIT,XKPLEC,SUMKS,TAU,
678 & PERCEN,CPERF
679          INTEGER NUMR,IProg
680
681          OLDFLX = 0.0
682
683          DO 40 I=2,11
684
685          c          Since the BC at the wall will be zero, then this moves
686 c          the indexing back one.
687
688          CPLAS= cmax*exp(-xlam*(real(i-1)*tau))
689          DENDUM = SUMKS-XLAM
690          ADUM=(CPLAS*XKPLEC+GICF+GECF)/DENDUM
691          BDUM = (XKPLEC*CMAX)/DENDUM
692          CINFIN=ADUM-(BDUM*EXP(-SUMKS*TAU*REAL(i-1)))
693          TIME = REAL(I-1)*TAU
694          WRITE(62,568)TIME,CPLAS
695          568          FORMAT(1X,F10.6,3X,F10.6)
696
697          397          format(1x,'cmax = ',f10.6,3x,'C at far-field=',f10.6)
698
699          IF (CPERF.GT.CINFIN) THEN
700              IProg = 2
701          ELSE
702              IProg = 1
703          ENDIF
704
705
706 c          10-21-94 (Added sometime in 4-94)
707 c          The following IF THEN statement was empirically added
708 c          for situation in which a Lönnroth or no net flux situation
709 c          is used in microdialysis. For some reason when the perfusion
710 c          fluid concentration started to get within 30 percent of the
711 c          far-field concentration then the flux gets sensitive..thus
712 c          reason for going up in percentage units at a slower rate.

```

```

713 c           Otherwise the program would bypass the stable value and
714 c           would diverge from the answer rather than converge. I do
715 c           not know that mathematical reason for this....but 30 percent
716 c           seems to work the best.
717
718 IF (CINFIN.GT.1.0E-6) THEN
719     PERDUM = (ABS(CPERF-CINFIN))/CINFIN
720     IF (PERDUM.LE.0.3) THEN
721         ADDER = 1E-4
722     ELSE
723         ADDER = 0.0005
724     ENDIF
725 ELSE
726     ADDER = 0.0005
727 ENDIF
728
729
730     PCNNEW = PERCEN
731
732 c           Calculate the approx. value for DELCON (0.05*cinfin)
733 c           IARG = 1
734     ARGOLD = 1.0E6
735     format(lx,'DCNEW = ',f10.6)
736 369
737
738 19     IF (IProg.EQ.1) THEN
739         DCNEW = (PCNNEW*CINFIN)+CPERF
740     ELSE
741         AMTLST = CPERF*PCNNEW
742         DCNEW = CPERF-AMTLST
743     ENDIF
744
745 C           Set up guess to determine the flux at the inner membrane
746 c           surface.
747 C           Use continuity equation to obtain guess
748
749     DELCON = DCNEW-CPERF
750     FLUXRI = (DELCON*QDIAL)/(2.0*3.14*RIN*XLEN)
751     CMEMRI = ((FLUXRI*RIN)/((35.0/13.0)*DDIAL))+DCNEW
752
753
754     ECFT(1) = CMEMRI
755
756
757 C           Note VALUE only goes to NUMR-1 because the BC is
758 c           included.
759
760     VALUE(1)=-ECFT(2)-ACOEFF(2)*CMEMRI
761     VALUE(10) = (FLUXRI*(RIN/ROUT)*RUNIT)/DMEM
762     DO 45 K=2,9
763         VALUE(K)=-ECFT(K)
764 45     CONTINUE
765
766 C           Call THOMAS calls the subroutine THOMAS to solve the
767 c           matrix of concentrations at each point.
768     CALL THOMEM(ECFTP1,ACOEFF,BCOEFF,CCOEFF,VALUE)
769 C
770
771 C           Note VALUE only goes to NUMR-1 because the BC is
772 c           included.
773
774     VALUE(NUMR-1)=-ECFT(NUMR-1)-(XKPLEC*CPLAS*TAU)
775 &     -((GICF+GECF)*TAU)-CCOEFF(NUMR-1)*CINFIN
776     VALUE(12) = -ECFT(12)-(XKPLEC*CPLAS*TAU)
777 &     -((GICF+GECF)*TAU)-ECFTP1(10)*ACOEFF(12)

```

```

778          DO 50 J=13,NUMR-2
779             VALUE (J)=-ECFT (J)-(XKPLEC*CPLAS*TAU)-((GICF+GECF)*TAU)
780 50          CONTINUE
781             ITHOM = 12
782             NUMEQ = NUMR-ITHOM
783
784 C          Call THOMAS calls the subroutine THOMAS to solve the
785 c          matrix of concentrations at each point.
786          CALL THOECF (ECFTP1,ACOEFF,BCOEFF,CCOEFF,VALUE,NUMEQ,ITHOM,NUMR)
787
788 C
789
790
791 C          Now check the difference in the FLUXrout and FLUX ecf and
792 c          set a tolerance of 0.1 for the absolute value
793 c          of the difference. Recall that ECFTP1(12) is the
794 c          value in the ECF at point 12 and ecftp1(10) is
795 c          the value of the concentration at the membrane outer
796 c          radius. DELR(11) is the radial increment in the ECF
797
798          FLUXEC = ((ECFTP1(12)-ECFTP1(10))/DELR(11))*DECF
799          FLUXRO = FLUXRI*(RIN/ROUT)
800          DIFFLX = (FLUXEC-FLUXRO)
801          CHGFLX = OLDFLX-DIFFLX
802          IF (IPROG.EQ.2.AND.CHGFLX.LT.0.0.AND.DIFFLX.GT.1.0E-4) THEN
803             IPROG = 1
804             PCNNEW = PERCEN
805             GOTO 19
806          ENDIF
807          OLDFLX = DIFFLX
808          ARGUM = ABS(DIFFLX/FLUXRO)
809
810          TOLER = 0.1
811
812          IF (IARG.EQ.2000) THEN
813             print*, 'over tolerance level IN RAMP'
814             GOTO 39
815          ENDIF
816
817
818
819          IF (ARGUM.GT.TOLER) THEN
820             IARG = IARG+1
821             PCNNEW = PCNNEW+ADDER
822             GOTO 19
823          ELSE
824             GOTO 29
825          ENDIF
826
827
828 29          DO 55 K=1,10
829             ECFT (K+1)=ECFTP1 (K)
830 55          CONTINUE
831             DO 60 K=ITHOM,NUMR-1
832                ECFT (K)=ECFTP1 (K)
833 60          CONTINUE
834
835          CALL DATOUT (ECFT, DELR, RUNIT, TAU, RIN, CINFIN, DCNEW, NUMR, I)
836 40          CONTINUE
837 39          RETURN
838          END
839
840
841          SUBROUTINE THOMEM (ECFTP1, THOMA, THOMB, THOMC, VALUE)
842             REAL ECFTP1 (700), THOMA (700), THOMB (700),

```

```

843      & THOMC(700),VALUE(700),THBETA(700),THGAMM(700)
844      INTEGER IT,NEQU
845 C          nequ = number of equations = numr-1
846 C          SOLVE A SET OF ALGEBRAIC EQUATIONS USING THE THOMAS
847 C          TECHNIQUE FOR TRIDIAGONAL EQUATIONS
848 C          THE THOMAS TECHNIQUE INVOLVES THREE DIFFERENT
849 C          SECTIONS:
850 C              1) DECOMPOSITION
851 C              2) FORWARD SUBSTITUTION
852 C              3) BACK SUBSTITUTION
853 C          CHANGED USED CARNAHAN EXAMPLE PG. 442
854
855 C          DO THE DECOMPOSITION
856 C          NEQU=10
857
858 C          1-20-94 Need to check and make sure that the indexing in
859 C          Thomas is correct. Need to move everything up by
860 C          one so that the coefficients match the values given
861
862 C          *****
863 C          PARAMETERS INTERNAL TO THOMEM
864 C          *****
865 C          THBETA = AN ARRAY TO HOLD THE "B" COEFFICIENTS BECAUSE
866 C          THE B COEFFICIENTS PASS THROUGH THIS ROUTINE MORE
867 C          THAN ONCE...THEREFORE THEY NEED TO BE PRESERVED.
868 C          THGAMMA = AN ARRAY NECESSARY FOR THE SOLVING OF THE
869 C          MATRIX
870
871 C          THBETA(1)=THOMB(2)
872 C          THGAMM(1)=VALUE(1)/THBETA(1)
873
874 C          DO 35 IT=2,NEQU
875
876 C          THBETA(IT)=THOMB(IT)-((THOMA(IT)*THOMC(IT-1))/THBETA(IT-1))
877 C          THGAMM(IT)=(VALUE(IT)-(THOMA(IT)*THGAMM(IT-1)))/THBETA(IT)
878
879 C          THBETA(IT)=THOMB(IT+1)-((THOMA(IT+1)*THOMC(IT))/THBETA(IT-1))
880 C          THGAMM(IT)=(VALUE(IT)-(THOMA(IT+1)*THGAMM(IT-1)))/THBETA(IT)
881
882 C          35 CONTINUE
883
884
885 C          ECFTP1(NEQU)=THGAMM(NEQU)
886 C          DO 45 KT=NEQU-1,1,-1
887
888 C          ECFTP1(KT)=THGAMM(KT)-((THOMC(KT+1)*ECFTP1(KT+1))
889 C          /THBETA(KT))
890 C          45 CONTINUE
891
892
893 C          RETURN
894 C          END
895
896
897
898 C          SUBROUTINE THOECF(ECFTP1,THOMA,THOMB,THOMC,VALUE,NUMEQ,ITHOM,
899 C          & NUMR)
900 C          REAL ECFTP1(700),THOMA(700),THOMB(700),
901 C          & THOMC(700),VALUE(700),THBETA(700),THGAMM(700)
902 C          INTEGER NUMEQ,ITHOM,IT,NEQU
903 C          nequ = number of equations = numr-1
904 C          SOLVE A SET OF ALGEBRAIC EQUATIONS USING THE THOMAS
905 C          TECHNIQUE FOR TRIDIAGONAL EQUATIONS
906 C          THE THOMAS TECHNIQUE INVOLVES THREE DIFFERENT
907 C          SECTIONS:

```

```

908 C          1) DECOMPOSITION
909 C          2) FORWARD SUBSTITUTION
910 C          3) BACK SUBSTITUTION
911 C          CHANGED USED CARNAHAN EXAMPLE PG. 442
912
913 C          print*, 'subroutine thomas'
914
915 C          DO THE DECOMPOSITION
916          NEQU=NUMEQ
917
918 C          1-20-94 Need to check and make sure that the indexing in
919 c          Thomas is correct. Need to maove everything up by
920 c          one so that the coefficients match the values given
921 c          3-6-94 ..changed indexing
922
923          THBETA(ITHOM)=THOMB(ITHOM)
924          THGAMM(ITHOM)=VALUE(ITHOM)/THBETA(ITHOM)
925
926          DO 35 IT=ITHOM+1, NUMR-1
927 c          1-20-94 ...Note this is where the change is in indexing.
928 c          3-6-94 ...changed it back..old indexing saved in comments
929
930          THBETA(IT)=THOMB(IT)-((THOMA(IT)*THOMC(IT-1))/THBETA(IT-1))
931          THGAMM(IT)=(VALUE(IT)-(THOMA(IT)*THGAMM(IT-1)))/THBETA(IT)
932
933 C          THBETA(IT)=THOMB(IT+1)-((THOMA(IT+1)*THOMC(IT))/THBETA(IT-1))
934 C          THGAMM(IT)=(VALUE(IT)-(THOMA(IT+1)*THGAMM(IT-1)))/THBETA(IT)
935
936 35          CONTINUE
937
938
939          ECFTP1(NUMR-1)=THGAMM(NEQU)
940          DO 45 KT=NUMR-1, ITHOM, -1
941 c          changed indexing is affected here too add 1 to coeffc.
942 c          3-6-94 ..undid change
943          ECFTP1(KT)=THGAMM(KT)-((THOMC(KT)*ECFTP1(KT+1))
944          &          /THBETA(KT))
945 45          CONTINUE
946
947 c          print*, 'jumping out of thomas'
948          RETURN
949          END
950
951
952          SUBROUTINE DATOUT(ECFT, DELR, RUNIT, DELT, RIN, CINFIN, DCNEW, NUMR, I)
953          REAL ECFT(700), DELR(700), DELT, SIMTIM, RADIAL, RIN
954          INTEGER NUMR, I
955
956 c          4-5-94 Counting in dataout was incorrect...did not
957 c          take into account the radial increment
958
959
960 c          RECOV = (DCNEW/ECFT(11))*100
961 c          WRITE(60, 279) RECOV
962 c279          FORMAT(1X, 'RECOVERY(&) = ', F10.6)
963 C          EXFRAC = DELCON/CINFIN
964 C          WRITE(60, 277) EXFRAC
965 C277          FORMAT(1X, 'EXTRACTION FRACTION = ', E15.5)
966          SIMTIM=(I-1)*DELT
967          WRITE(6, 578) SIMTIM
968 578          FORMAT(1X, 'TIME UNIT = ', F10.6)
969
970          WRITE(65, 289) SIMTIM, DCNEW
971          WRITE(60, 289) SIMTIM, DCNEW
972 289          FORMAT(1X, F12.5, 2X, f12.5)

```



```

973 c      This subroutine will output the file so that it can be
974 c      imported into Excel. From Excel the user can determine
975 c      which time points of the simulation will be saved
976 c      or discarded.
977
978
979      write(60,298)RIN,ecft(1)
980 298      FORMAT(1X,f12.5,2x,f12.5,)
981 c      output membrane
982      DO 70 J=2,11
983 c      Calculate the radial distance for each concentration
984      RADIAL=RIN+((J-1)*RUNIT)
985 c      xnorm=ecft(j)/cinfin
986 C      WRITE(60,299)RADIAL,ECFT(J),xnorm
987 C299      FORMAT(1X,f12.5,2x,f12.5,2x,f12.5)
988      WRITE(60,299)RADIAL,ECFT(J)
989 299      FORMAT(1X,f12.5,2x,f12.5)
990
991 70      CONTINUE
992
993 c      output rest in steps of ten
994 c      Because of variable output need a logical statement
995 c      icount=0
996
997      DO 75 J=12,25
998      RADIAL=RADIAL+DELR(J-1)
999      WRITE(60,299)RADIAL,ECFT(J)
1000 75      CONTINUE
1001
1002
1003      DO 80 J=26,NUMR-1
1004      icount = icount+1
1005      RADIAL=RADIAL+DELR(J-1)
1006 C      xnorm=ecft(j)/cinfin
1007      if (icount.eq.10) then
1008 C      WRITE(60,899)RADIAL,ECFT(J),xnorm
1009 C899      FORMAT(1X,f12.5,2x,f12.5,2x,f12.5)
1010      WRITE(60,899)RADIAL,ECFT(J)
1011 899      FORMAT(1X,f12.5,2x,f12.5)
1012      icount = 0
1013      endif
1014 80      CONTINUE
1015      RADIAL=RADIAL+DELR(NUMR-1)
1016      write(60,301)radial,cinfin
1017 301      FORMAT(1X,f12.5,2x,f12.5)
1018
1019
1020      RETURN
1021      END
1022

```